A REAL TIME MONITORING AND FORECAST VERIFICATION INDEX OF MISO & REAL TIME PREDICTION OF MISO AT IITM .

MISO2

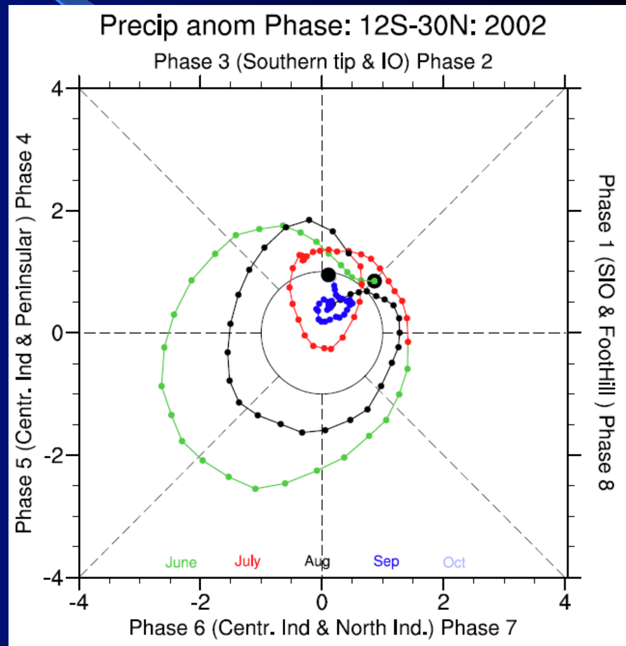

MISO1

B. N. Goswami
Indian institute of Tropical Meteorology, Pune

Outline

- Background
  - Need for Real Time Monitoring and Forecast Verification Index for MISO
  - Distinction between MJO and MISO and Inadequacy of the RMM Indices
- Philosophy, Methodology and Success of The New MISO Index (Suhas et. al. 2013)
- Application of MISO indices for verification ISV forecasts by the CFSv.1 and CFSv.2
- Real time MISO forecasting at IITM

Annual cycle of Precipitation over central India

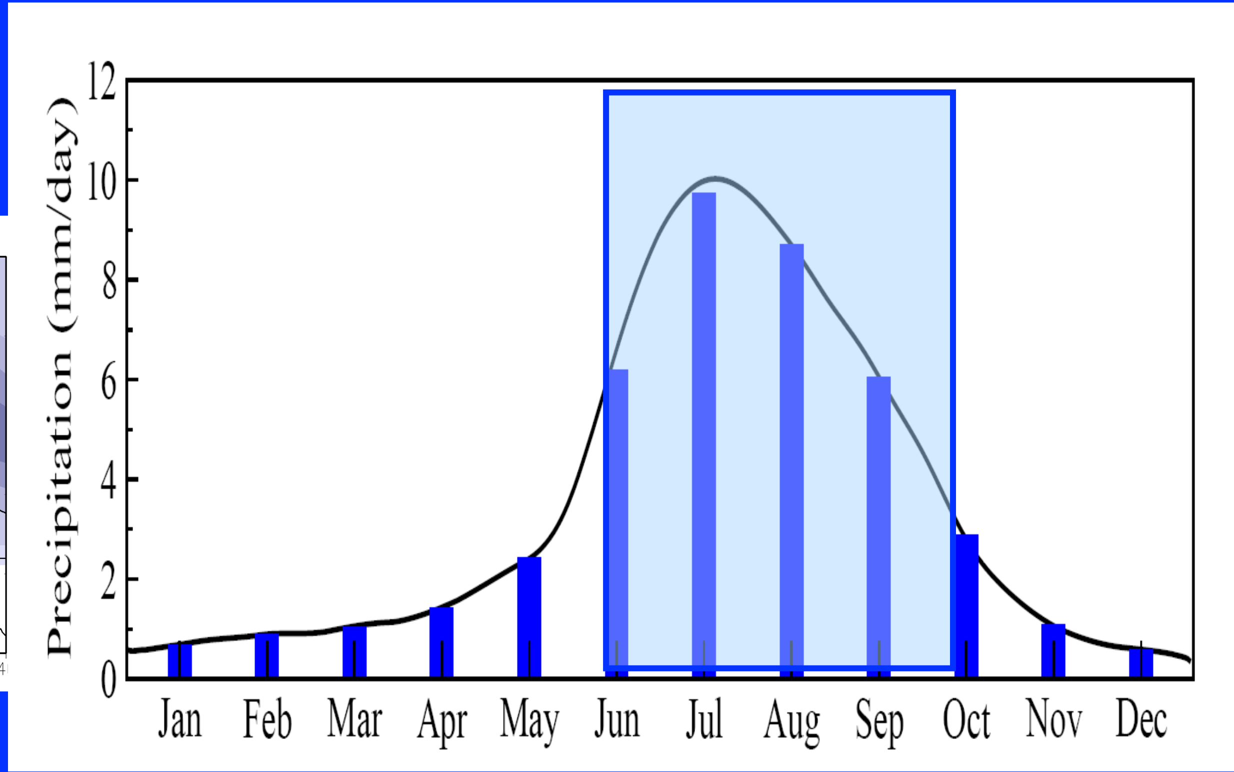

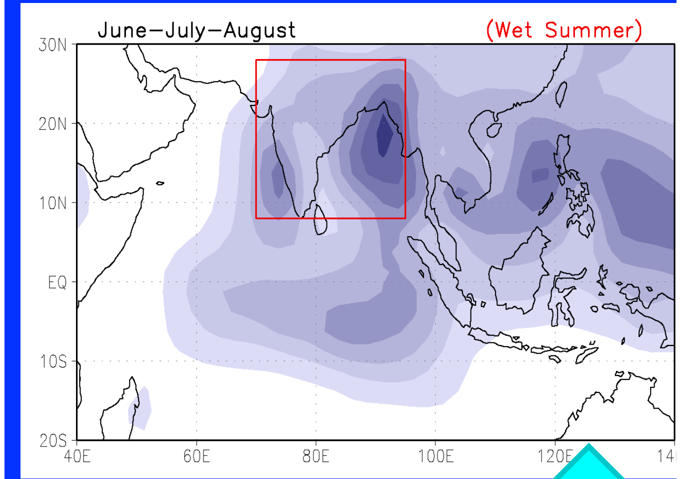

Seasonal mean JJAS precipitation

Daily Precipitation over India for two years

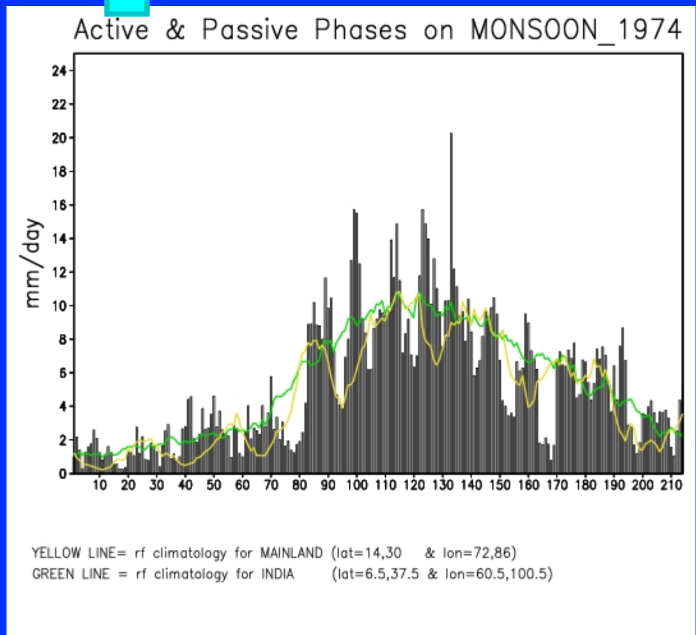

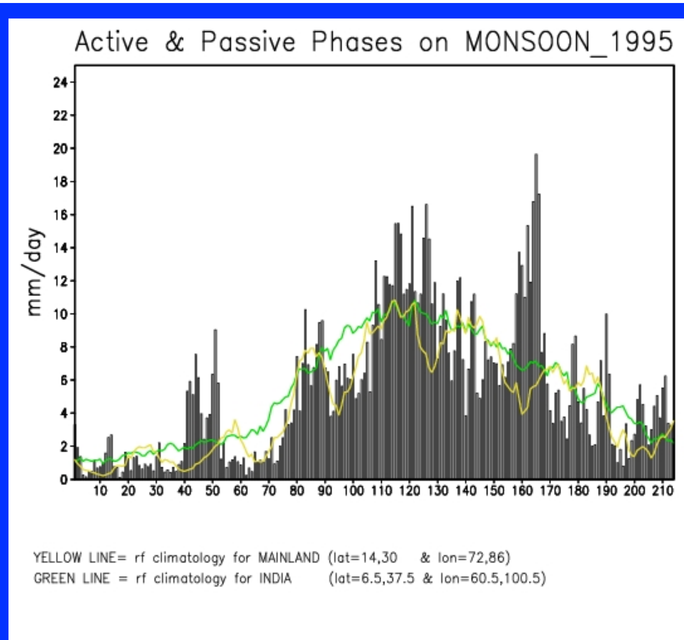

Indian Meteorologists were aware of sub-seasonal fluctuations in the form of

Active-break spells (cycles)

For a long time. e.g. Ramamurthy, 1962, 1969

Daily rainfall (mm/day) over central India for three years, 1972, 1986 and 1988

The smooth curve shows long term mean.

Red shows above normal or wet spells while blue shows below normal or dry spells

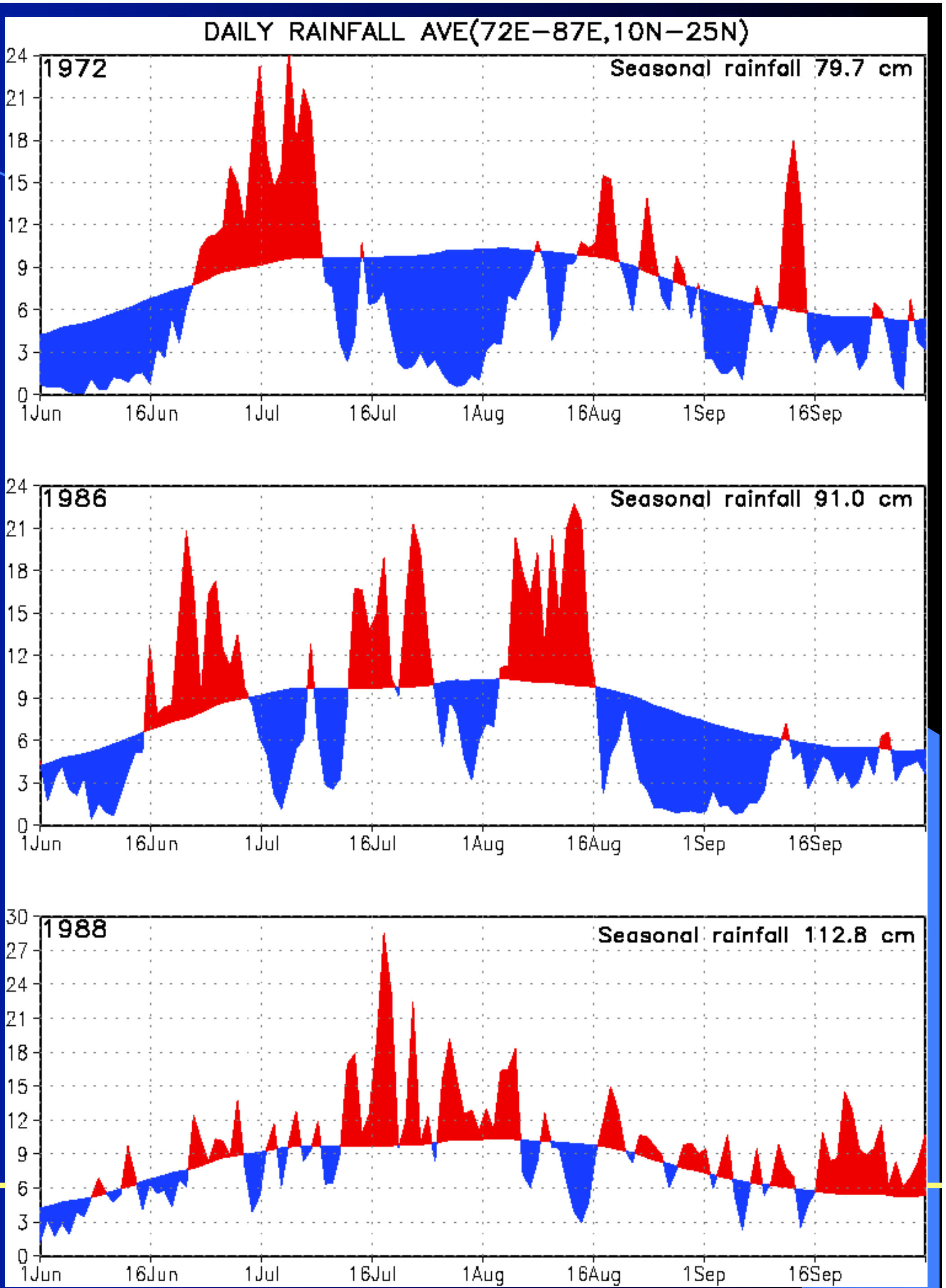

MISO is not confined only within India and has a large scale spatial structure

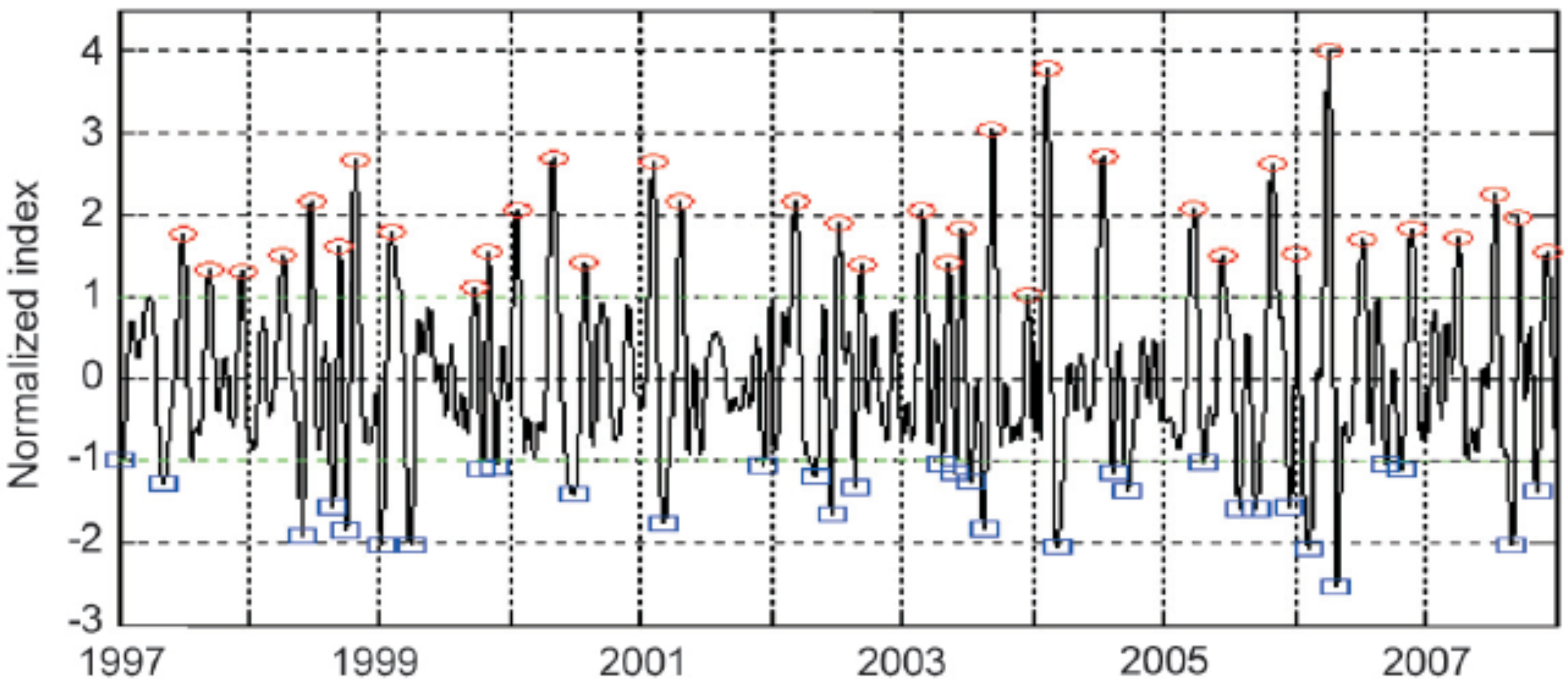

Figure 2.4. Time series of normalized monsoon ISO index between June 1 and September 30 (122 days) for a sample of 11 (1997–2007) summer seasons. The ISO index is defined as 10 to 90-day filtered GPCP rainfall anomaly averaged between 70°E–90°E and 15°N–25°N. The time series is normalized by its own standard deviation. Open circles and squares indicate peaks of active and break conditions, respectively.

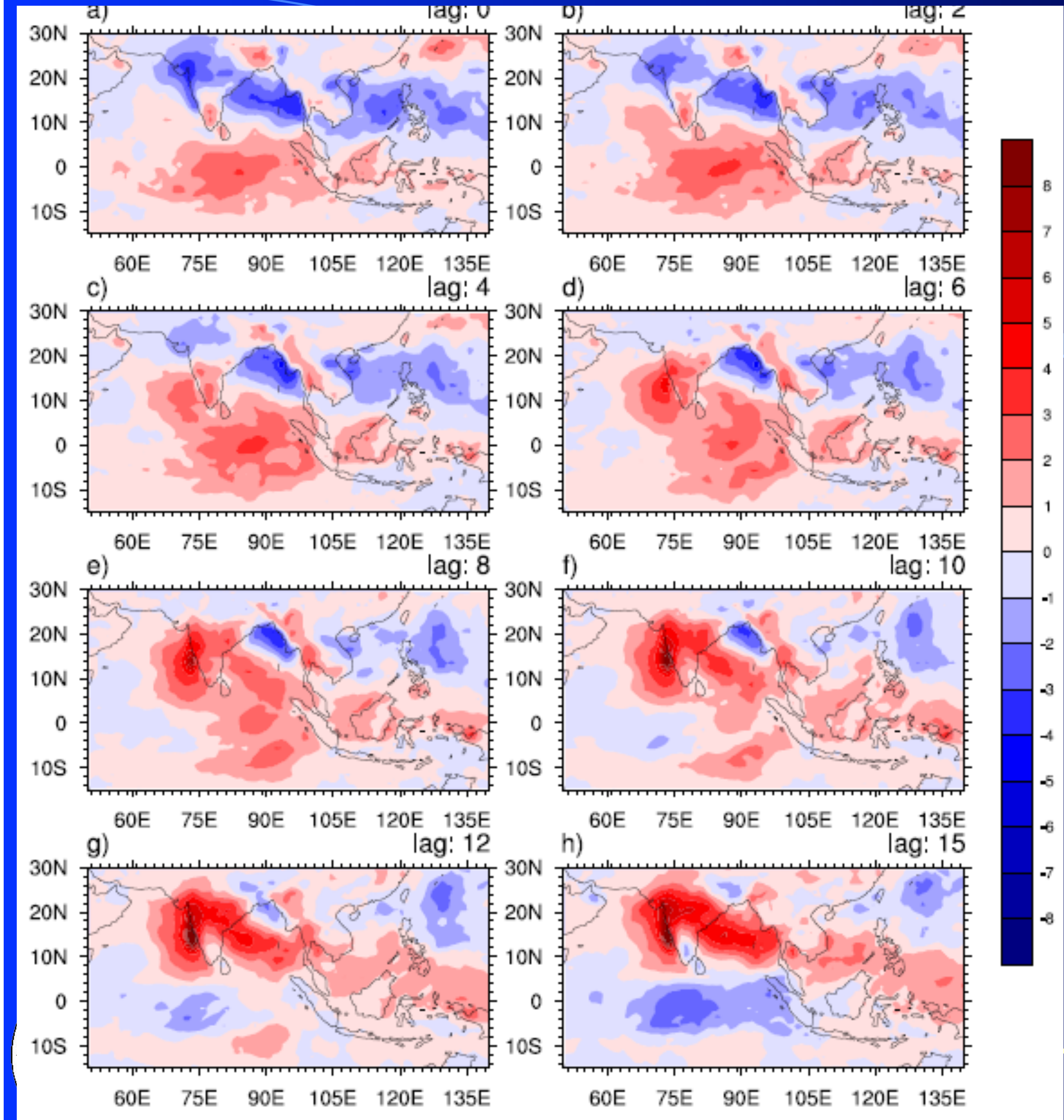

(GPCP JJAS)

MISO evolution one half cycle

- ➢Large east-west scale
- ➢Meridional dipole Over Indian region
- ➢NW-SE tilt of the rainband

Courtesy : Suhas E

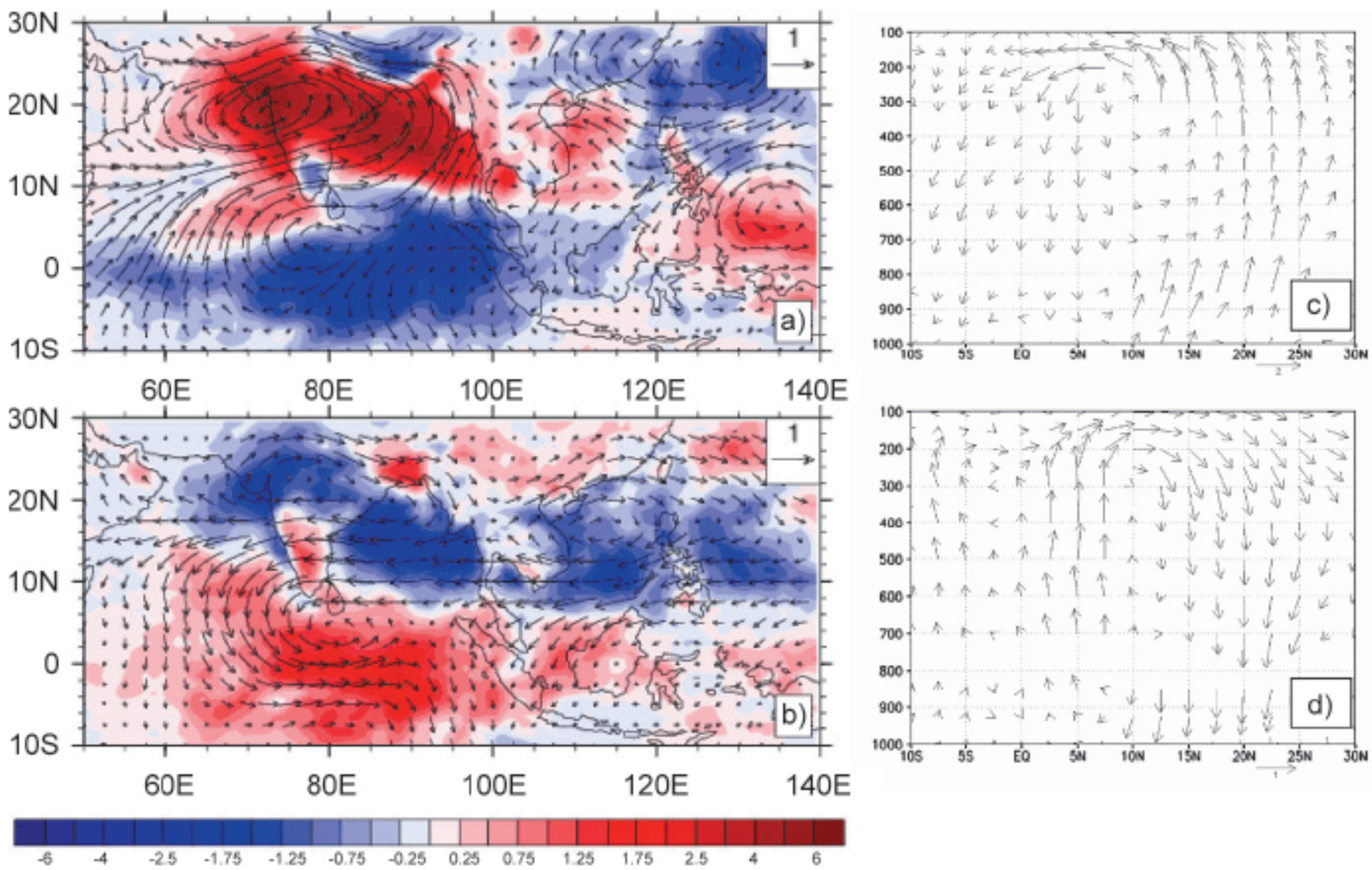

Figure 2.5. Horizontal and vertical structure of dominant ISV. Regressed 10 to 90-day filtered GPCP (shaded, mm day^{-1}) and zonal and meridional wind anomalies at 850 hPa (vectors, m s^{-1}) with respect to the ISO index (Figure 2.4) at (a) 0 lag (active condition) and (b) 14-day lag (break condition). (c) and (d) The anomalous regional Hadley circulation associated with active and break conditions, respectively. Regressed meridional and vertical wind anomalies at a number of vertical levels averaged over 75°E–85°E. Vertical wind anomalies (hPa s^{-1}) have been scaled up by a factor of 100.

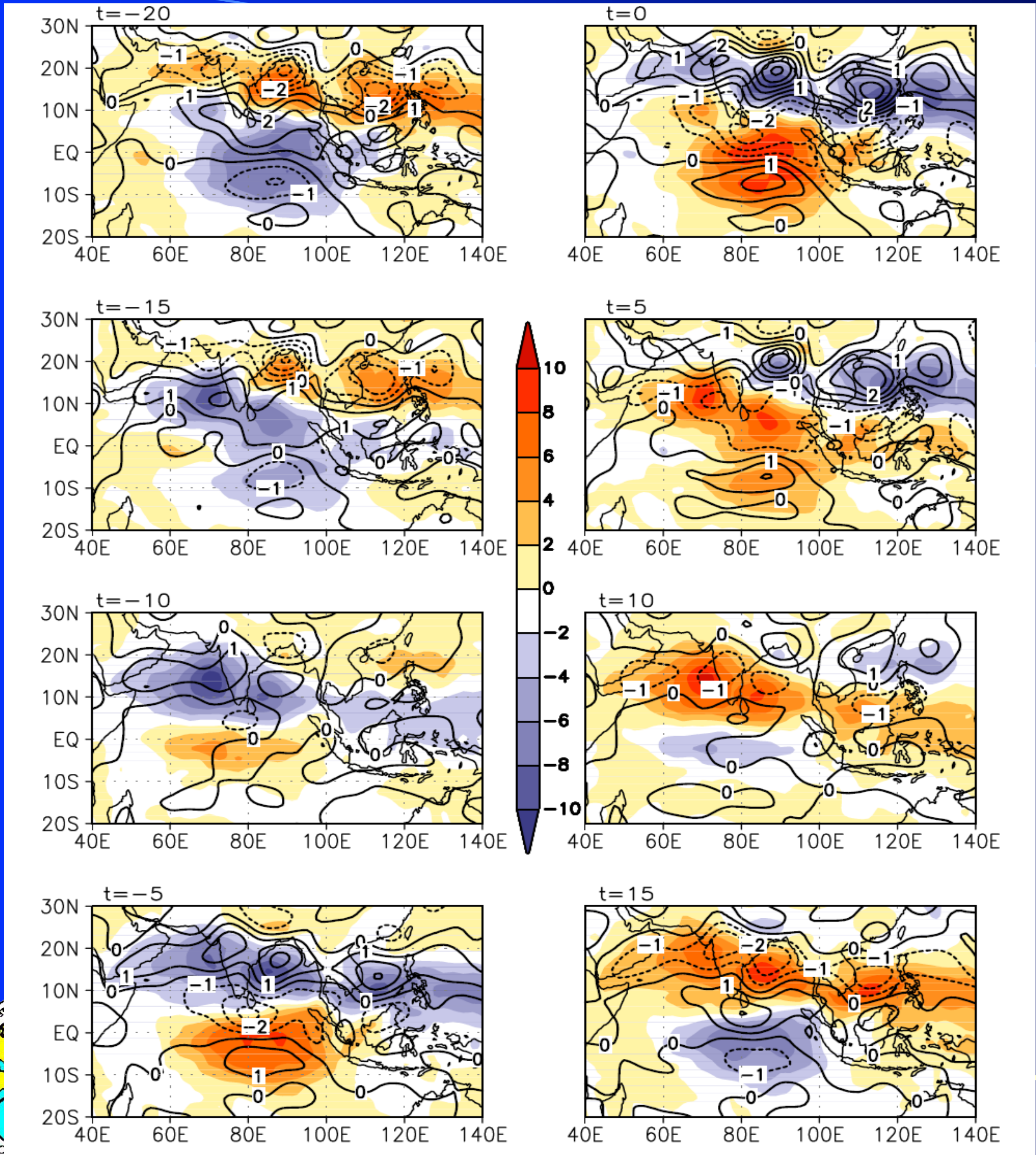

Large scale structure: relationship between OLR and 850 hPa vorticity

Regressed OLR (shaded) and 850 hPa relative vorticity (contour) w.r.t a reference time series of 10-90 day filtered OLR over CI

Goswami, 2005: ISV book

Clim Dyn (2012) 38:1989–2000
DOI 10.1007/s00382-011-1159-1

Bimodal representation of the tropical intraseasonal oscillation

Kazuyoshi Kikuchi · Bin Wang · Yoshiyuki Kajikawa

- **MJO : First EEOF mode (pc1 and pc2) from time filtered (25-90 days) OLR during DJF**

- **BISO : First EEOF mode (pc1 and pc2) from time filtered (25-90 days) OLR from JJA**

$$\|\mathrm{OLR}_{\mathrm{mode}}(t)\| = \sqrt{PC^2_{1,\mathrm{mode}}(t) + PC^2_{2,\mathrm{mode}}(t)}$$

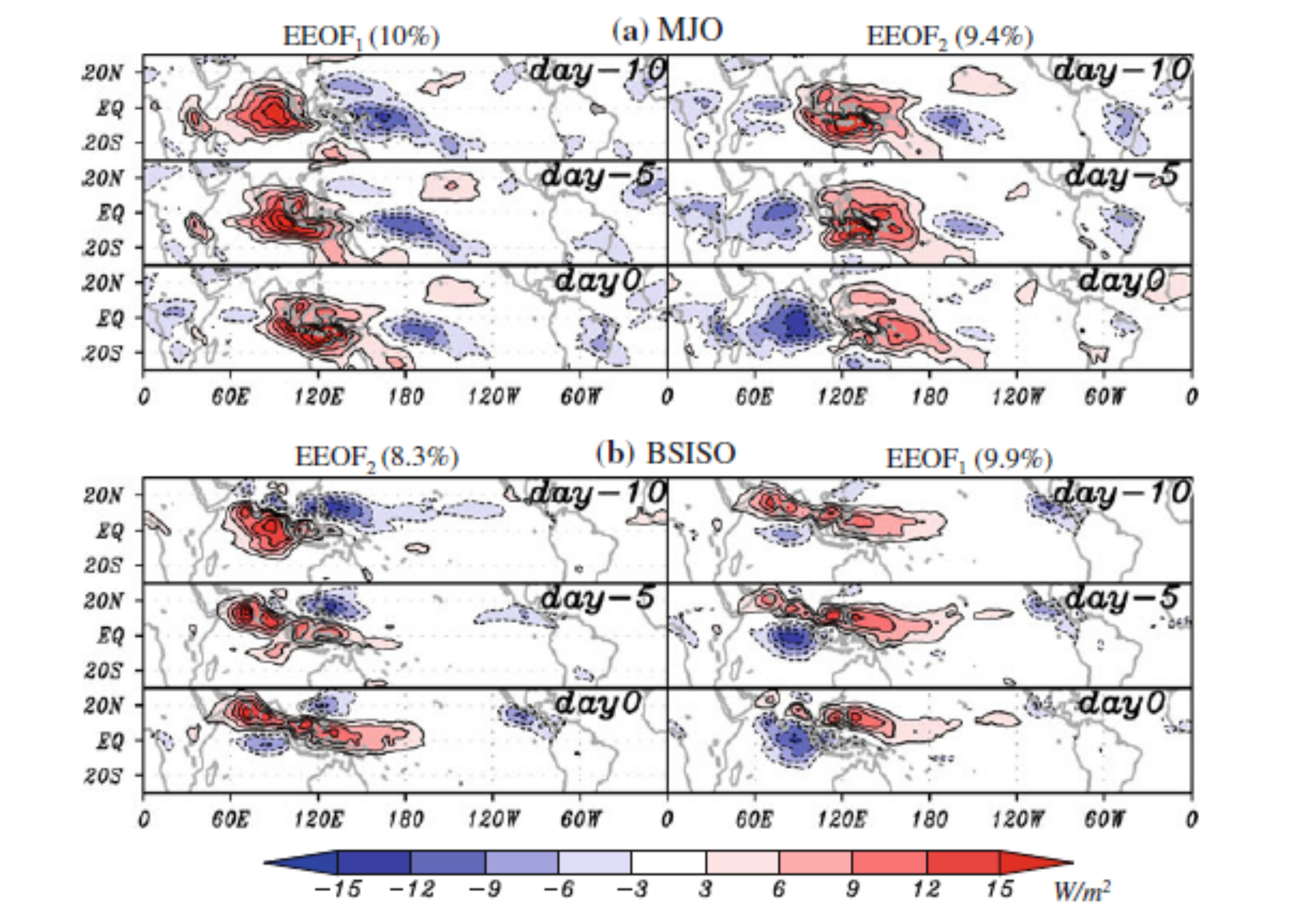

MJO captures the eastward propagating mode and BISO is a northward propagating mode (Kikuchi et al. 2012)

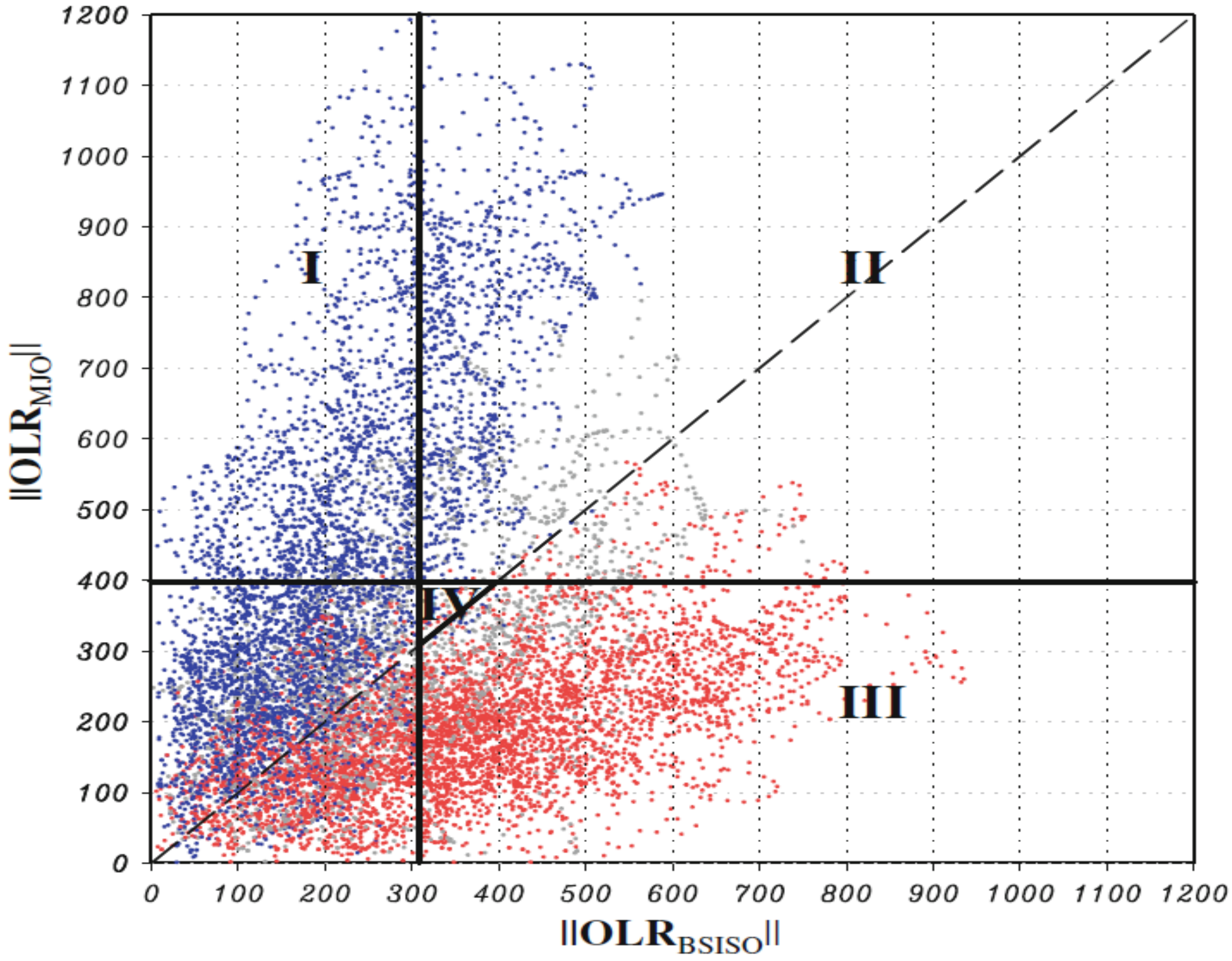

Fig. 4 Scatter plot of ISO amplitude in terms of the BSISO mode (*x* axis) and the MJO mode (*y* axis) for the period 1979–2009. *Solid lines* parallel to the *x* and *y* axes represent one standard deviation of each ISO mode ($\sqrt{PC_1^2 + PC_2^2}$) during the period each EEOF analysis was performed. *Dashed line* represents the situation when both the MJO mode and the BSISO mode have the same variance. According to the later discussion about Fig. 8, three seasons are in different colors (June–October in *red*, December–April in *blue*, otherwise in *gray*)

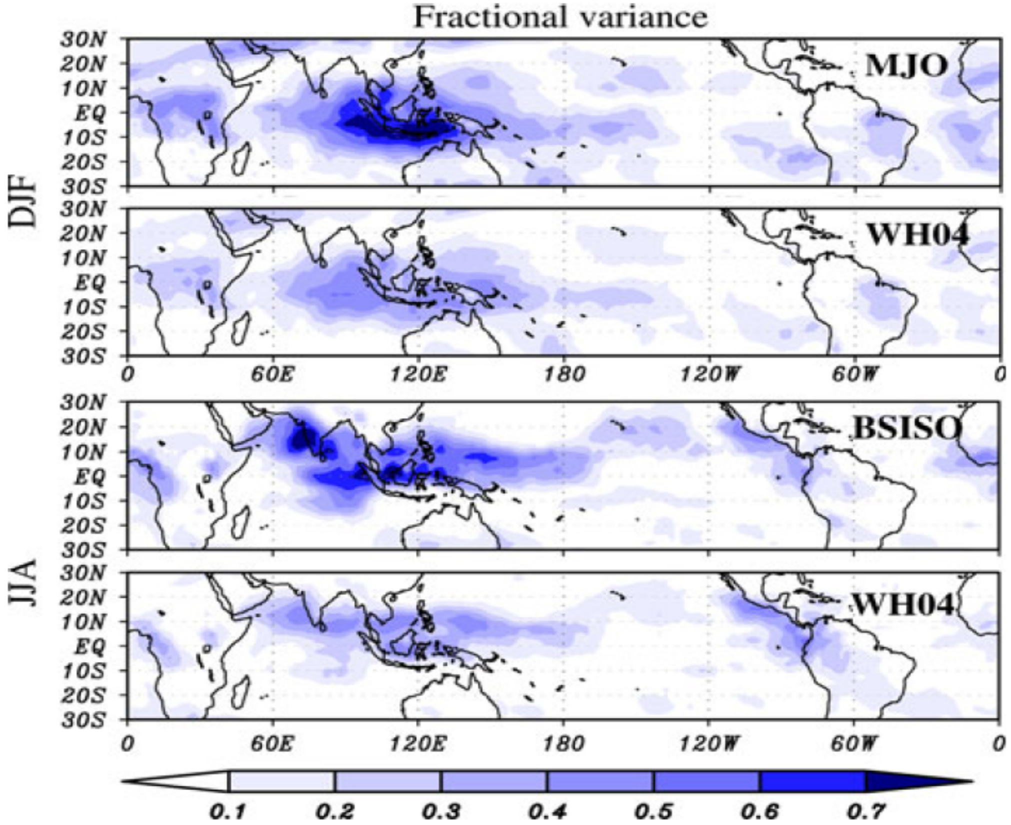

Fig. 6 Fractional variance of ISO composites in terms of OLR based on the bimodal ISO index (*upper panels*) and WH04 index (*lower panels*) during boreal winter (*left panels*) and summer (*right panels*) for the period 1979–2009. The fractional variance is defined as the ratio of the variance of the ISO composite which undergoes through its life cycle to the total variance of the intraseasonal (25–90 day) fluctuation. The composite lifecycle with WH04 index was constructed in the same manner as WH04. The lifecycle with the bimodal ISO index was constructed in a similar way, which was descried in Sect. 4.1 except that, for a fair comparison, the criterion for determining significant ISO events based on A^* was adjusted so that the total number of days (samples) used to construct the composite are the same between the two indices (1,726 for DJF and 1,579 for JJA)

A New MISO Index and Real time Monitoring of MISO in precipitation

- **Even June-Lee et al. index, in addition to require 2 modes for representation of MISO, does not adequately represent the Indian summer MISO, misses 30-60 day variance.**
- **All efforts so far do not use precipitation directly. To represent the active/break spells, an MISO index in precipitation will be more useful.**
- **All existing indices used so far are inadequate in capturing the variance of the northward propagating MISO**

An Indian monsoon intraseasonal oscillations (MISO) index for real time monitoring and forecast verification

E. Suhas • J. M. Neena • B. N. Goswami

Clim Dyn
DOI 10.1007/s00382-012-1462-5

MISO evolution one half cycle

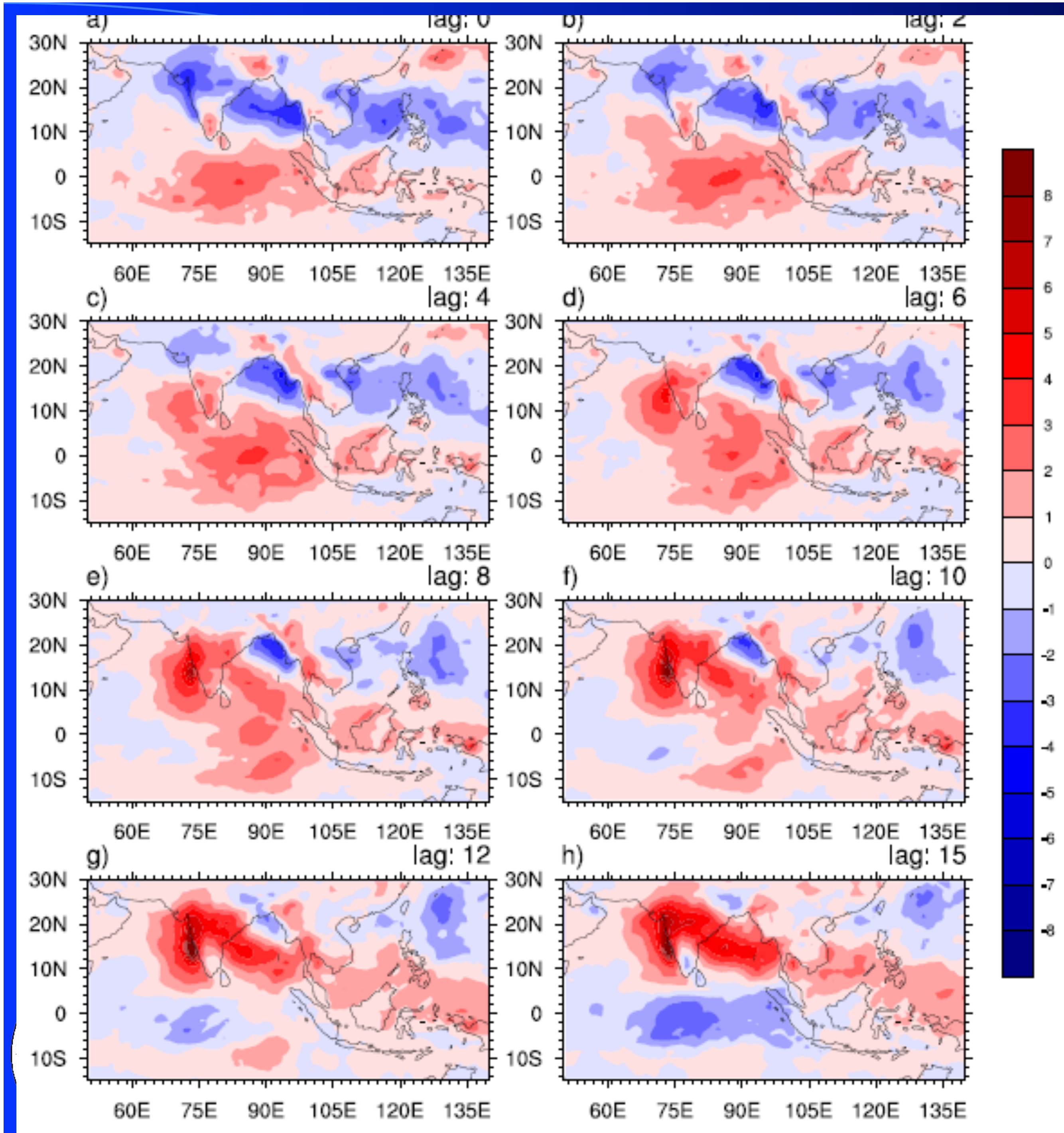

Lag composite of MISO of 25-90 day (GPCP JJAS) precipitation w.r.t. a reference time series of 25-90 day filtered precip averaged over (10.5N–25.5N, 70.5E–85.5E)

Conceptual framework behind developing this Index

- Choose GPCP daily precipitation analysis to apply directly to rainfall
- Employ EEOF technique to capture the northward propagation
- Average between 60.5 and 95.5 E as interested in capturing the northward propagation

Methodology

- **Remove climatological mean and annual cycle.**
- **Average rain anomalies between 60E- 100E.**
- **Augment the original anomaly data with different time lags**
- **Compute the EOFs (eigen values) of the augmented matrix.**
- **Projection of 1st two EEOFs on to the data gives corresponding PCs.**

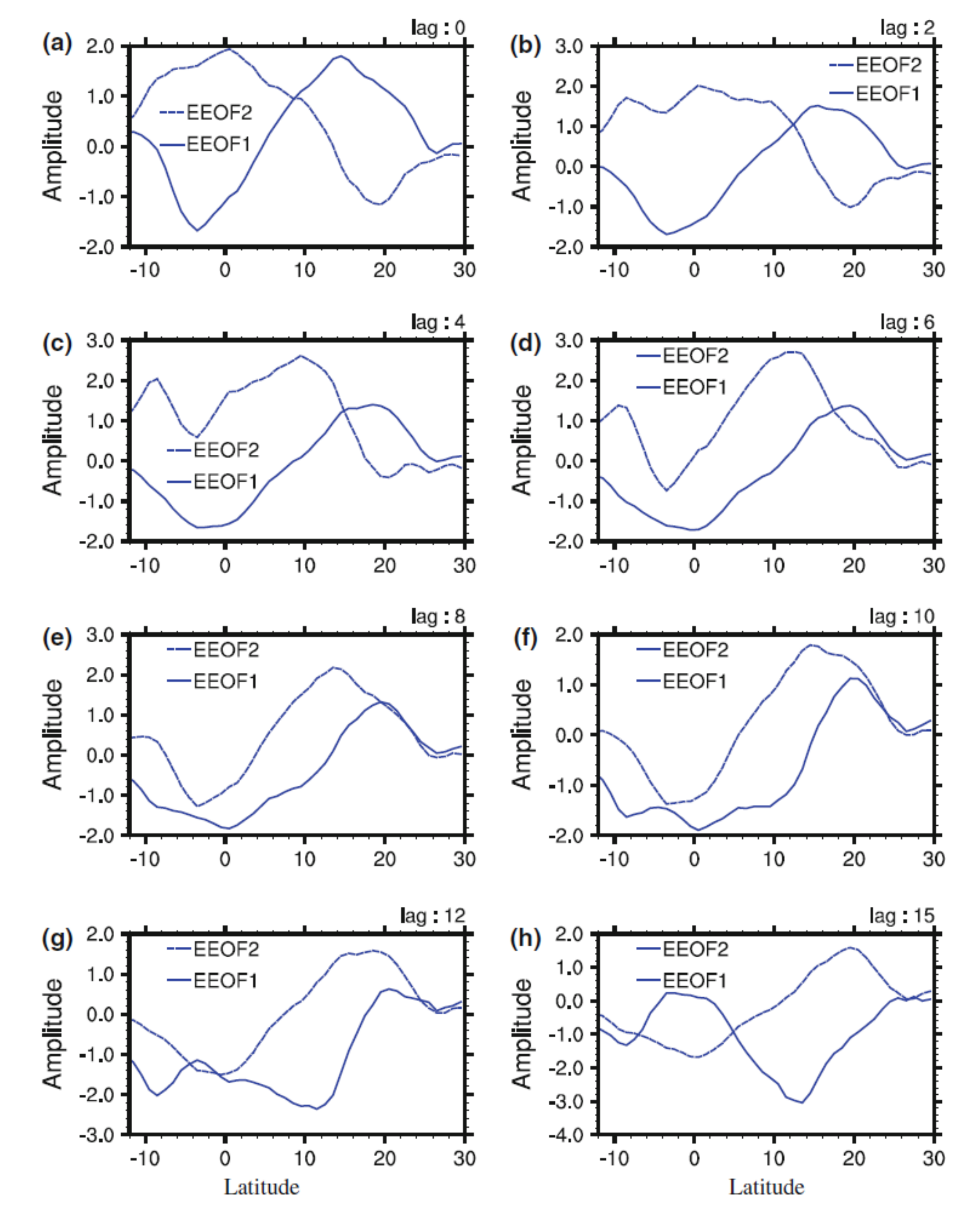

Fig. 2 First two EEOF modes of longitudinally (60.5°E–95.5°E) averaged rainfall anomalies are shown for eight different lags. These two modes together explain about 23 % of the total variance. Amplitudes of the EEOFs are arbitrary

Fig. 3 The first two PCs of EEOF of rainfall anomalies for four JJAS seasons are plotted together. The PCs are normalized by its own standard deviation

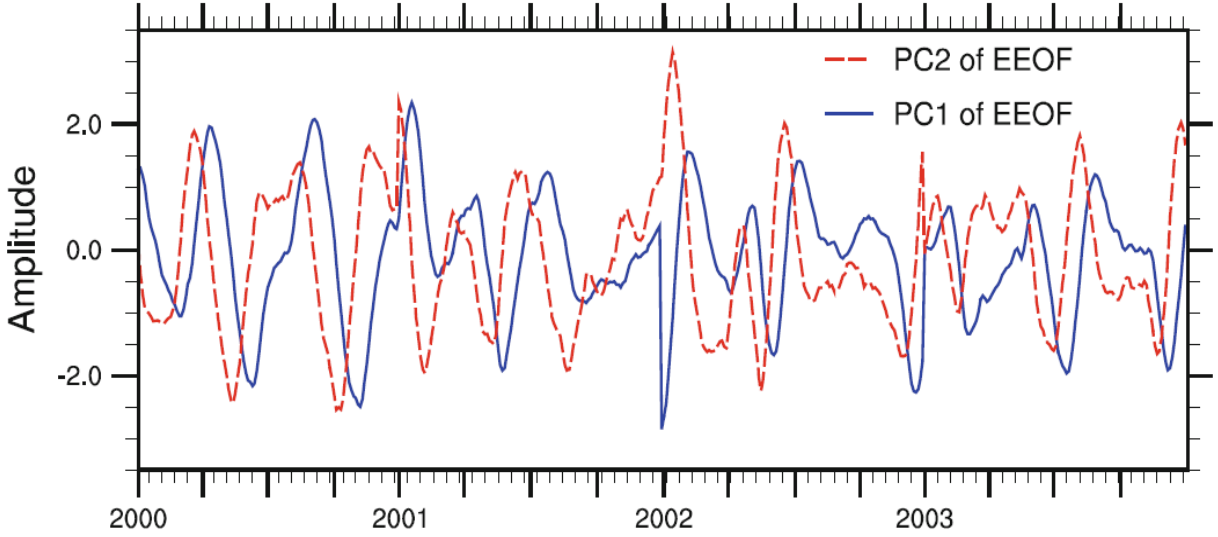

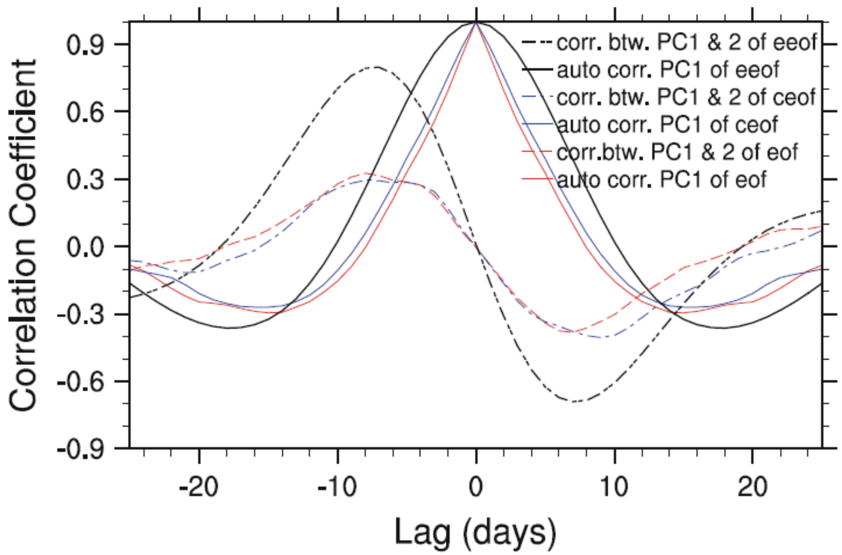

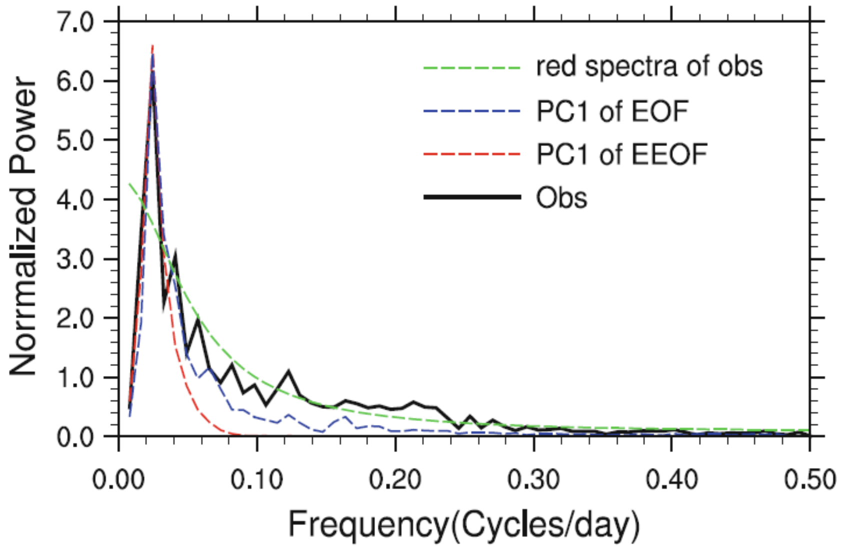

Fig. 4 Auto correlations of PC1 (*solid lines*) and cross-correlation between PC1 and PC2 (*dashed lines*) of eeof, ceof and eof analysis, at different lags

Fig. 6 Power spectra of PC1 of eof (*blue line*) and eeof (*red line*) analysis compared with that of rainfall anomalies (*black line*) averaged over the ISM domain (10.5°N–25.5°N, 70.5°E–85.5°E) for the 1997–2008 JJAS seasons. The red spectra of rainfall anomaly at 95 % confidence level is shown by *dashed green lines*

GPCP

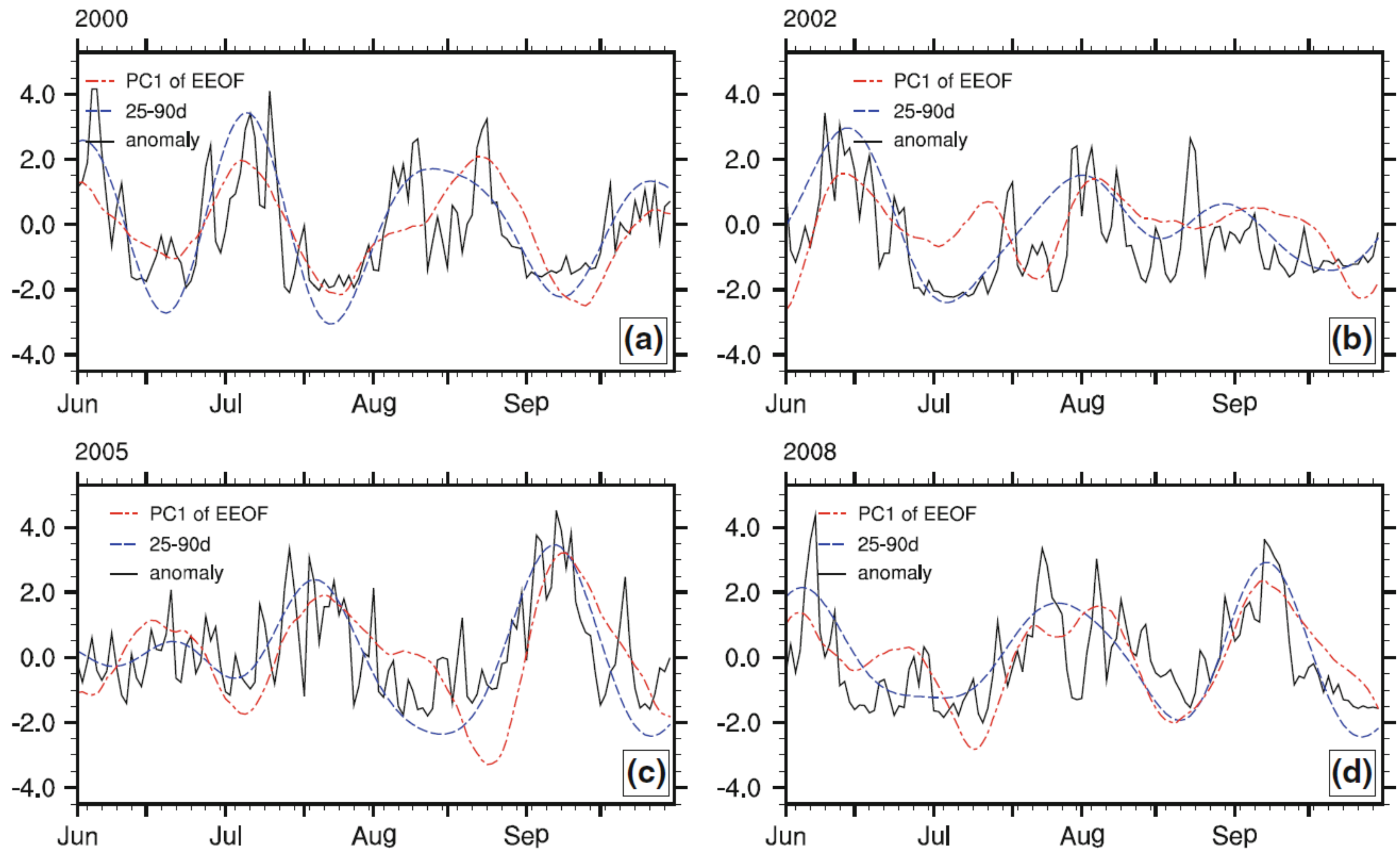

ig. 7 PC1 of EEOF analysis (*red dashed line*) compared with band-pass filtered (25–90 day, *blue dashed line*) and unfiltered (*black solid line*) ainfall anomalies averaged over the ISM domain (10.5°N–25.5°N, 70.5°E–85.5°E) for four different JJAS seasons

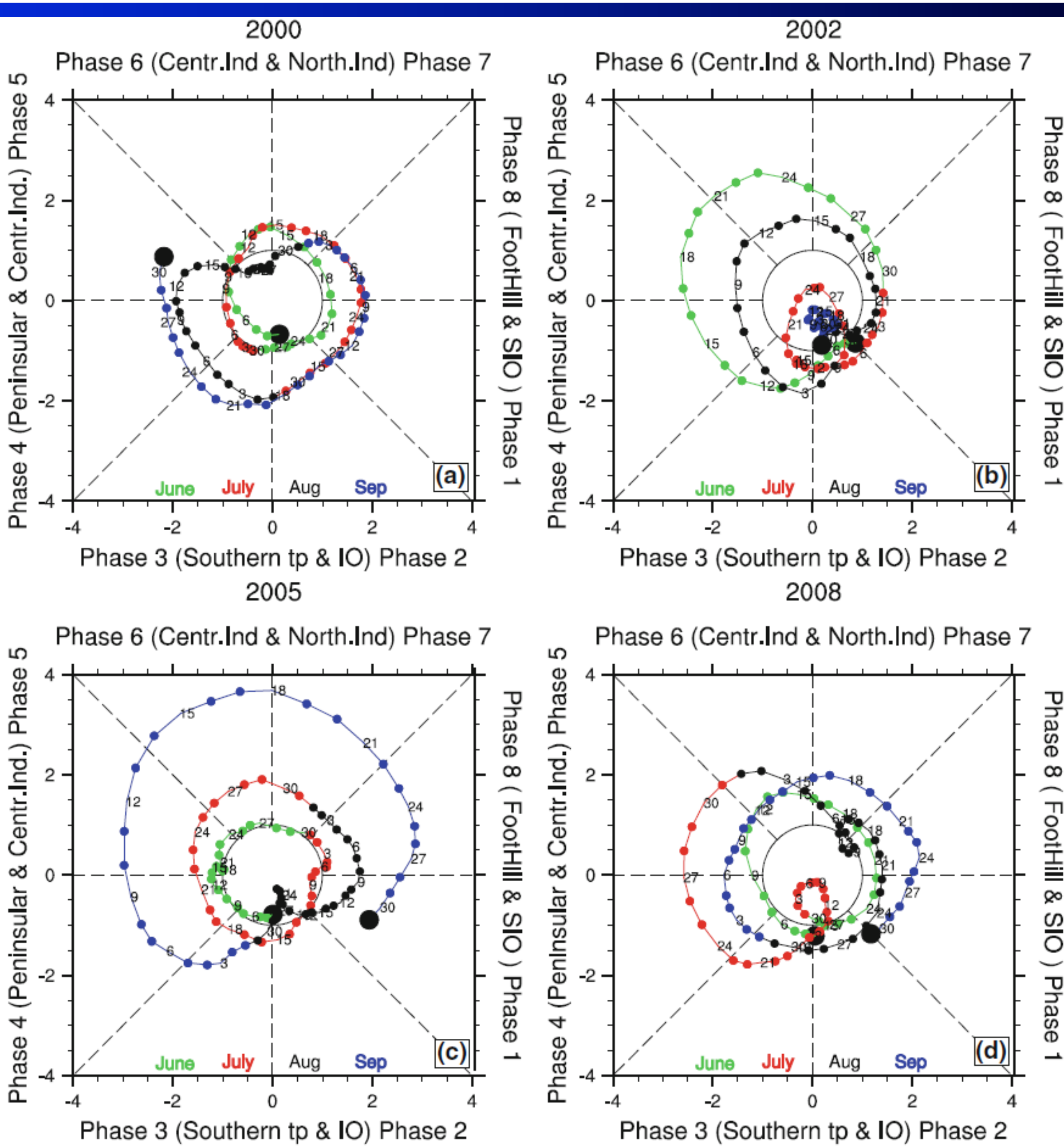

Fig. 8 The evolution of the MISO represented in the phase space constructed by the first two PCs of the EEOF analysis (MISO1 and MISO2) for four different JJAS seasons. The approximate locations of active phase of rainfall are denoted. A clockwise motion in the MISO phase space indicates northward propagation. The MISO indices are normalized with their corresponding standard deviation

Phase composite of precipitation anomaly

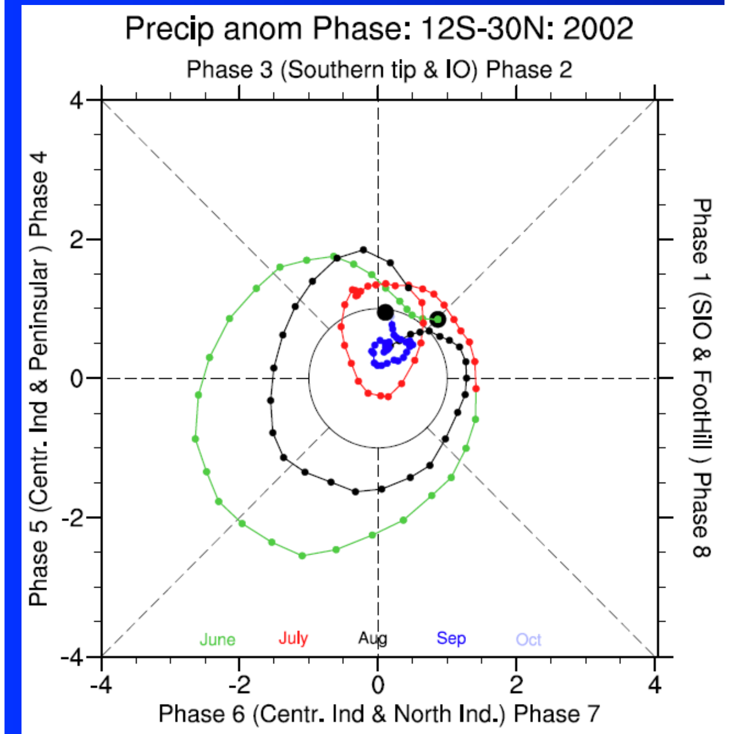

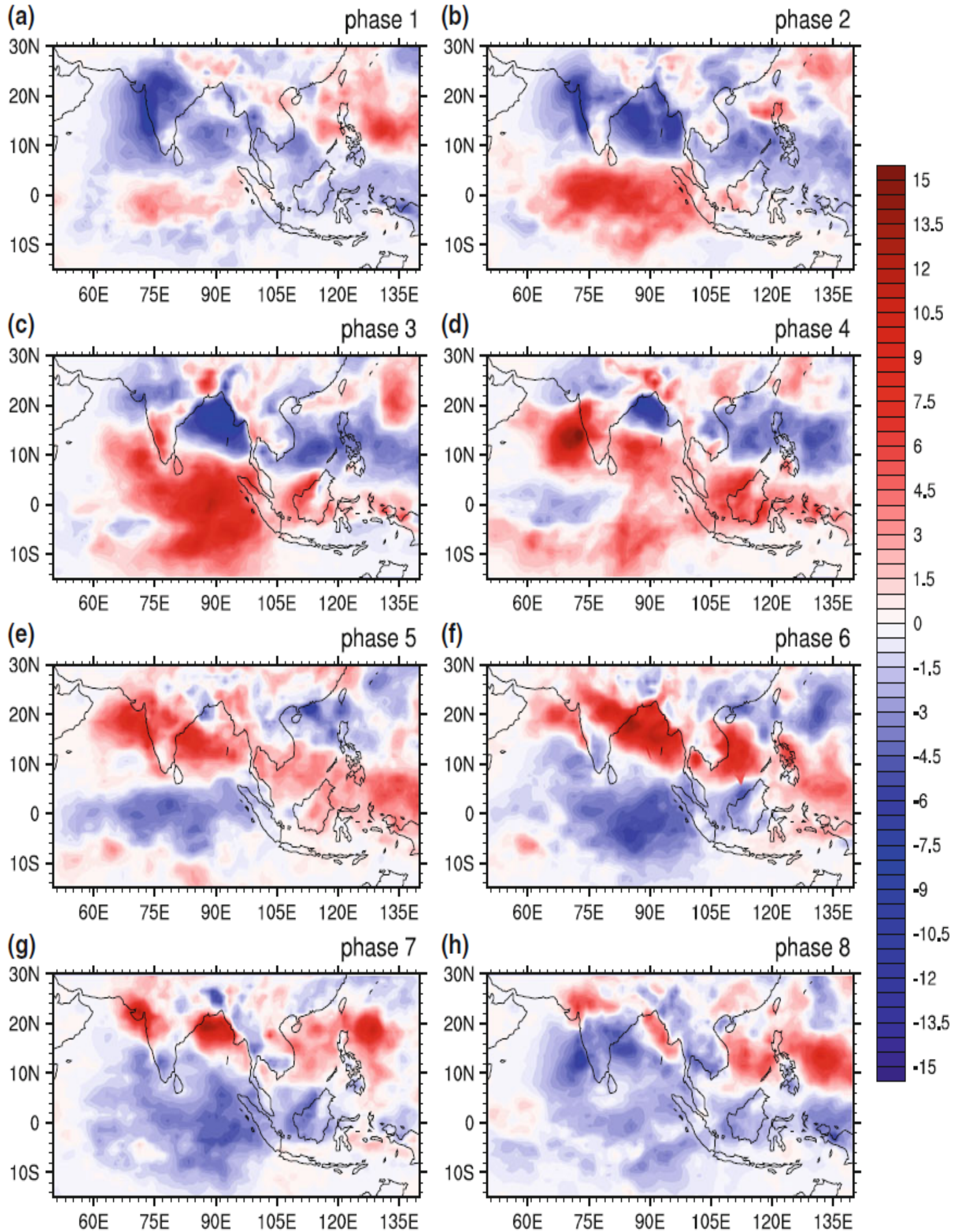

Fig. 10 Composite life cycle of the MISO during eight different phases identified from the MISO1 and MISO2 phase space. The composite is constructed from unfiltered rainfall anomalies (mm/day) for the 1997–2008 JJAS seasons

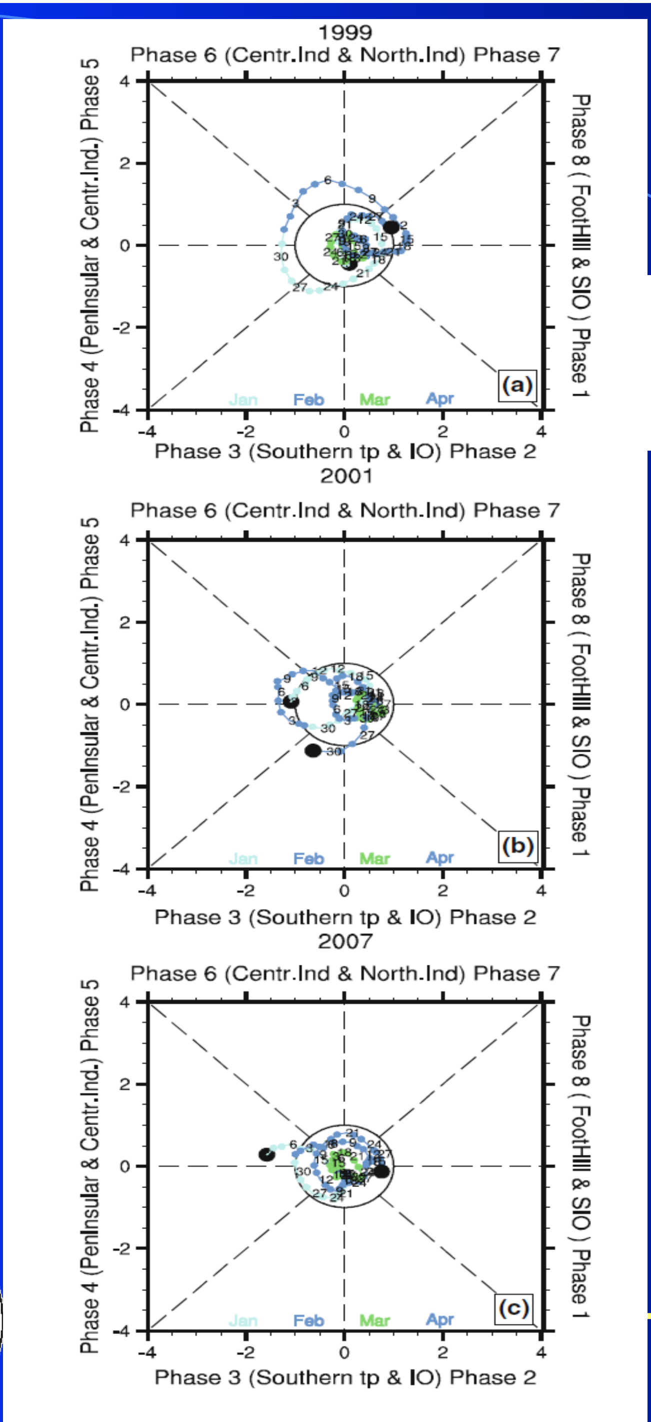

◀ Fig. 9 Same as Fig. 8 but for January, February, March and April months

During Boreal winter, the ISV does not project on the MISO.

Improvement of forecast skill of active-break spells of Asian summer monsoon in a coupled ocean-atmosphere model

B.N. Goswami[1], E. Suhas[2], J. M. Neena [3], A.K. Sahai[1], A. Suryachandra Rao[1], S. Abhilash[1], Arun Kumar[4]

[1]Indian Institute of Tropical Meteorology, Pune, India
[2]Scripps Institution of Oceanography, University of California San Diego, USA
[3]JIFRESSE-UCLA, Los Angeles, California, USA
[4]National Centre for Environmental Prediction, Washington, D.C., USA

Table 1: Description of the models and the forecast experiments.

No	Model	Model Details	Forecast Experiment
1	CFSv1 (NCEP Fully Coupled, Saha et.al. 2006)	Atmosphere: NCEP GFS(T62L64) Ocean: GFDL MOM3 Vertical levels - 40 Domain - 74°S to 64°N. Zonal resolution -1°. Meridional resolution - 1/3° between 10°S and 10°N, gradually increasing through the tropics until becoming fixed at 1° poleward of 30°S and 30°N. Prescribed sea ice.	A series of 45-day forecast integrations starting from 1st May to 29 September at 5 day intervals (total 31 starting dates in a season) for 7 years from 2001-2007 have been carried out in Prithvi HPC of IITM. The atmospheric initial conditions obtained from NCEP/DOE Reanalysis (R2) data (Kanamitsu et al. 2002), Ocean initial conditions from the NCEP Global Ocean Data Assimilation (GODAS) (Behringer and Xue , 2004). Each initial condition was perturbed to generate additional 10 members. Thus total 11 member integrations for each 31 start date were carried out for next 45 days.The ensemble mean corresponds to average of total 11 members.
2	CFSv2 (NCEP Fully Coupled, Saha et.al. 2011)	Atmosphere: NCEP GFS(T126L64) Ocean: GFDL MOM4 Vertical levels - 40 Domain - Global Horizontal resolution - 0.25 deg between 10S-10N and 0.5 deg towards poles. An interactive sea ice model included.	The data were downloaded from Climate Forecast System Reanalysis and Reforecast data available from NCDC website: http://nomads.ncdc.noaa.gov/. The 45 day forecasts from every 0Z, 6Z, 12Z and 18Z cycle over a period of 10 years (2000-2009) carried out at NCEP with CFSv.2 are used. 11 member ensembles were created with initial conditions every 5 days in the following way, e.g, for 31st May start date: 45 days integrations for 00Zof 31st May, 18Z,12Z, 06Z and 00Z of 30th May, 18Z, 12Z, 06Z and 00Z of 29th May and 18Z, 12Z of 28th May. The forecast valid from 31st May to next 40 days were considered from all the members.

Forecast skill of CFS

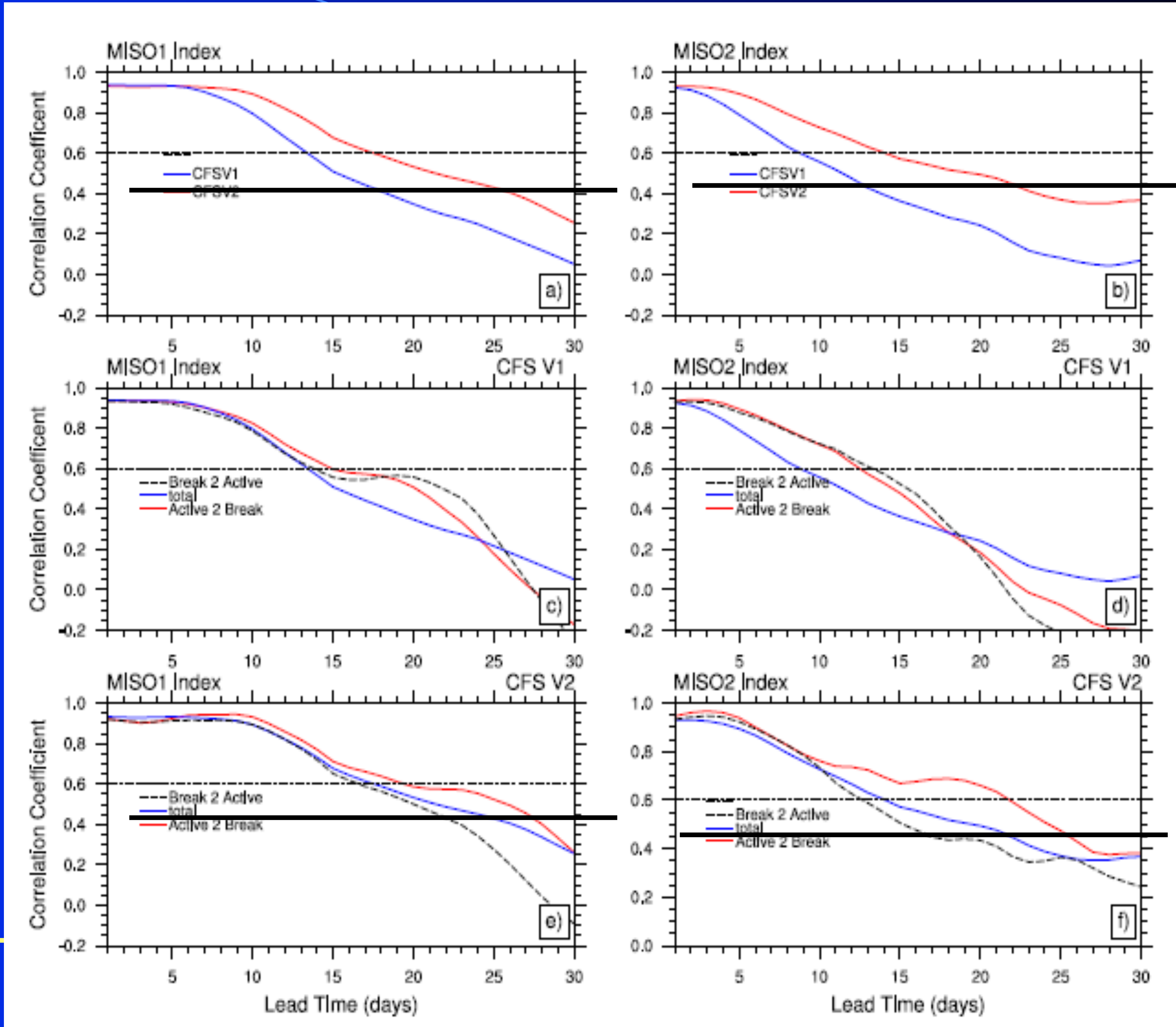

EEOF1 of GPCP, CFSv1 and CFSv2

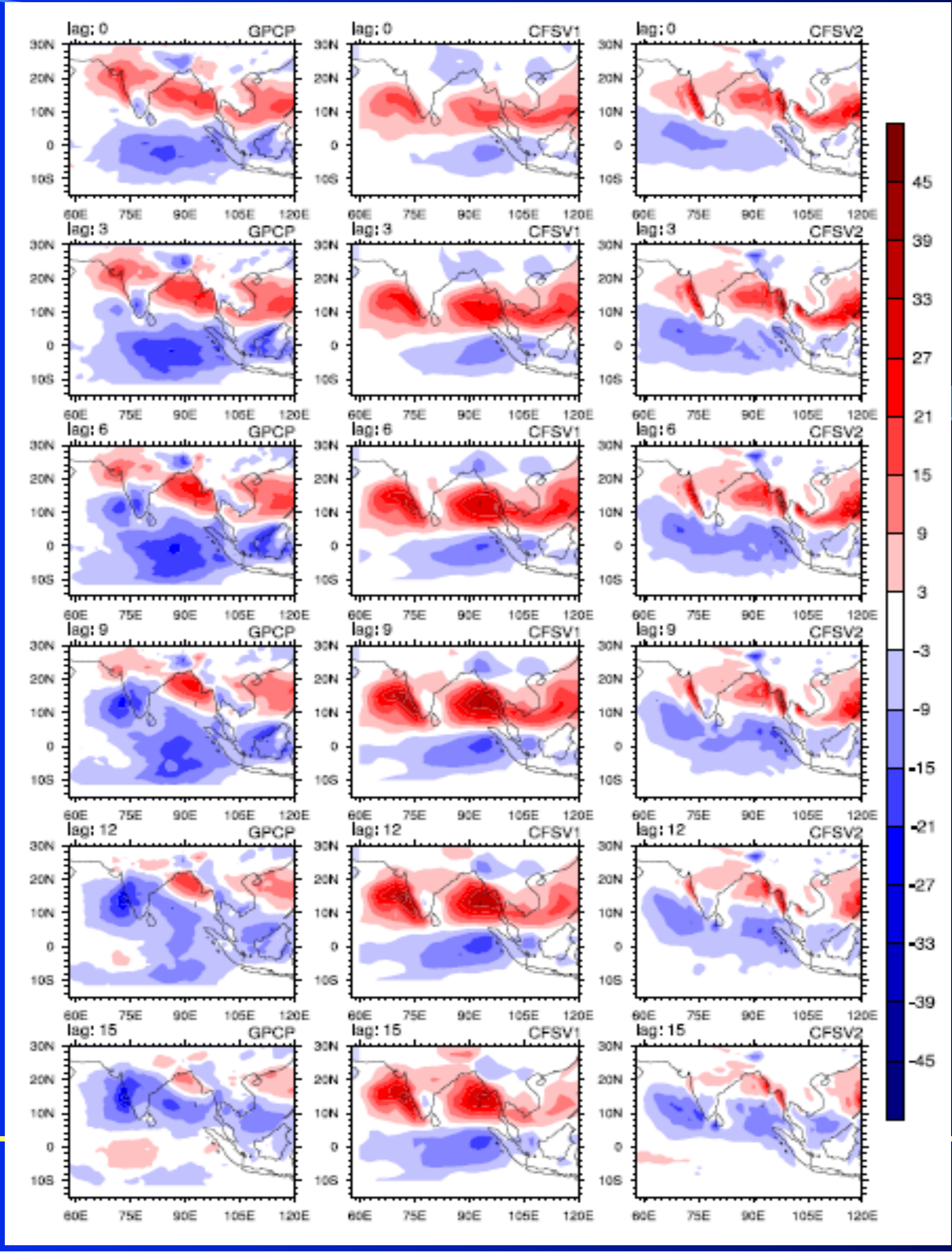

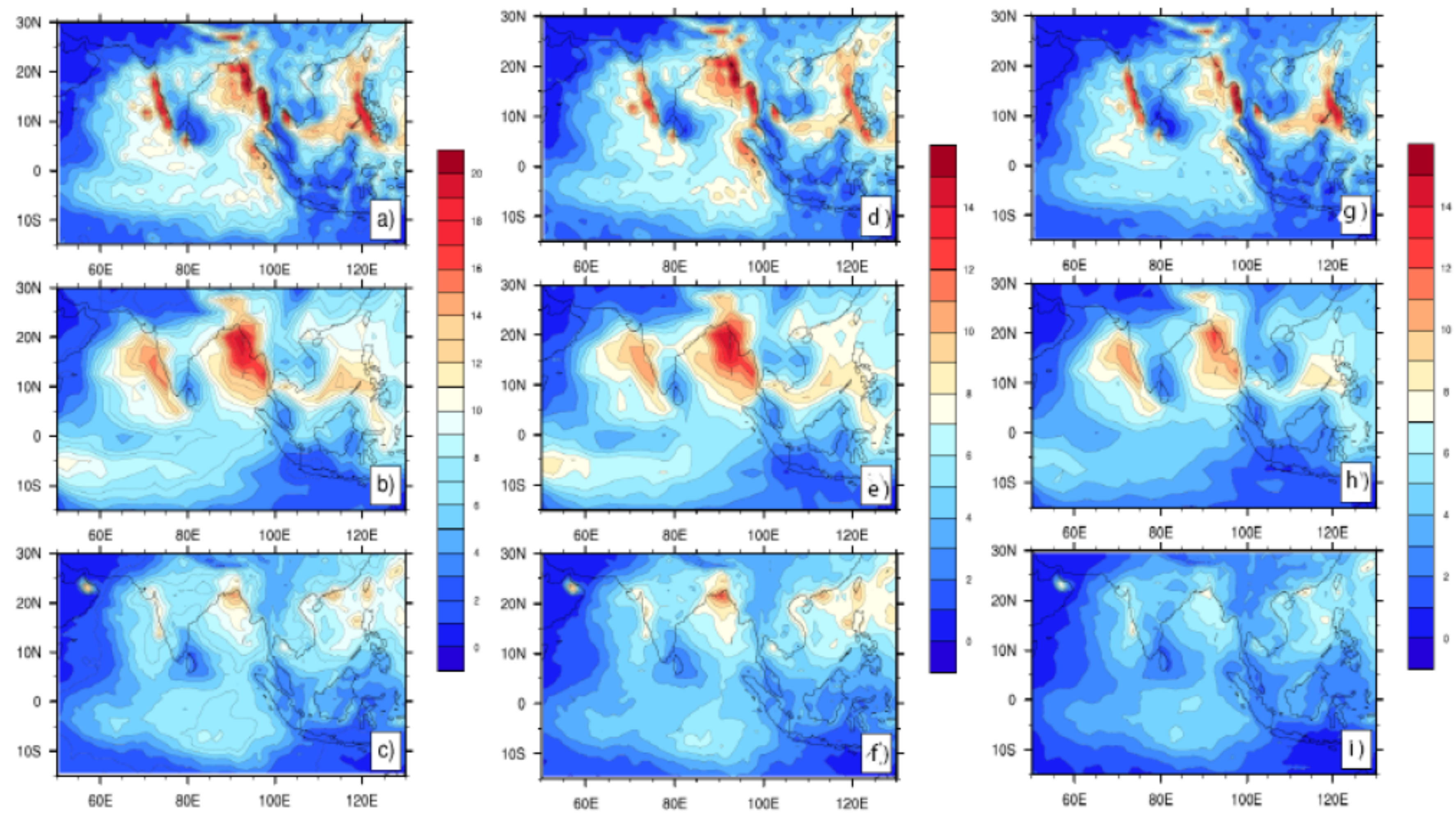

Figure 5: Variance of rainfall during June-September in the intraseasonal time scale in observation compared with simulated variance in the same time scales by the two versions of the model. Variance from observation, of 10-90 filtered anomalies from (a) CFSv.2 , (b) CFSv.1 and (c) GPCP. (d)-(f) are same as (a)-(c) but for 10-25 day filtered anomalies and (g)-(i) are same as (a)-c) but for 25-90 day filtered anomalies.

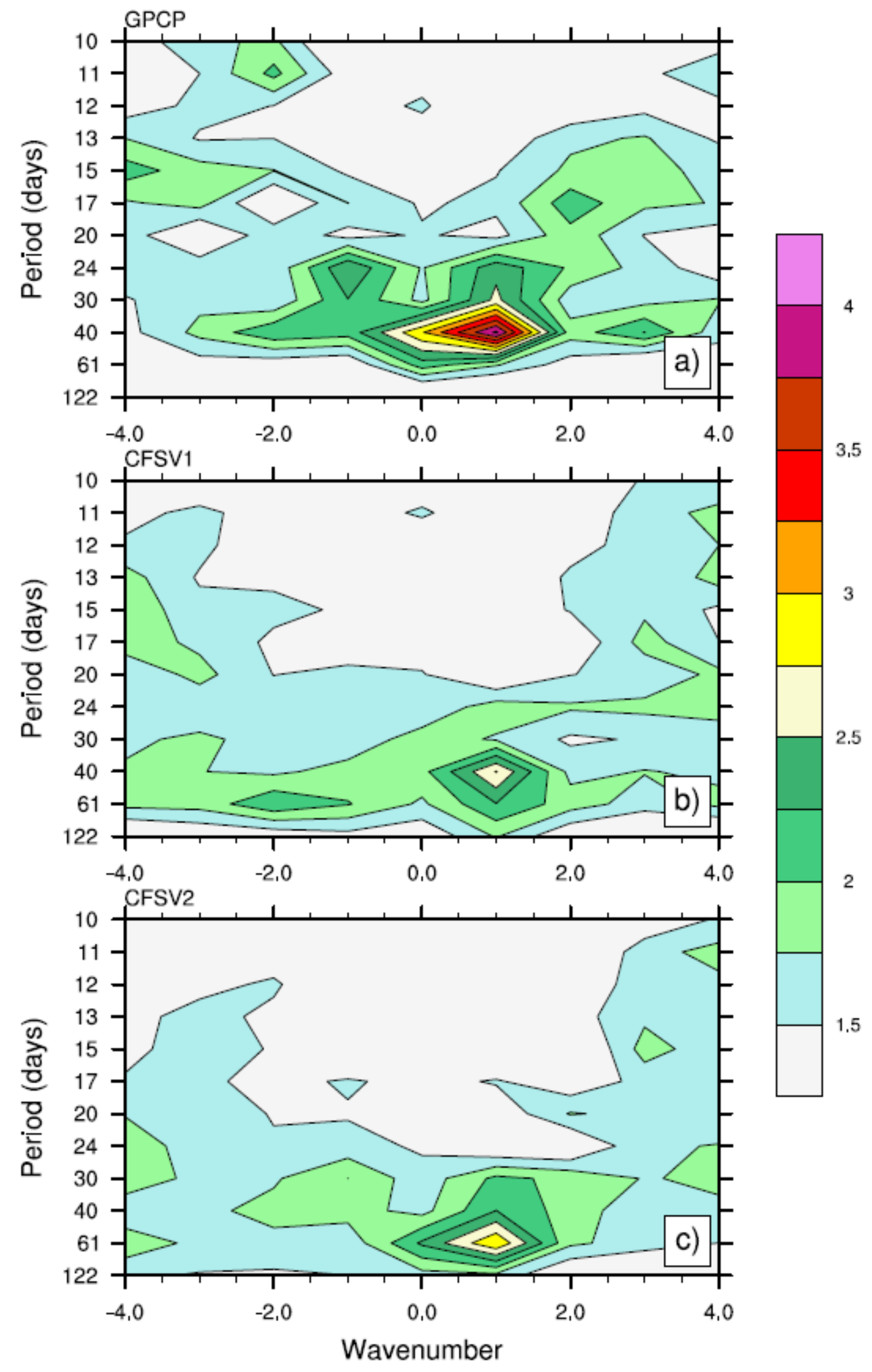

Northward propagating space-time spectra of precipitation in
a) GPCP
b) CFSv.1
c) CFSv.2

IITM MISO Forecast System and R & D to improve the skill of MISO forecasts

Atmospheric and oceanic initial conditions	**obtained from National Climate Data Centres (NCDC) NOAA Operational Model Archive and Distribution System (NOMADS) online model data server.**

Model	Resolution	Forecast Lead	Hindcast period
CFSv2	T126~100km	45 days -11-Member ensemble	2001-2012 (28 Start dates in one year during monsoon season)
CFSv2	T382~38km	45 days -11 member ensemble	2001-2012 (28 Start dates in one year during monsoon season)
GFS	-do-	45 days	-do-
GFSbc (Forced by Bias corrected CFSv2 SST)	-do-	45 days	-do-

Variable	Dataset	Reference
Precipitation	IMD	Rajeevan et al. 2006
	TRMM-merged	Mitra et al., 2003
Reanalysis Data	NCEP Reanalysis data	Kalney et. al 1996
SST	OISST	http://www.ncdc.noaa.gov/sst/

Hindcast Statistics

CFSv2 T126/T382
vs
GFSbc

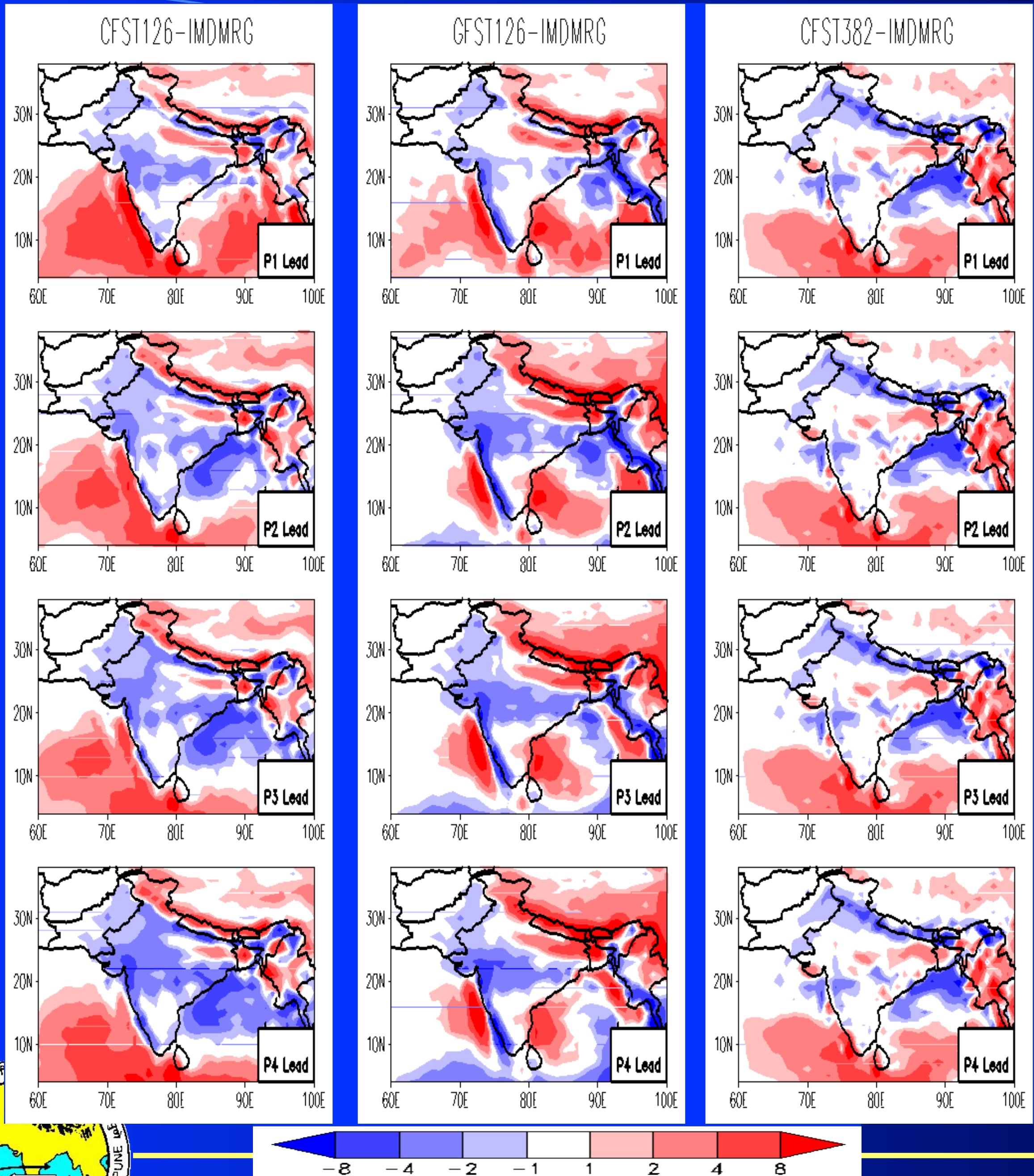

T382 Seasonal Climatology Has improved

CC & RMSE For T126, T382 & GFSbc Over MZI

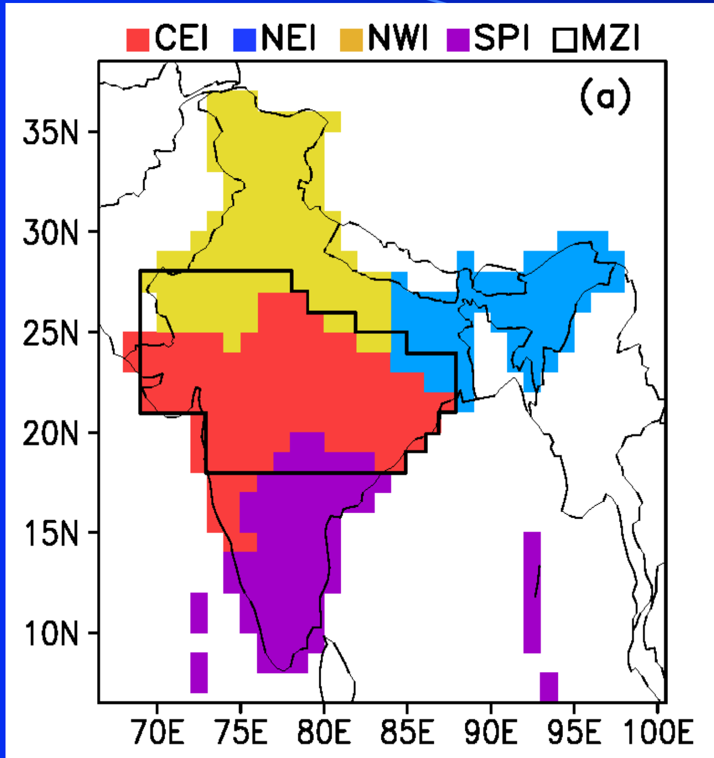

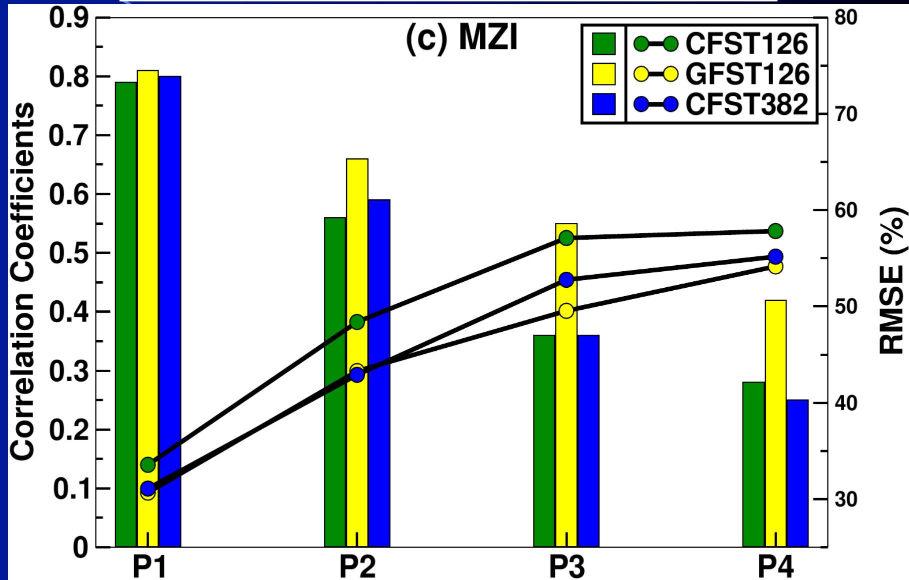

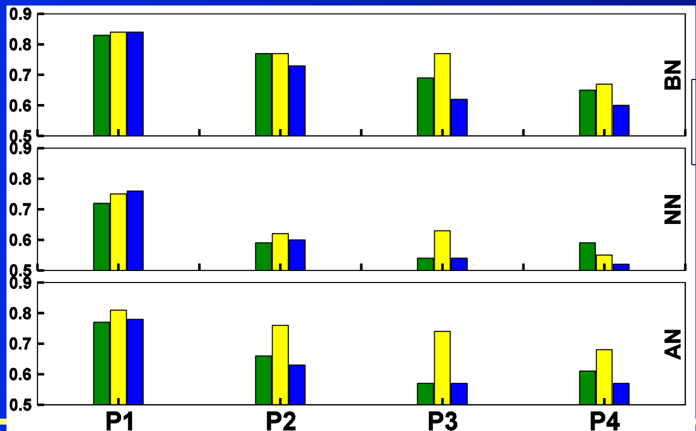

ROC Area Under Curve for Forecasted categories For MZI

MISO

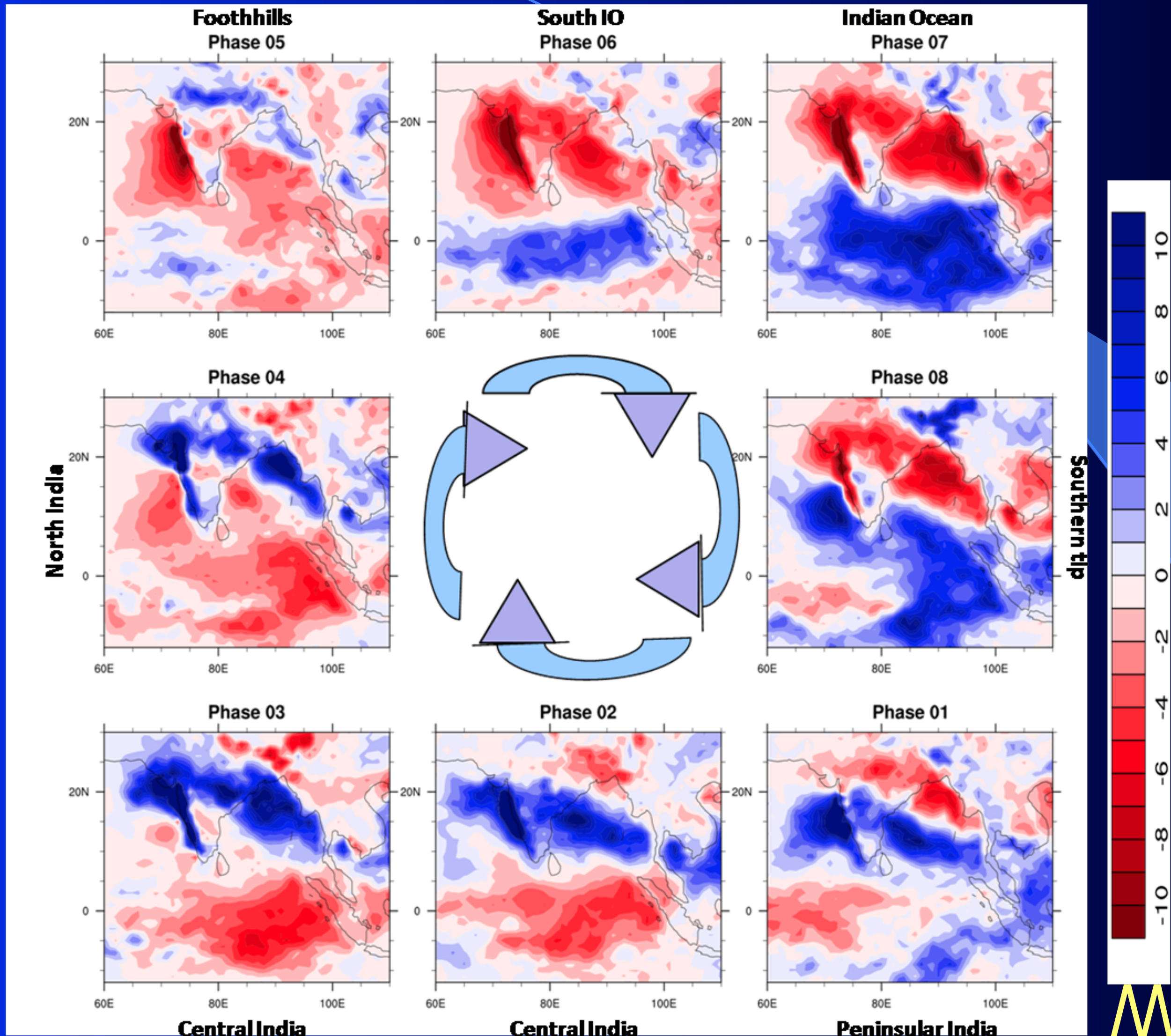

Foothhills
Phase 05
South IO
Phase 06
Indian Ocean
Phase 07
Phase 04
Phase 08
Phase 03
Phase 02
Phase 01
North India
Southern tip
Central India
Central India
Peninsular India
20N
0
60E
80E
100E
10
8
6
4
2
0
-2
-4
-6
-8
-10

Monitoring for 2007 and 2009

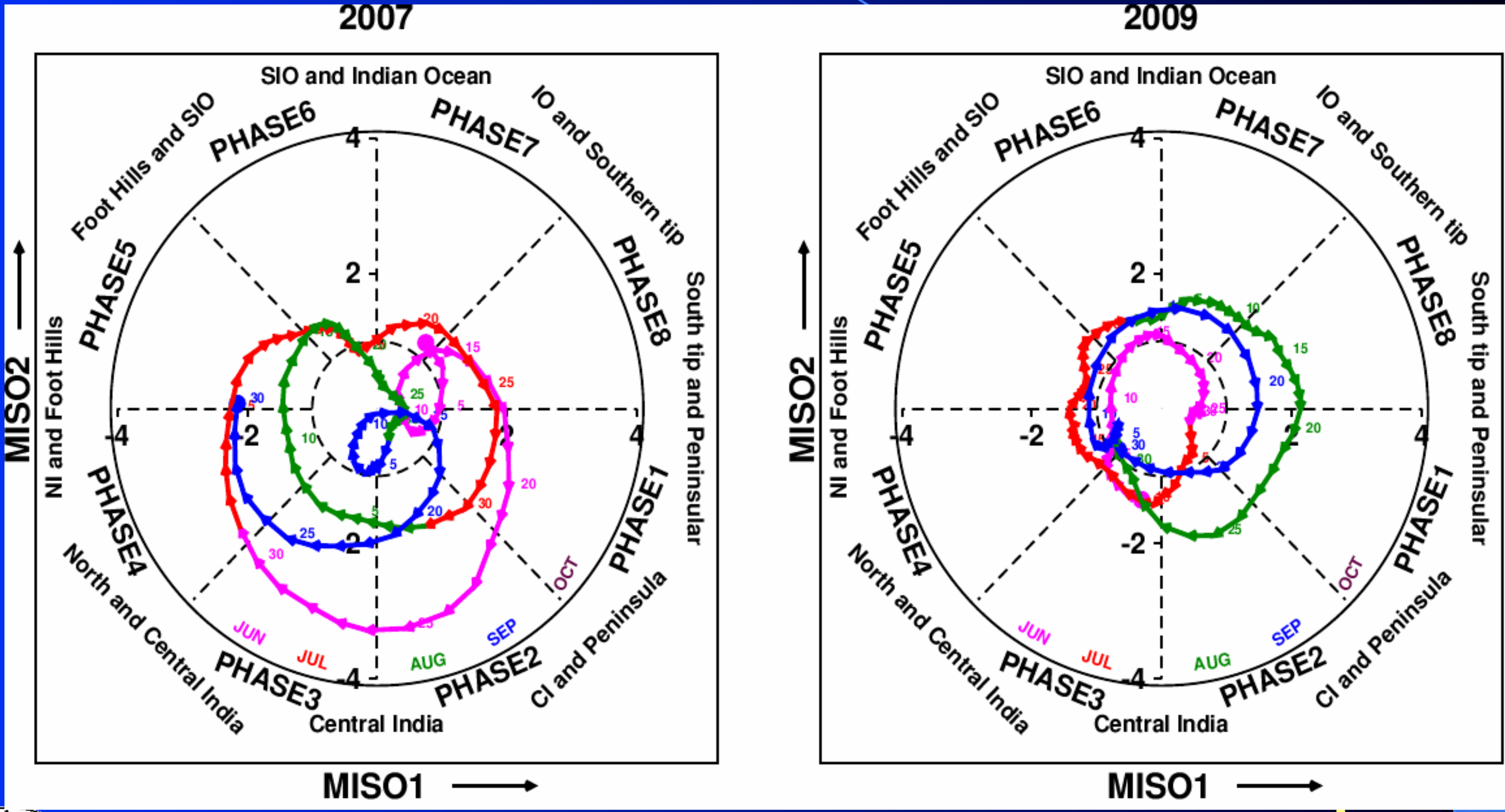

Skill in predicting MISO Indices

(CC between predicted and observed MISO indices)

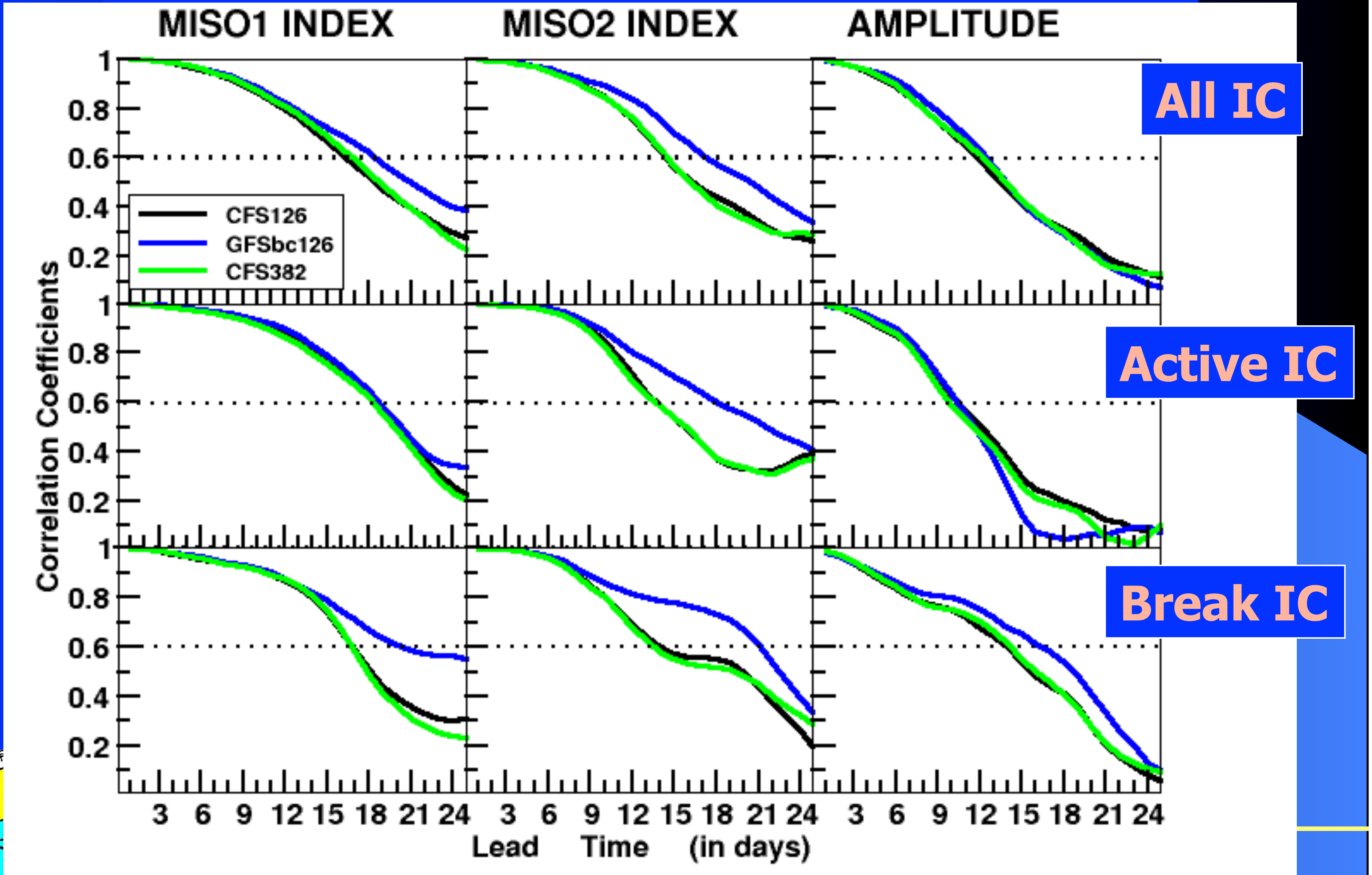

Predicted and observed rainfall anomalies and probabilities for three categories over monsoon zone During 2011

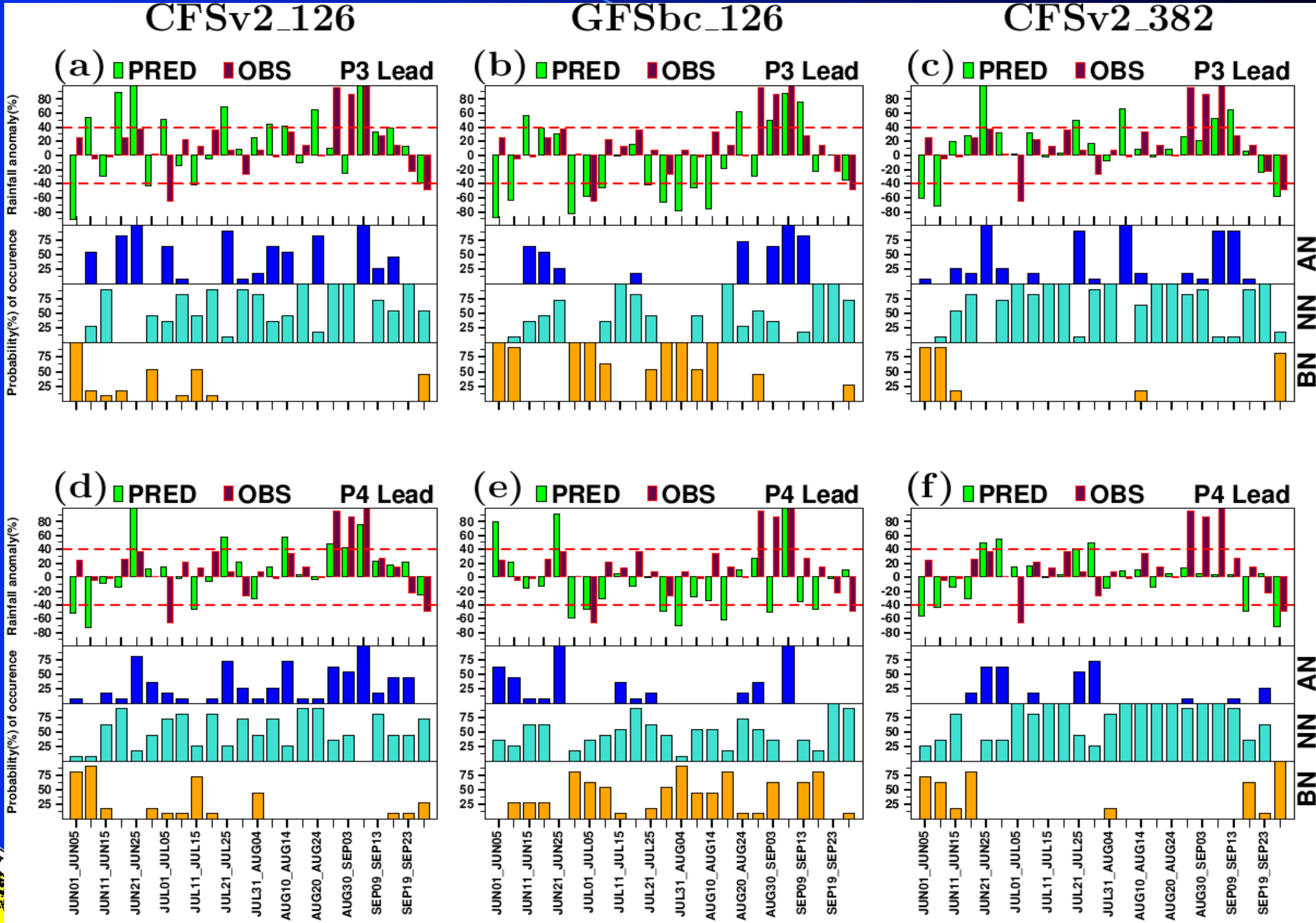

Outcome of the experiments

Bias Correction as well as High Resolution

- The dry bias over the Indian land region slightly reduced in all lead pentads in the bias corrected GFSv2 compared to CFSv2T126. While T382 run exhibit large reduction in climatological biases … But no significant operational usefulness of CFST382 forecast over T126 forecast of MISO.
- The pentad lead prediction skill of ensemble mean deterministic and probabilistic forecasts from GFSv2bc is significantly higher than CFSv2, both T126 and T382, for all lead pentads.
- GFSv2bc is superior to CFSv2 in predicting large-scale low-frequency components of MISO and is clearly an artifact of correcting the SST bias. Biases are similar in T126 and T382 resolutions.
- The real-time dissemination of extended range (~3 weeks) forecast in the high resolution NCEP CFSv2 framework could be a challenging task for the operational forecasters, owing to time constraints and computational management.

… contd

Inter-annual variation in skill of individual models

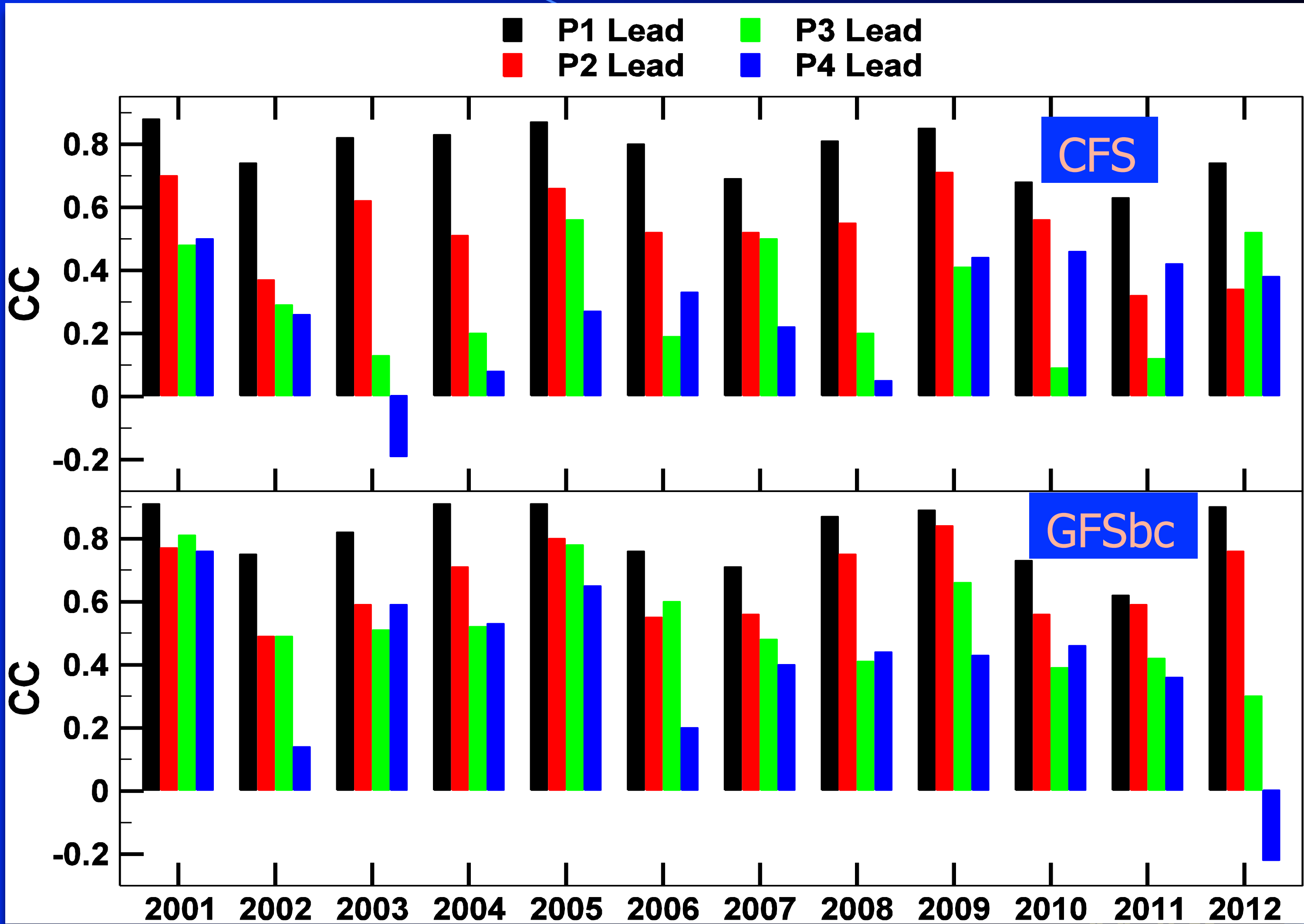

As far as Users concerned, Forecast consensus is very much Important

Generation of Multi-model Ensemble (MME) Forecasts Using CFST126, CFST382 and GFSbc

CFS Grand Ensemble Prediction System (CGEPS)

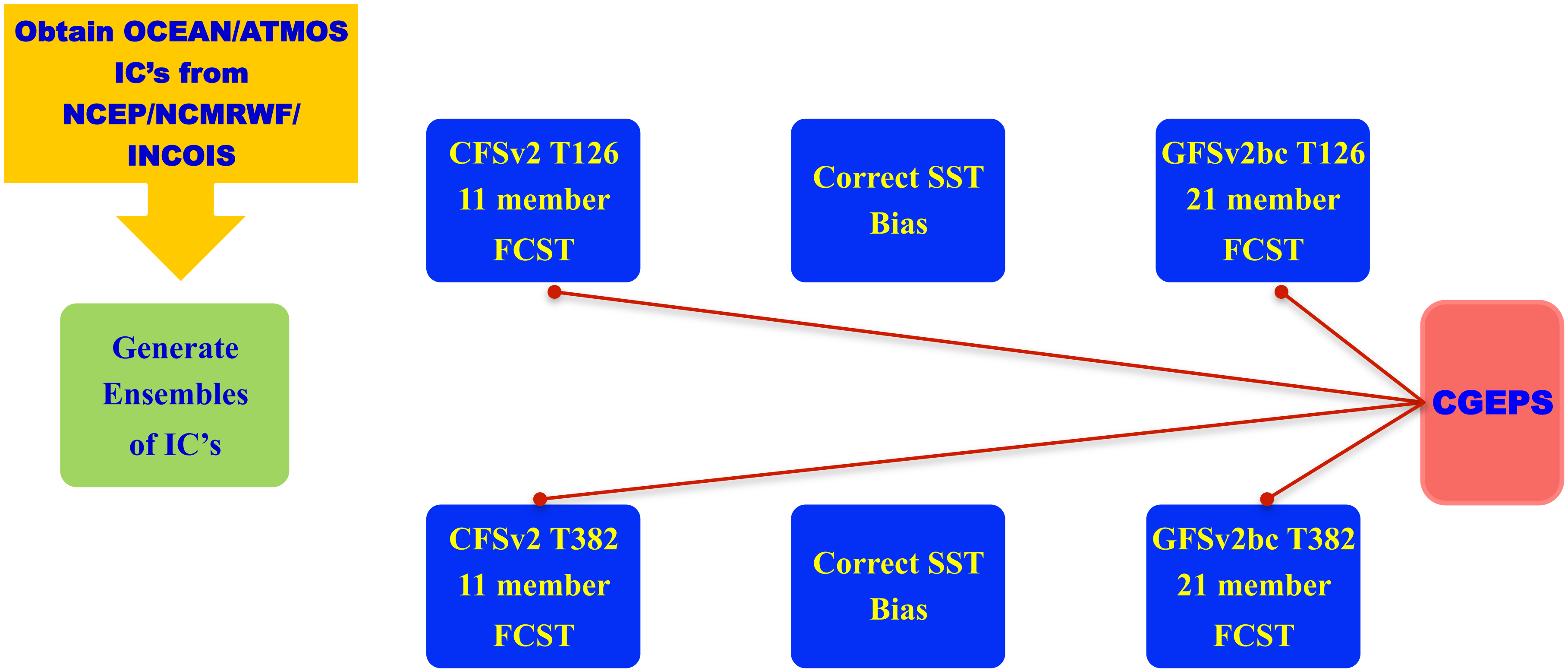

Preliminary results from MME:

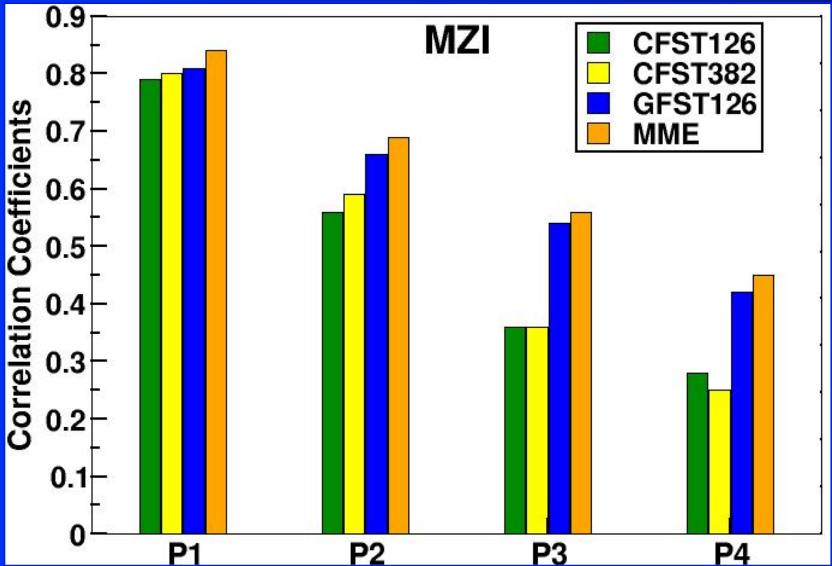

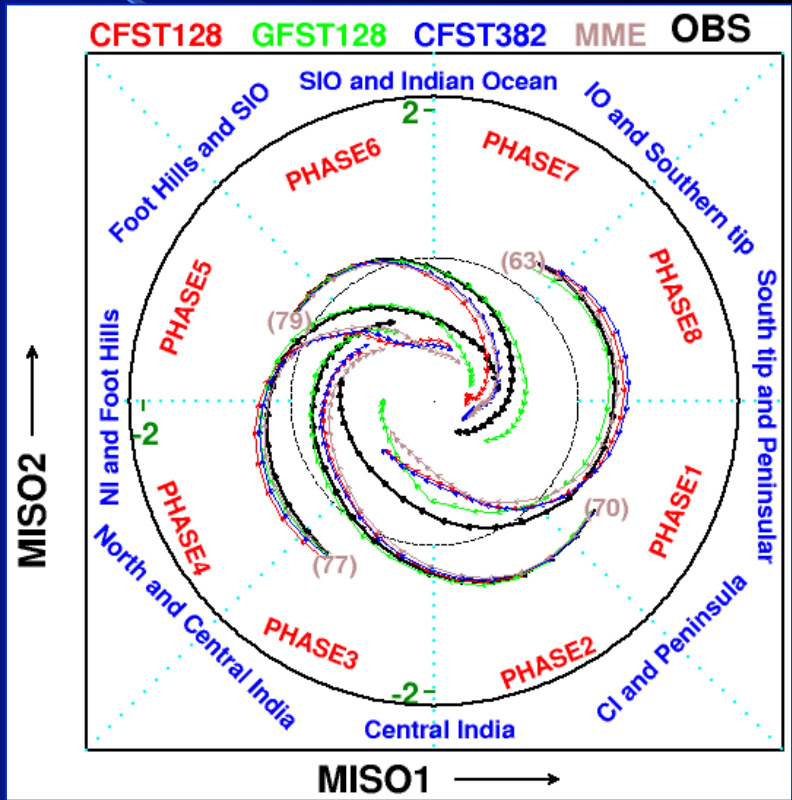

Real time prediction strategy
&
Skill of real time predictions

Strategy: Ensemble Prediction using CFSv2

- Ocean and Atmospheric Initial conditions (IC) are obtained from NCEP.
- Technique was developed to perturb ICs to generate 11 members. (Abhilash et al., 2013)
- Model has been integrated at low resolution (T126, ~100km, termed as CFS126 hereafter; Abhilash et al. 2014) and high resolution (T382, ~38km, termed as CFS382 hereafter; Sahai et al. 2014) for 45 days for each 11 ICs at five day intervals starting from 16th May (Eg: 16 May, 21 May, 26 May, 31 May, 05 Jun........etc). Climatology has been calculated from 10-year hindcast.
- Bias correction in daily forecasted SST from CFS126 for each lead time has been done by removing the daily mean bias for corresponding lead time (model climatology-observed climatology) from forecasted daily SST (Sahai et al., 2013; Abhilash et al., 2013). This model is hereafter termed as GFSbc.

Generation of CGEPS

- **In the formulation of MME from CGEPS, 21 ensembles of GFSbc, 11 ensembles of CFS126 and 11 ensembles of CFS382 have been used (Abhilash et al. 2014, submitted).**
- **Hence, total 43 ensemble members were produced independently from 3 variants of CFS model to generate the CGEPS and forecast consensus is done by making simple average among the members.**

Daily evolution of rainfall and wind at 850hPa

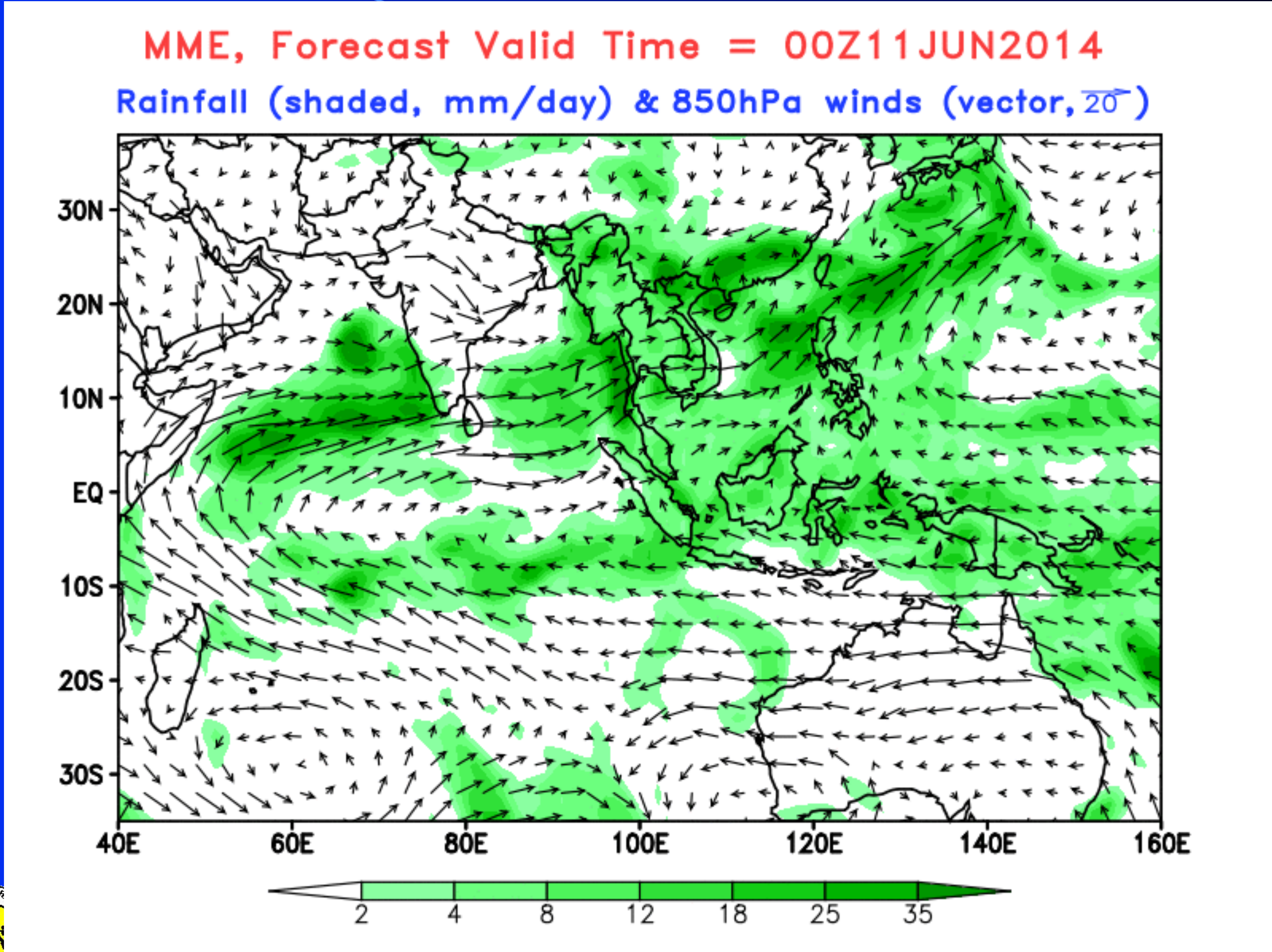

Forecast Verification 2013

Chief features:

1. Monsoon Onset
2. Rapid advancement
3. Extreme events
4. Delayed withdrawal

Rapid advancement of monsoon was well-predicted from 5 Jun IC

Wind (850hPa) and Rainfall

NCEP/TRMM Analysis

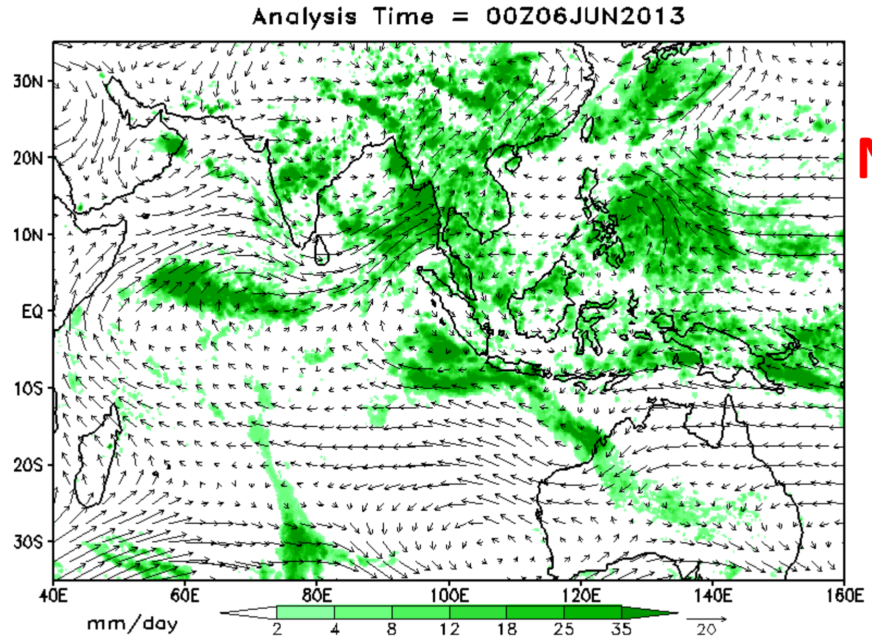

CFSv2

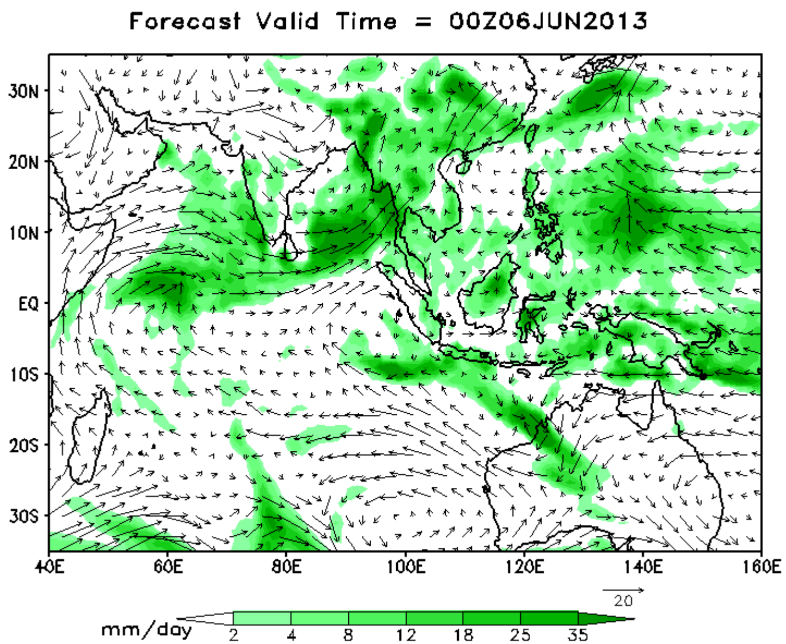

GFSbc

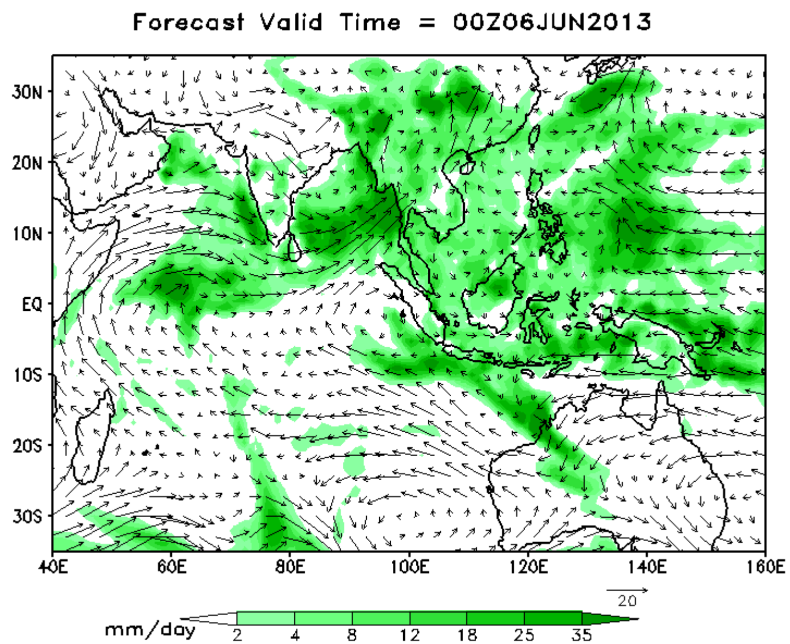

Uttarakhand Heavy Rainfall event is captured 10-12 days in advance from 05 June Initial Condition

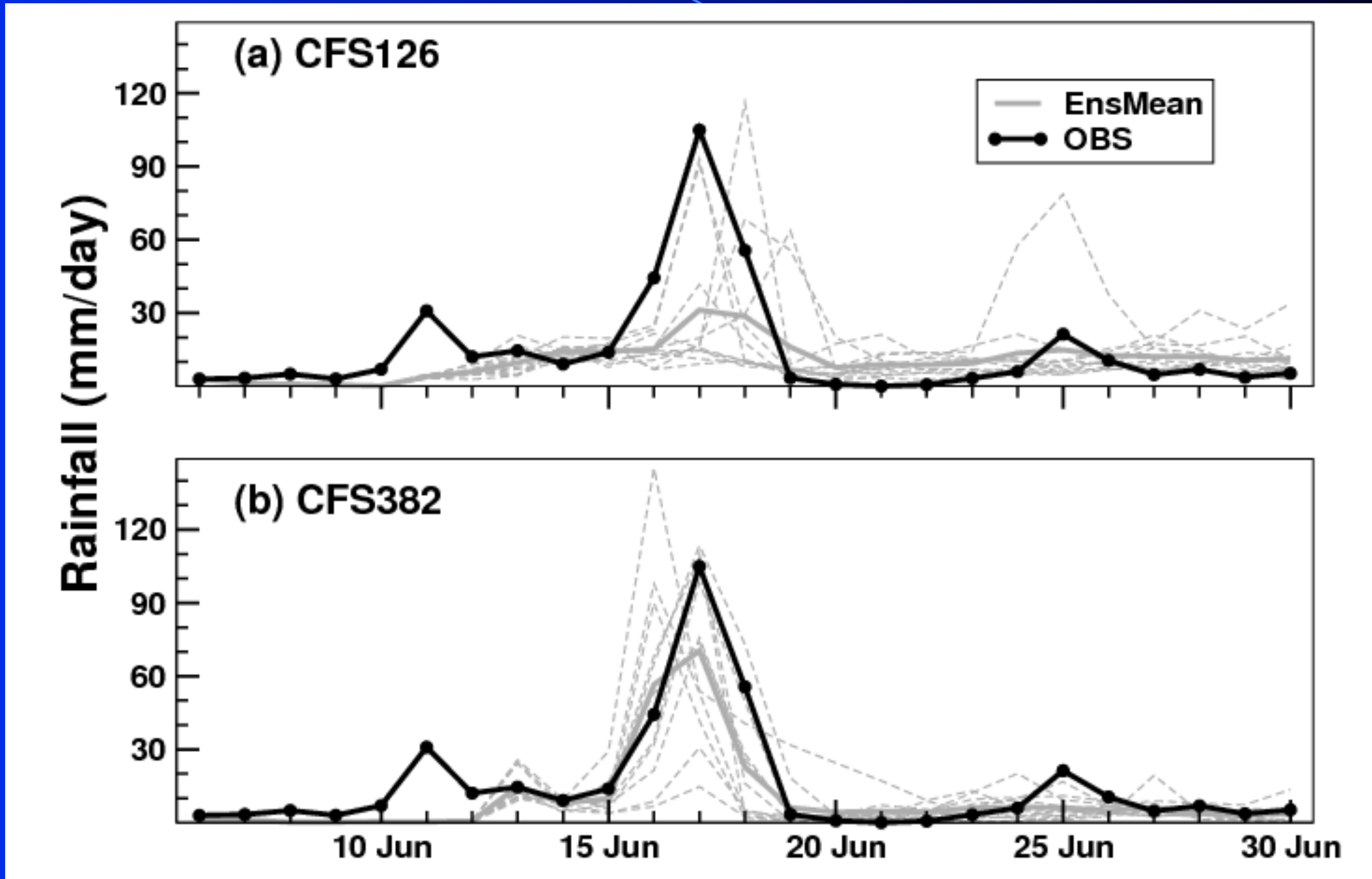

Revival of monsoon was well predicted from 08 September IC, which helped IMD in declaring the withdrawal of monsoon

CFST126

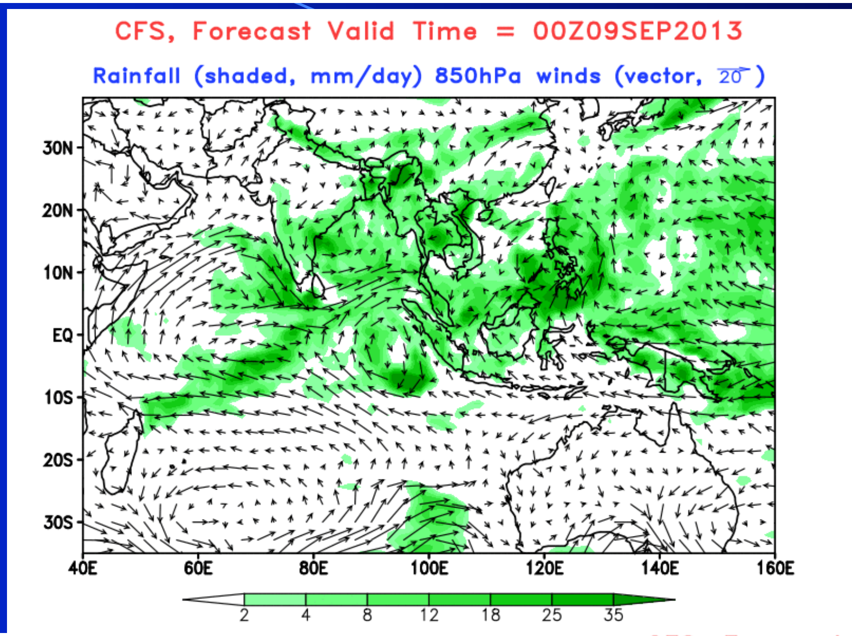

GFSbc

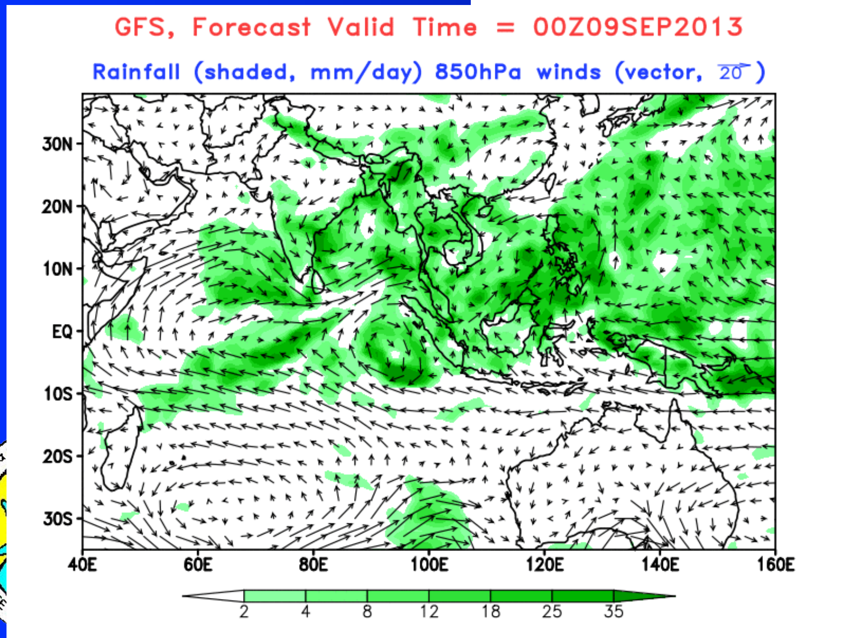

CFST382

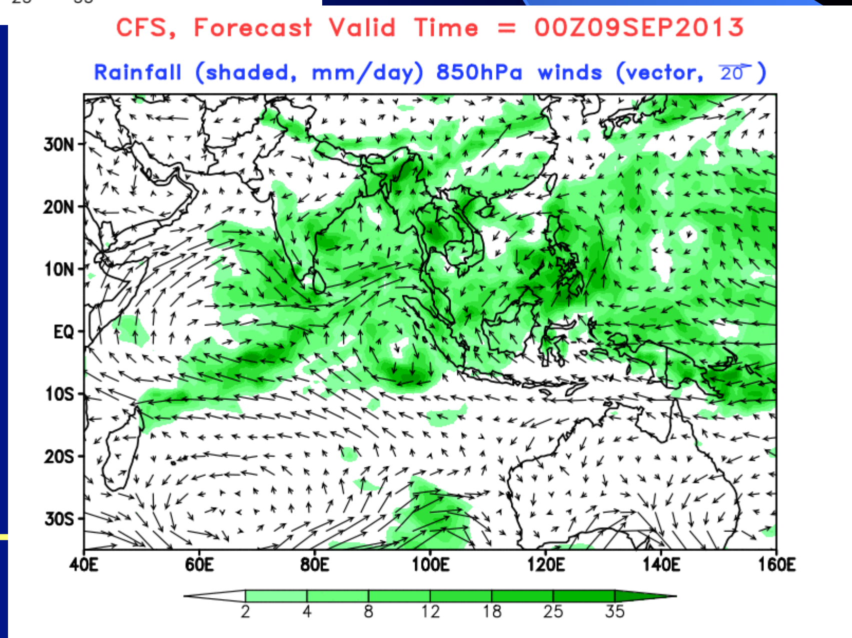

CFS, CEI

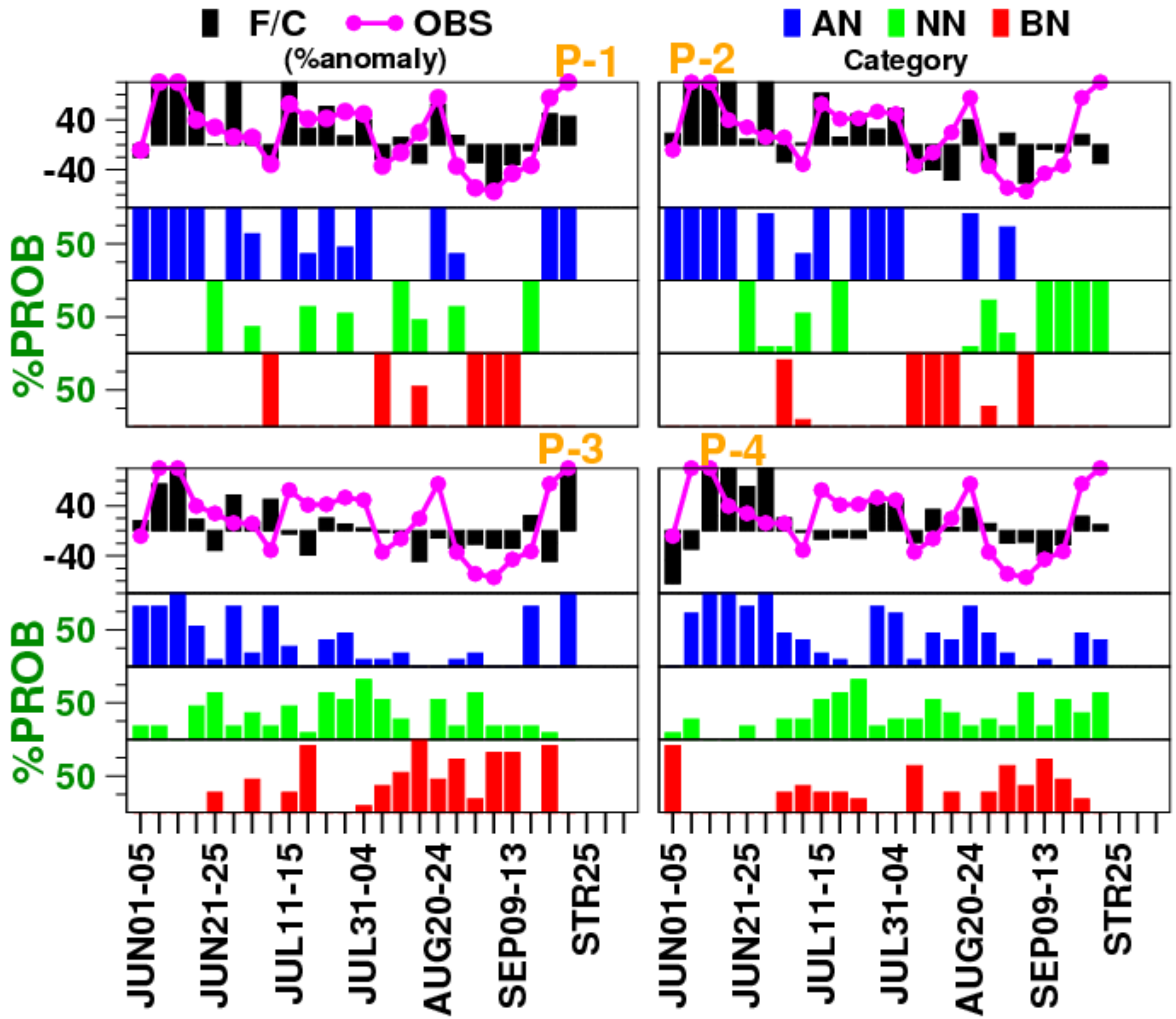
F/C
OBS
(%anomaly)
AN
NN
BN
Category
P-1
P-2
P-3
P-4
40
-40
50
%PROB
JUN01-05
JUN21-25
JUL11-15
JUL31-04
AUG20-24
SEP09-13
STR25

GFSbc, CEI

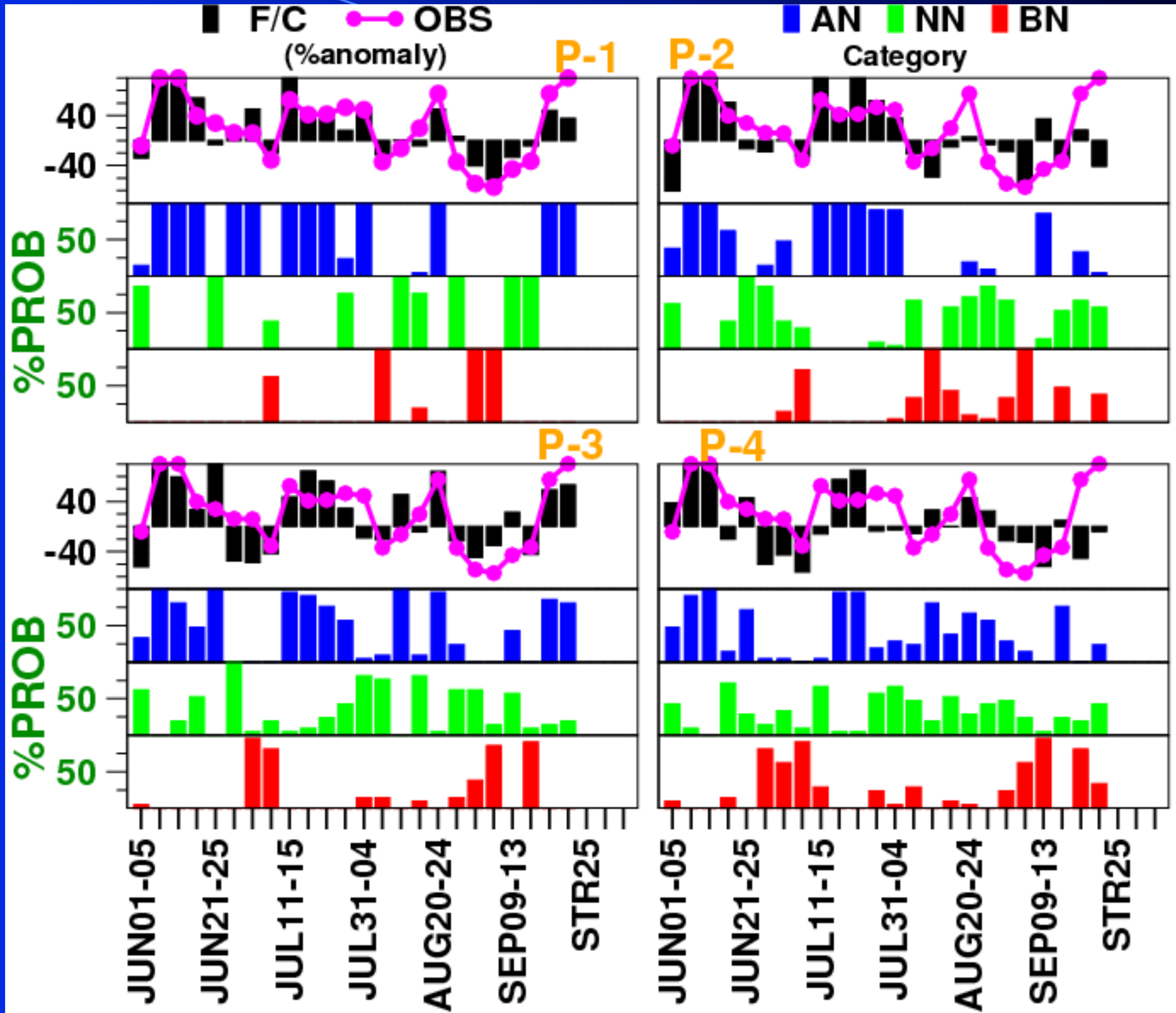

F/C
OBS
(%anomaly)
AN
NN
BN
Category
P-1
P-2
P-3
P-4
40
-40
50
%PROB
JUN01-05
JUN21-25
JUL11-15
JUL31-04
AUG20-24
SEP09-13
STR25

Observed and Predicted percentage anomalies are shown for 2013 over Monsoon Zone

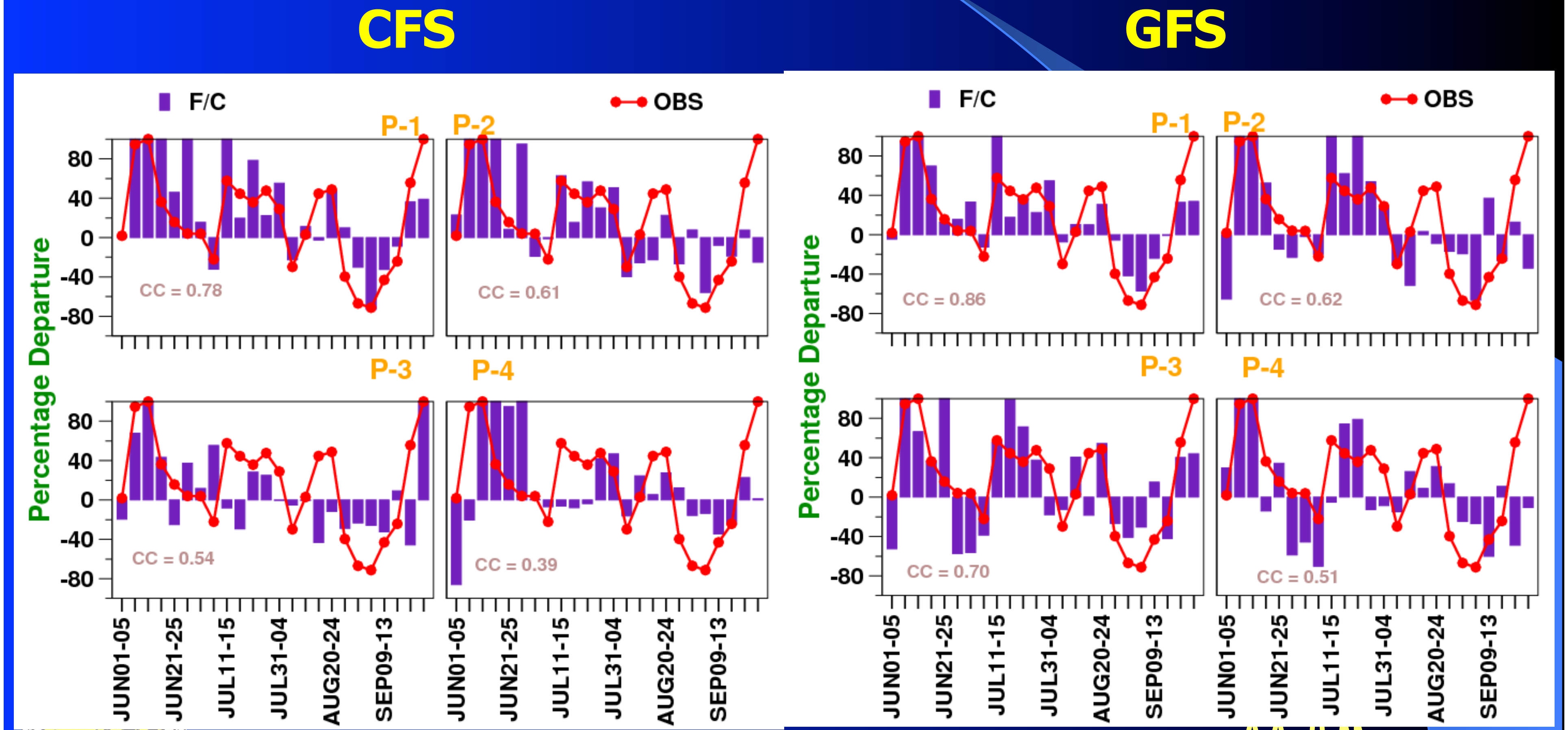

Monitoring of MISO and verification

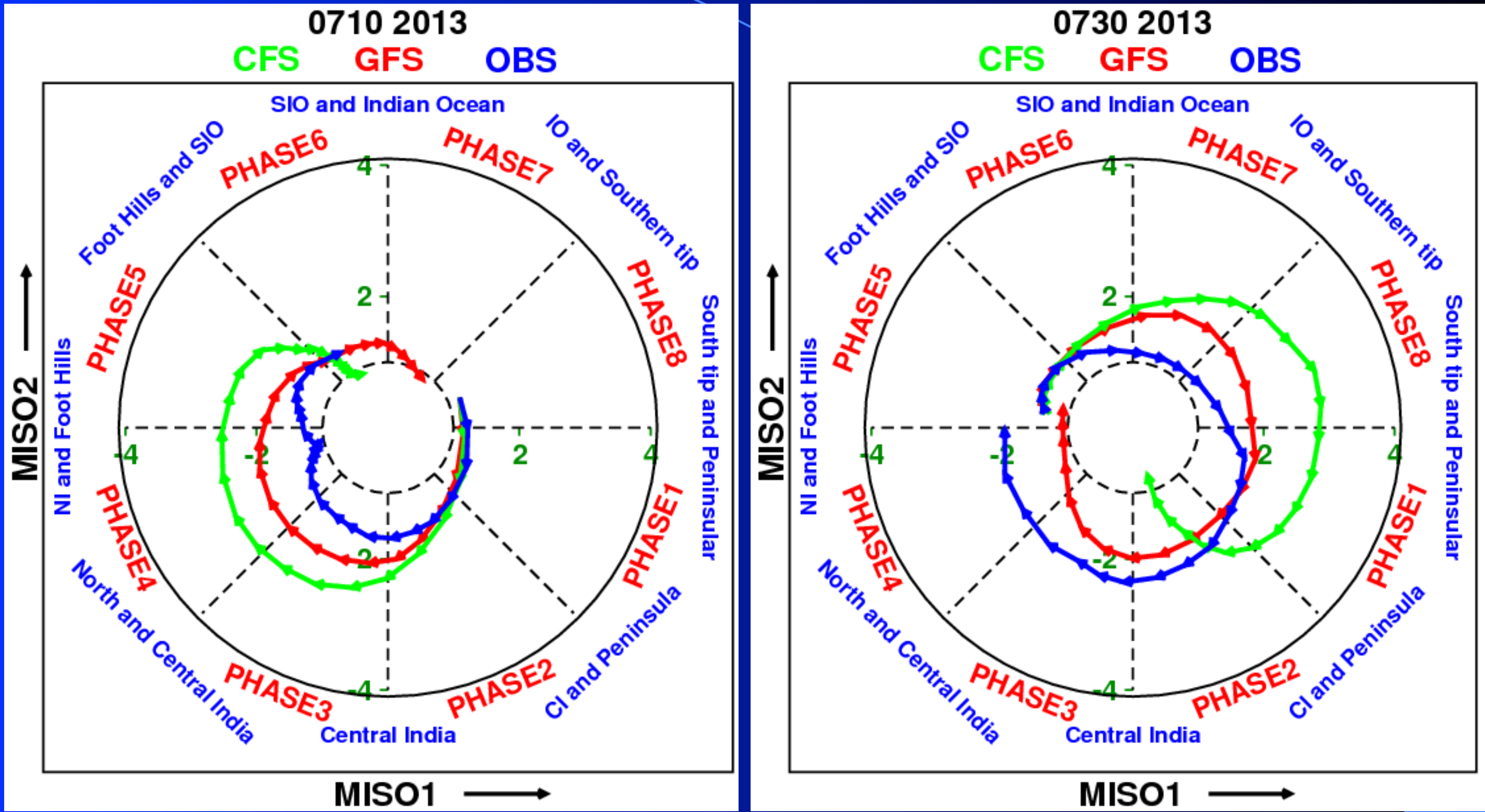

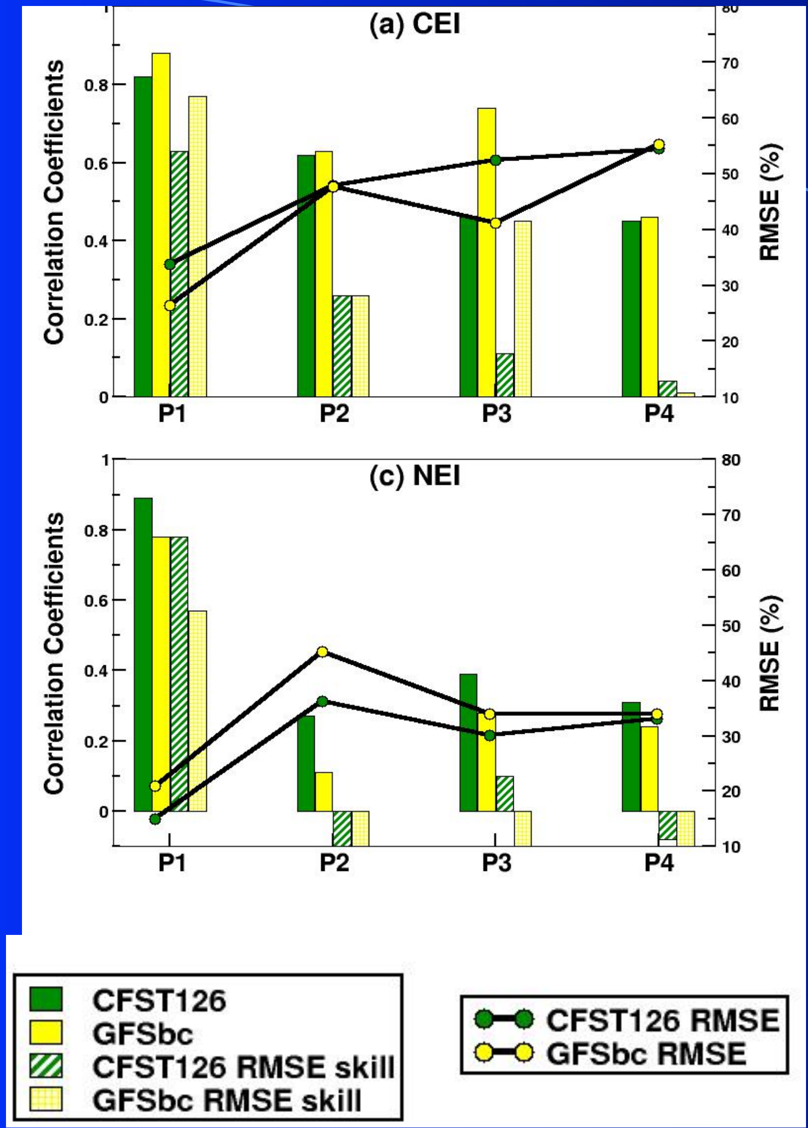

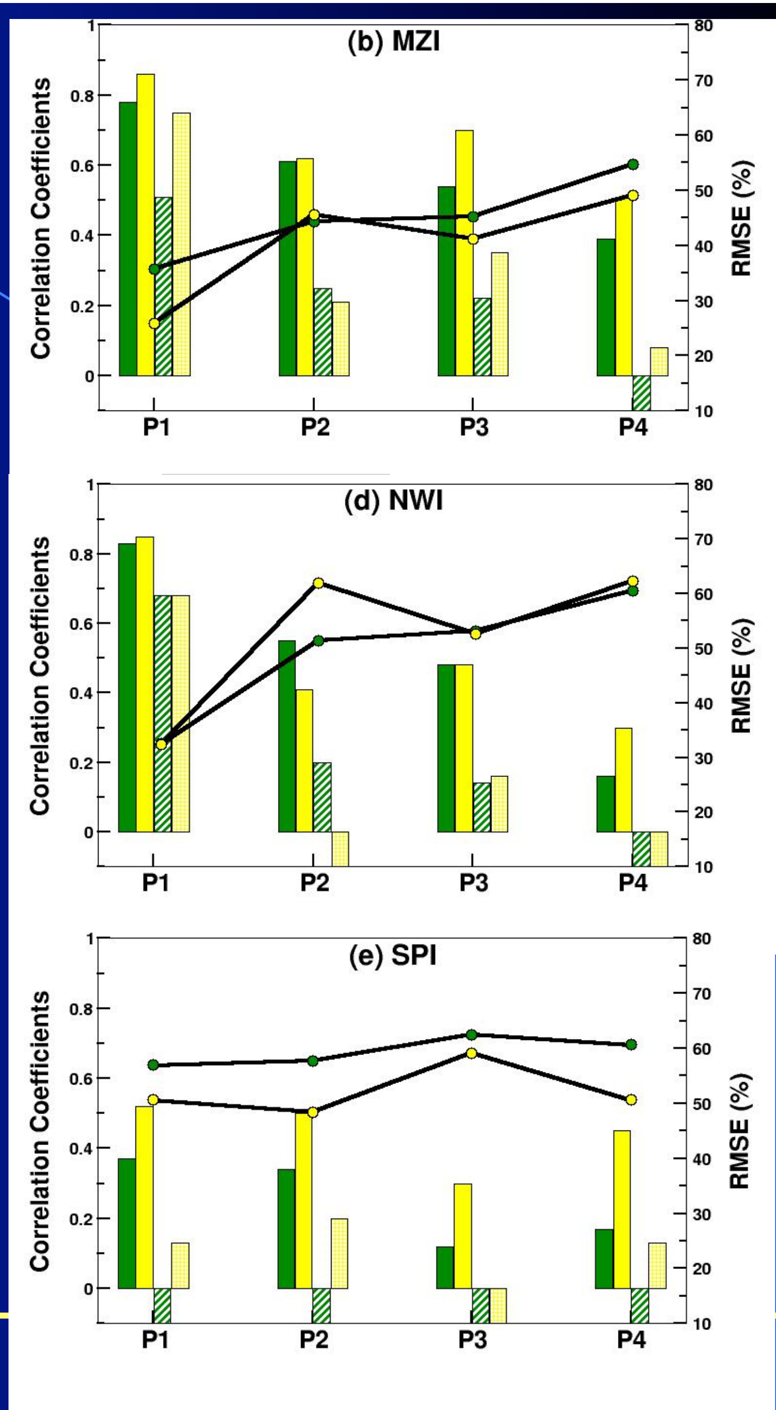

Pentad correlation skills, RMSE and RMSE skills over 5 homogeneous regions

Summary

- ESSO-IITM has developed indigenous Ensemble Prediction System (EPS) based on CFSv2. Hindcast skill for 2001-2010 and forecast for 2011-2012 has shown potential for ERF upto 20 days.
- Role of Bias correction in forecasted SST from CGCM shows improved skill in the extended range prediction.
- Increasing model resolution alone will not improve the prediction of MISO
- Monitoring of large-scale monsoon intraseasonal oscillations is being done using newly developed MISO index.
- The ERP skill from MME using CGEPS further improved and encouraging.
- Real-Time Dynamical Extended Range Forecast using Ensemble prediction System developed in NCEP CFSv2 and which is being updated every 5 days and displayed in IITM website: http://www.tropmet.res.in/erpas/

Conclusion

- **MJO indices are inadequate to represent MISO**

- **A new and effective MISO index has been proposed by Suhas et al. (2012) that is very useful in real time monitoring as well as forecast verification of MISO**

- **The coupled models have become good to give useful MISO forecast about 20 days in advance!**

Thank You

Real Time Monitoring of Monsoon Intraseasonal Oscillation during 2012 using a high Resolution merged rainfall data

Rajib Chattopadhyay, A. K. Mitra, A. K. Srivastava, A. K. Sahai[1] and B. N. Goswami[1]
Indian Institute of Tropical Meteorology, Pune, India
NCMRWF,NOIDA, New Delhi, India
India Meteorologial Department, Pune, India

- GPCP is not available on real time. Hence, a merged precip data set has been prepared with TRMM and IMD gridded product
- With historical data over the TRMM period, this data is available on real time throughout the year
- MISOs during 2012 were monitored in real time with our Index

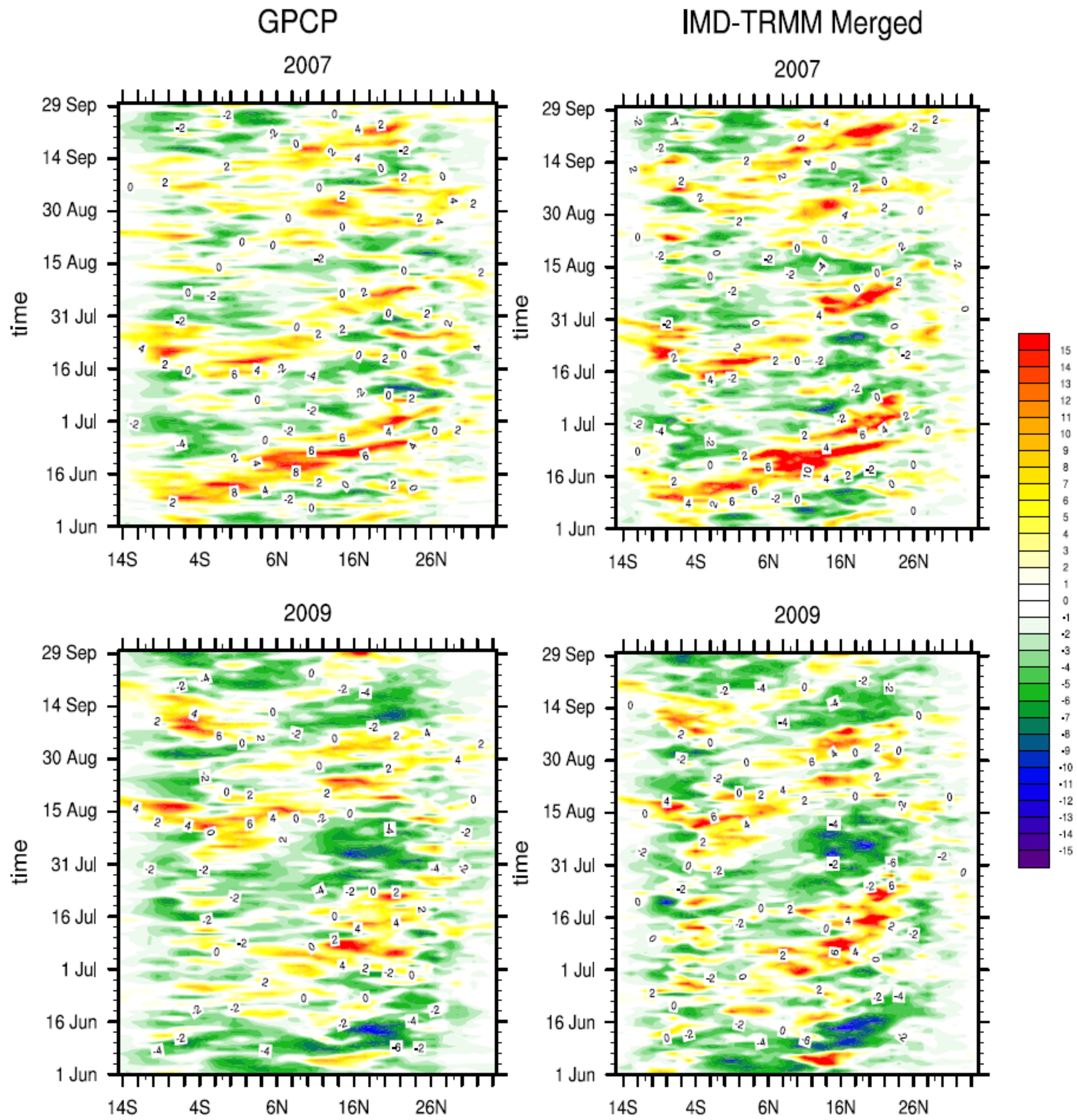

Figure 4: Plot comparing the rainfall derived from IMD-TRMM merged (left panels) and GPCP merged data for 2 extreme years 2007 (top) and 2009(bottom).

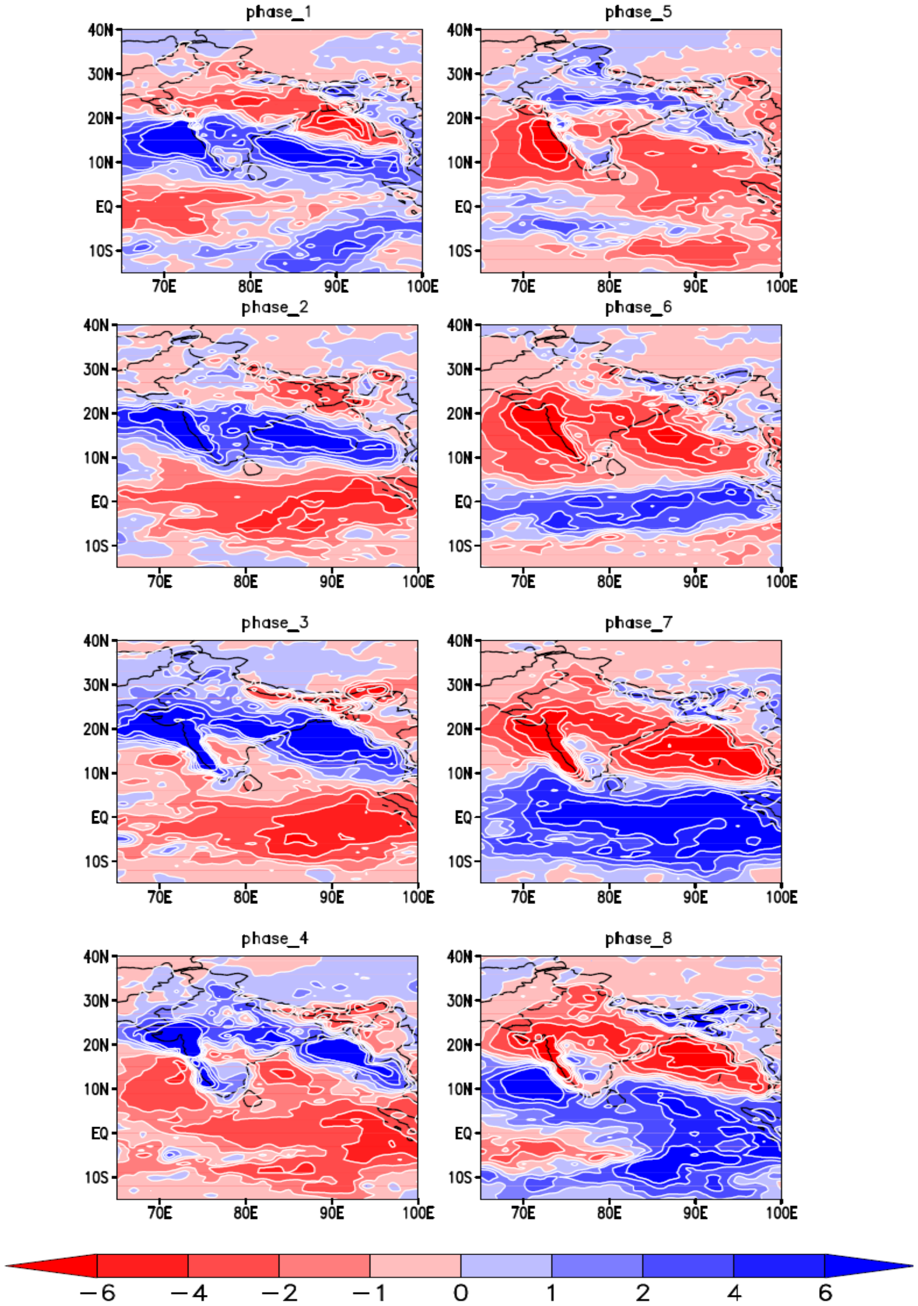

Figure 1: The Composite plot for rainfall anomalies for the days clustered in each phases in [MISO1, MISO2] phase space.

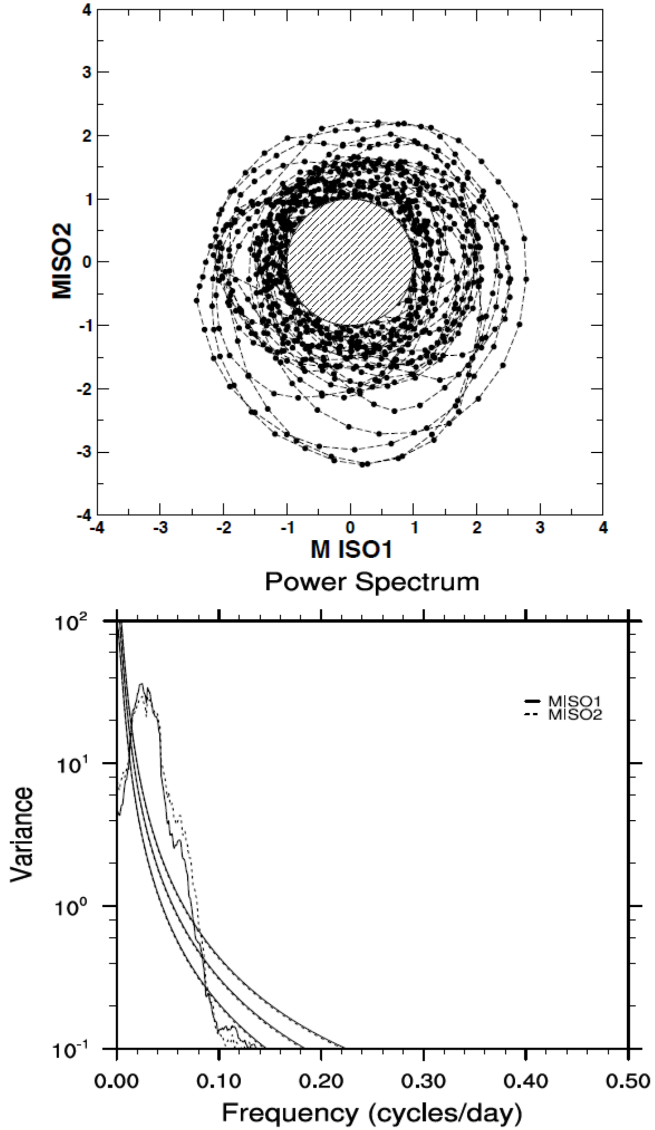

Figure 2: (a)The cloud of phase points represented by the amplitudes of MISO1 and MISO2 phase space. (b) Power spectrum of the MISO1 and MISO2 time series.

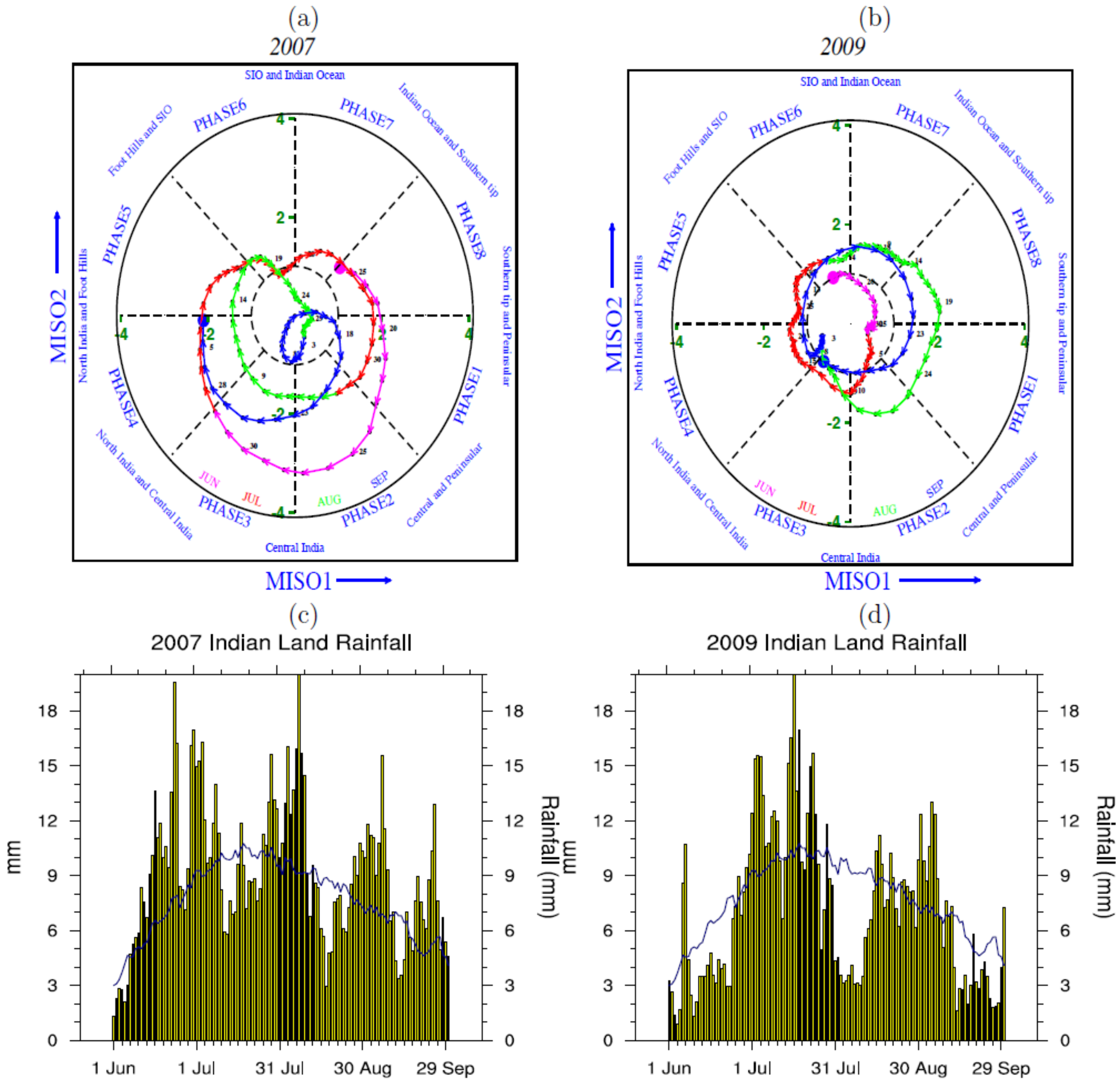

Figure 5: (top)MISO phase plot for 2007 and 2009.(bottom) Rainfall Evolution(yellow bar) and daily climatology(blue curve).

(a)

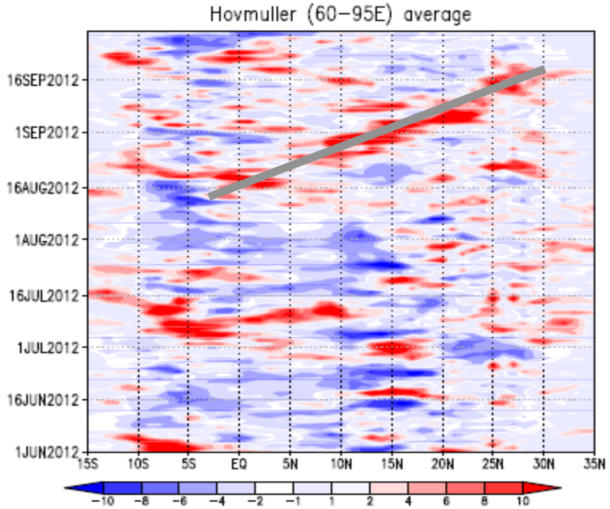

(b)

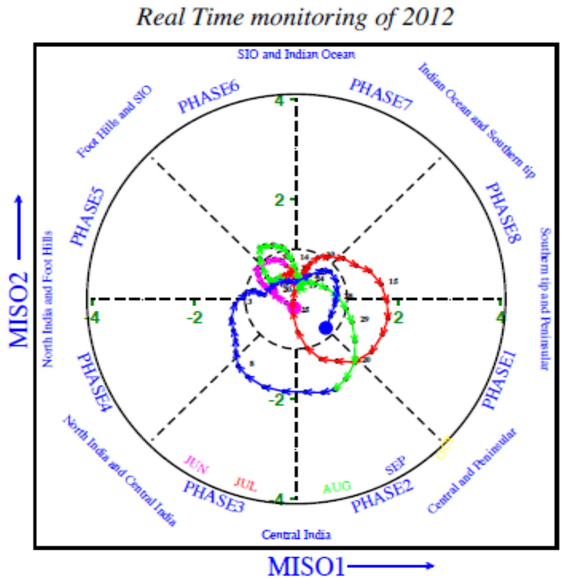

'igure 8: (a) Hovmuller plot for the year 2012 (b) MISO phase plot.

Pentad wise rainfall predicted by MME

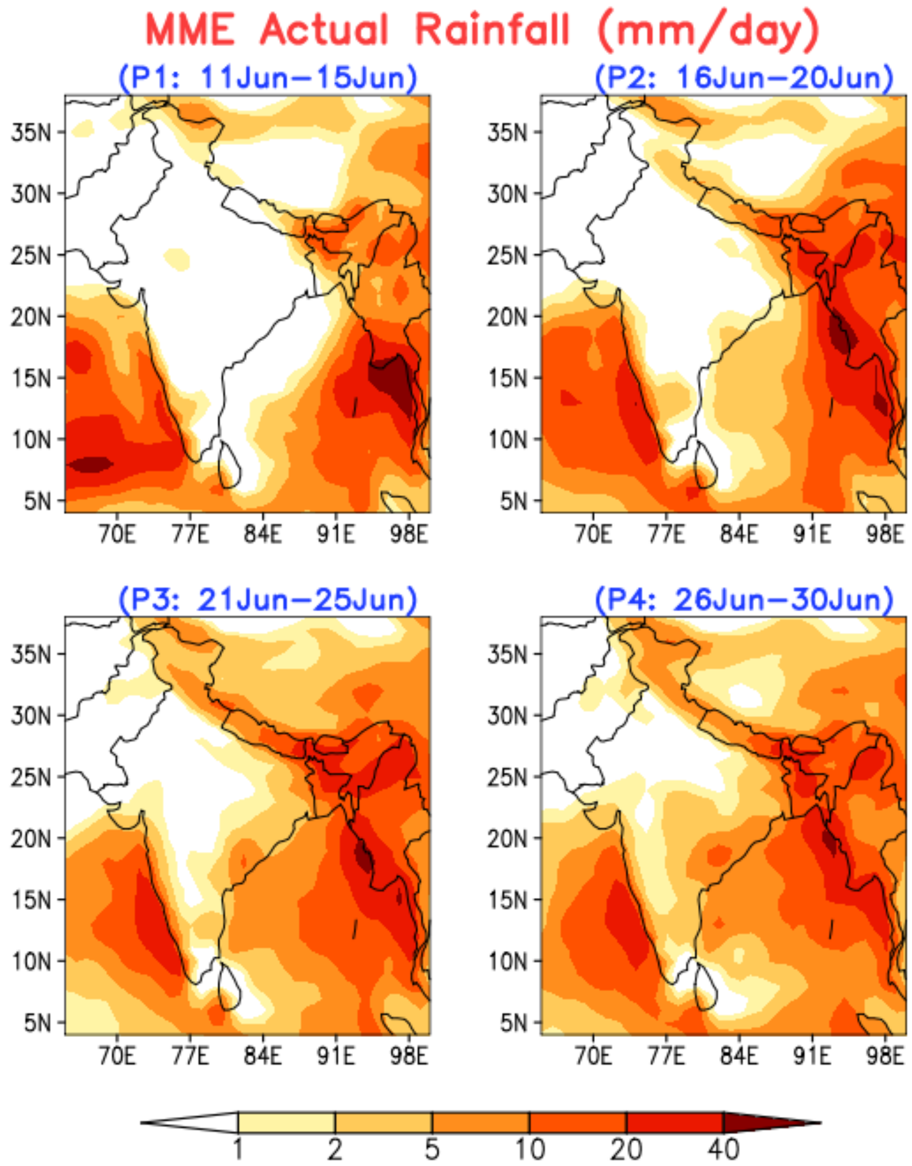

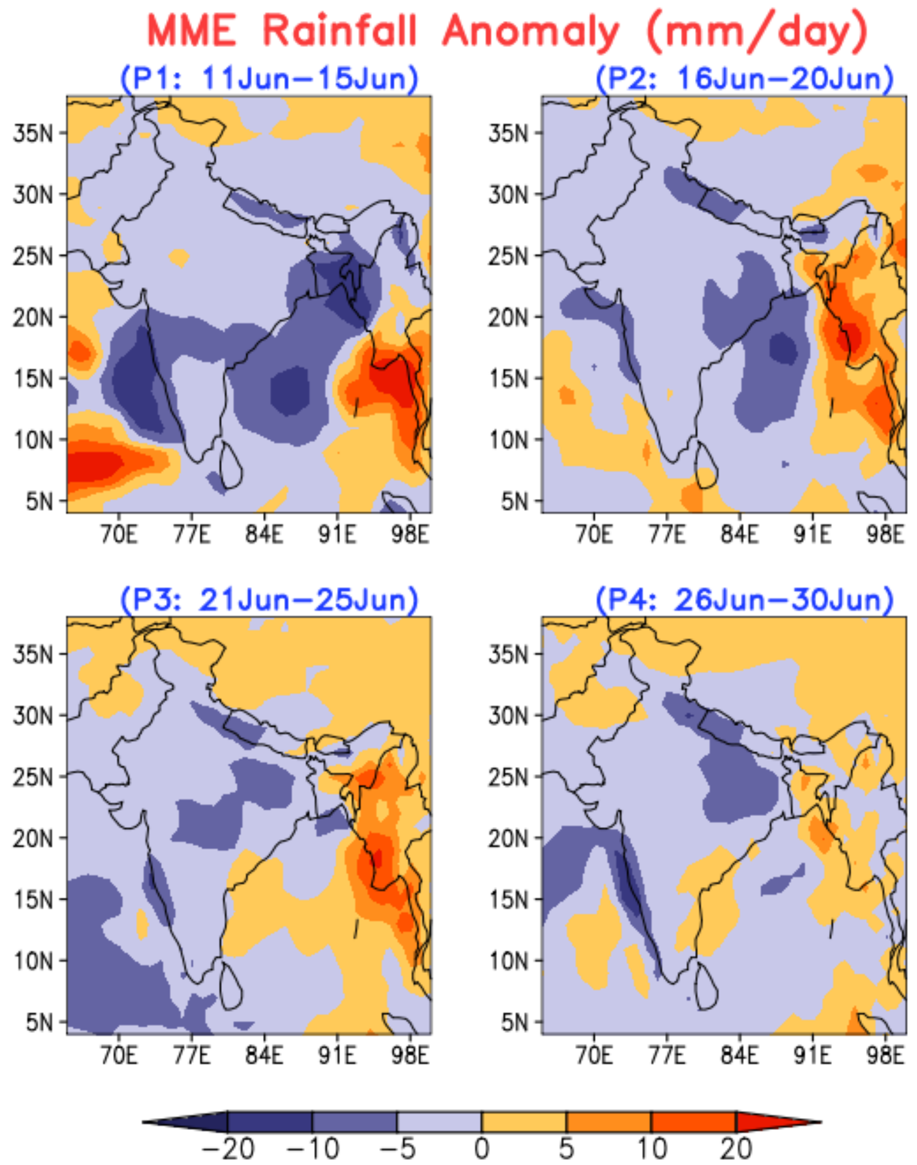

Area averaged rainfall over homogeneous regions predicted by MME

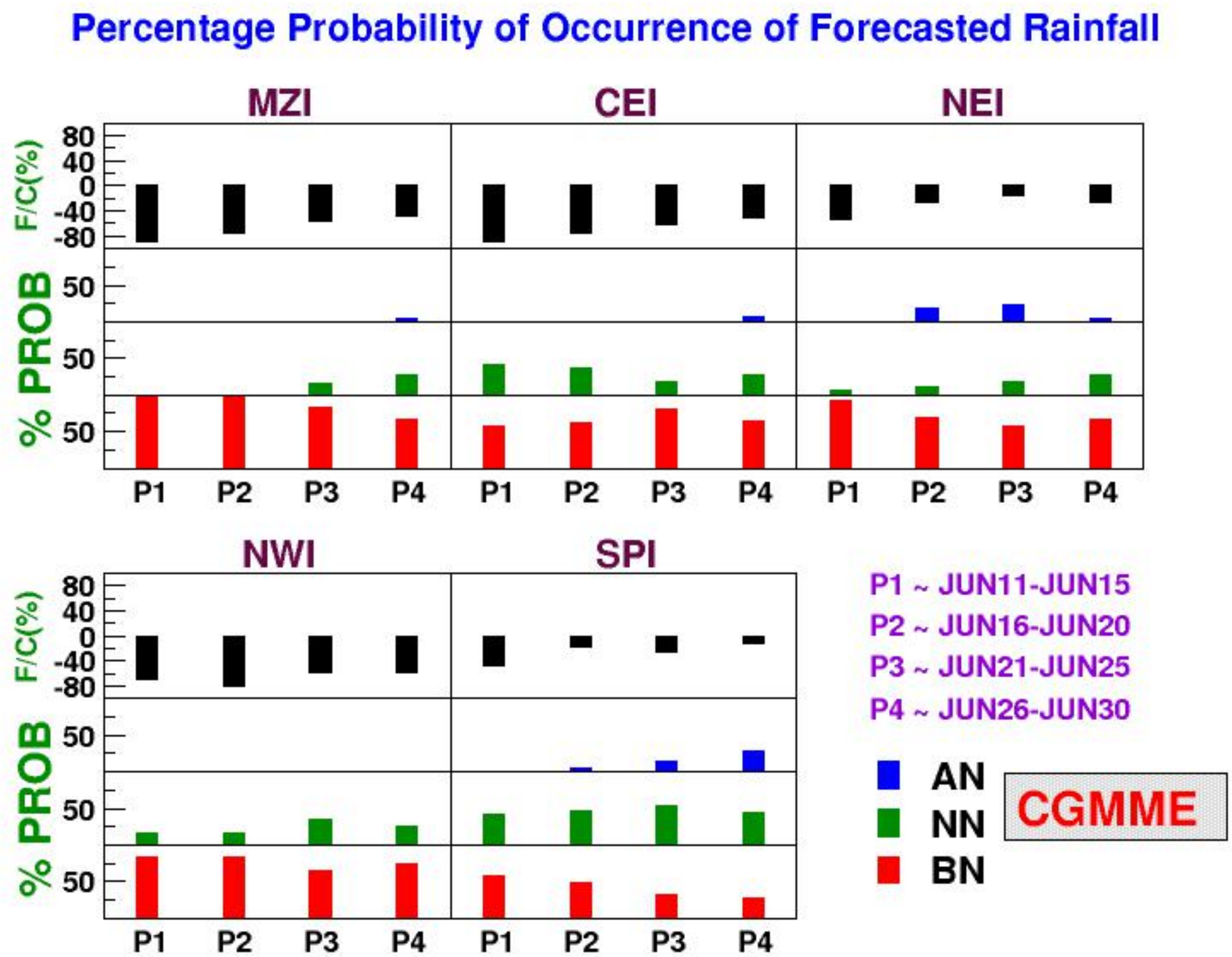

Verification of area averaged rainfall over homogeneous regions predicted by MME

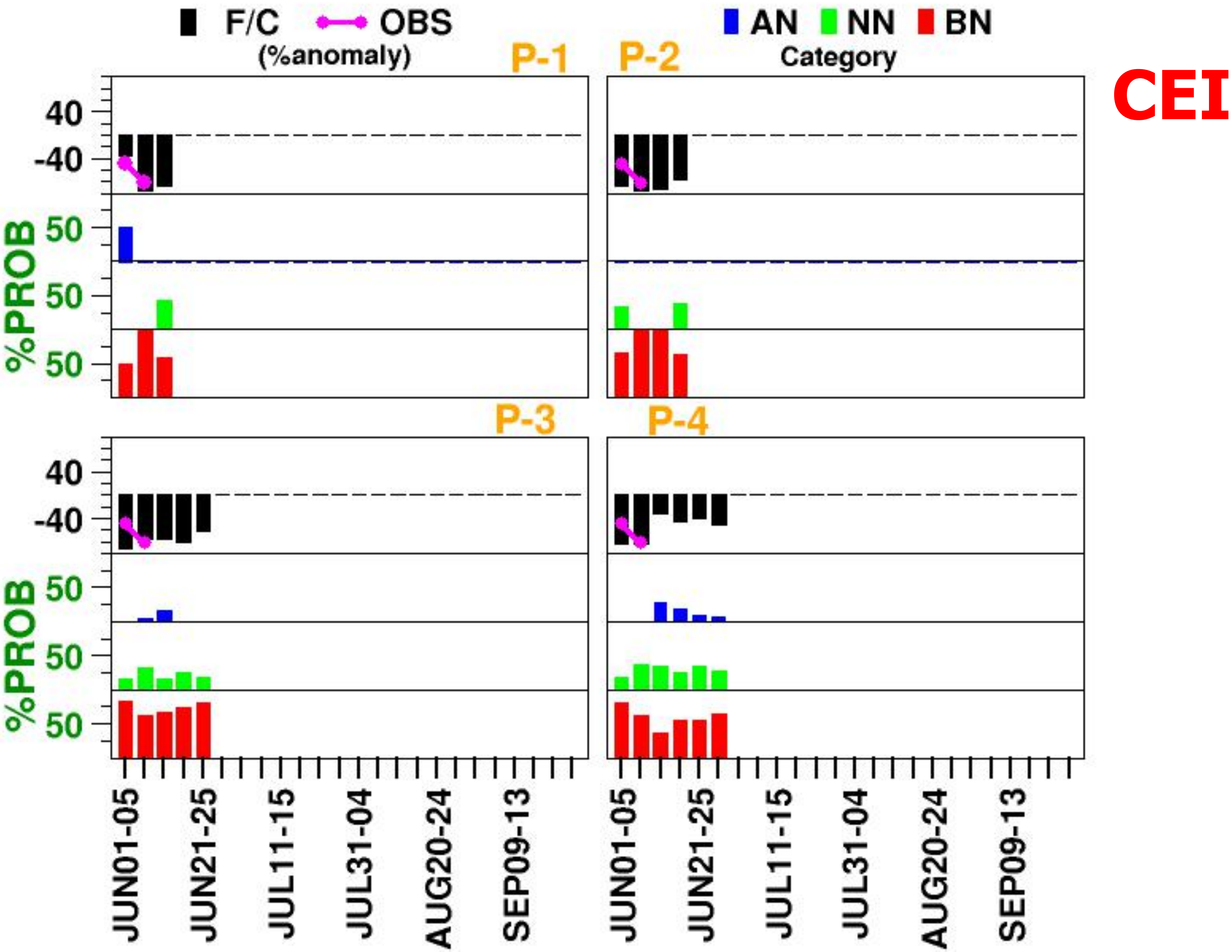

Verification of area averaged rainfall over homogeneous regions predicted by MME

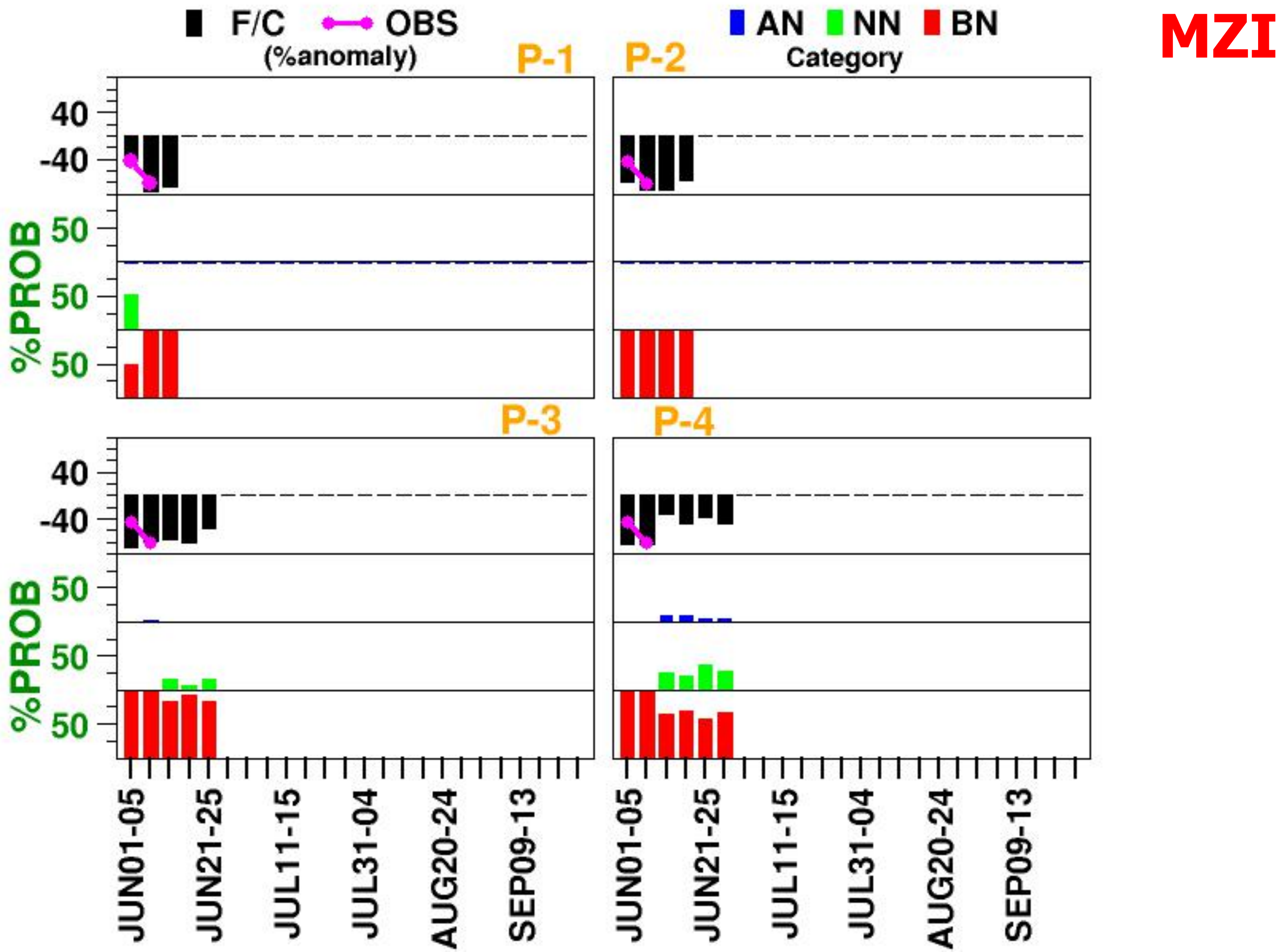

Verification of area averaged rainfall over homogeneous regions predicted by MME

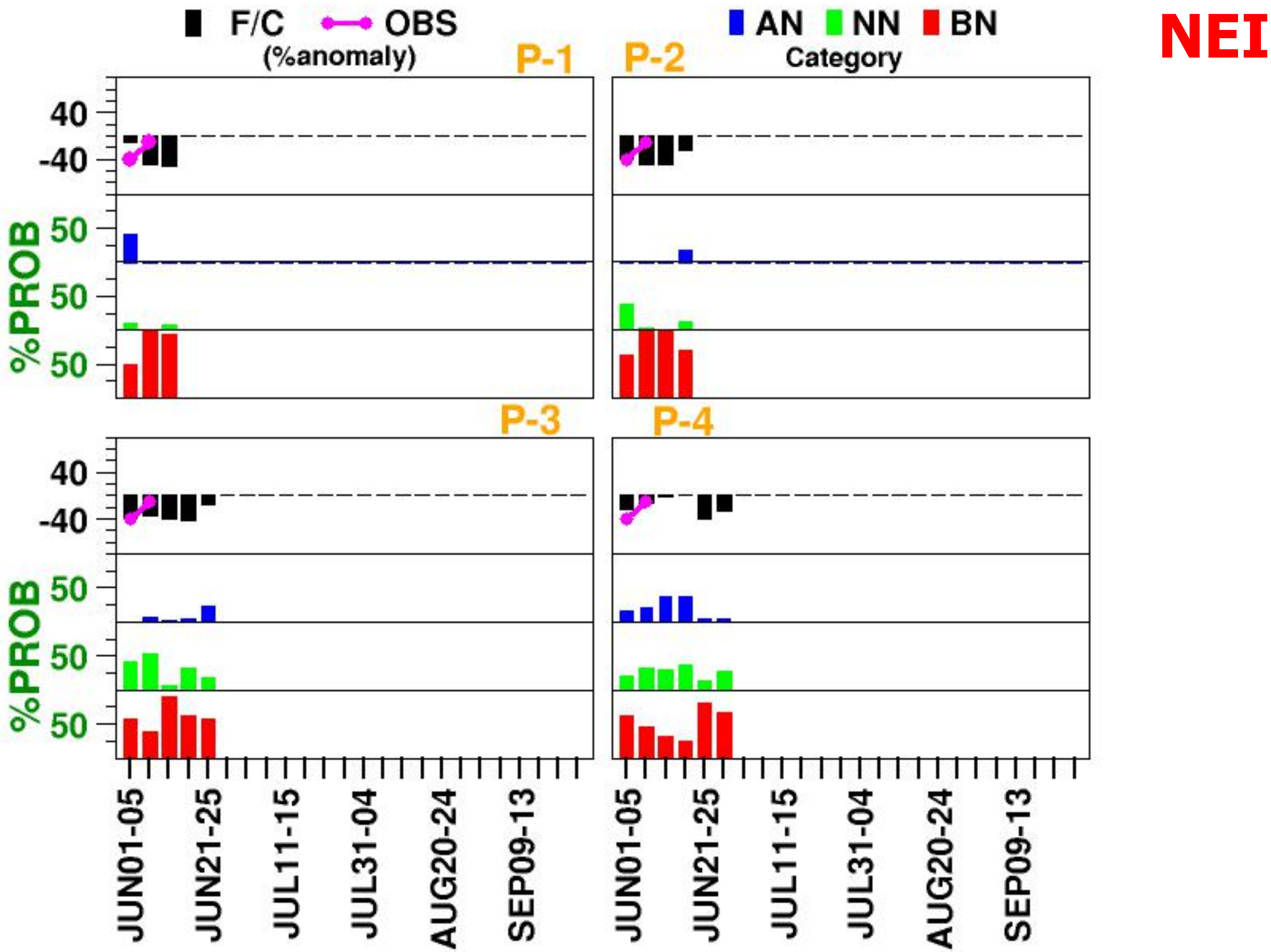

Verification of area averaged rainfall over homogeneous regions predicted by MME

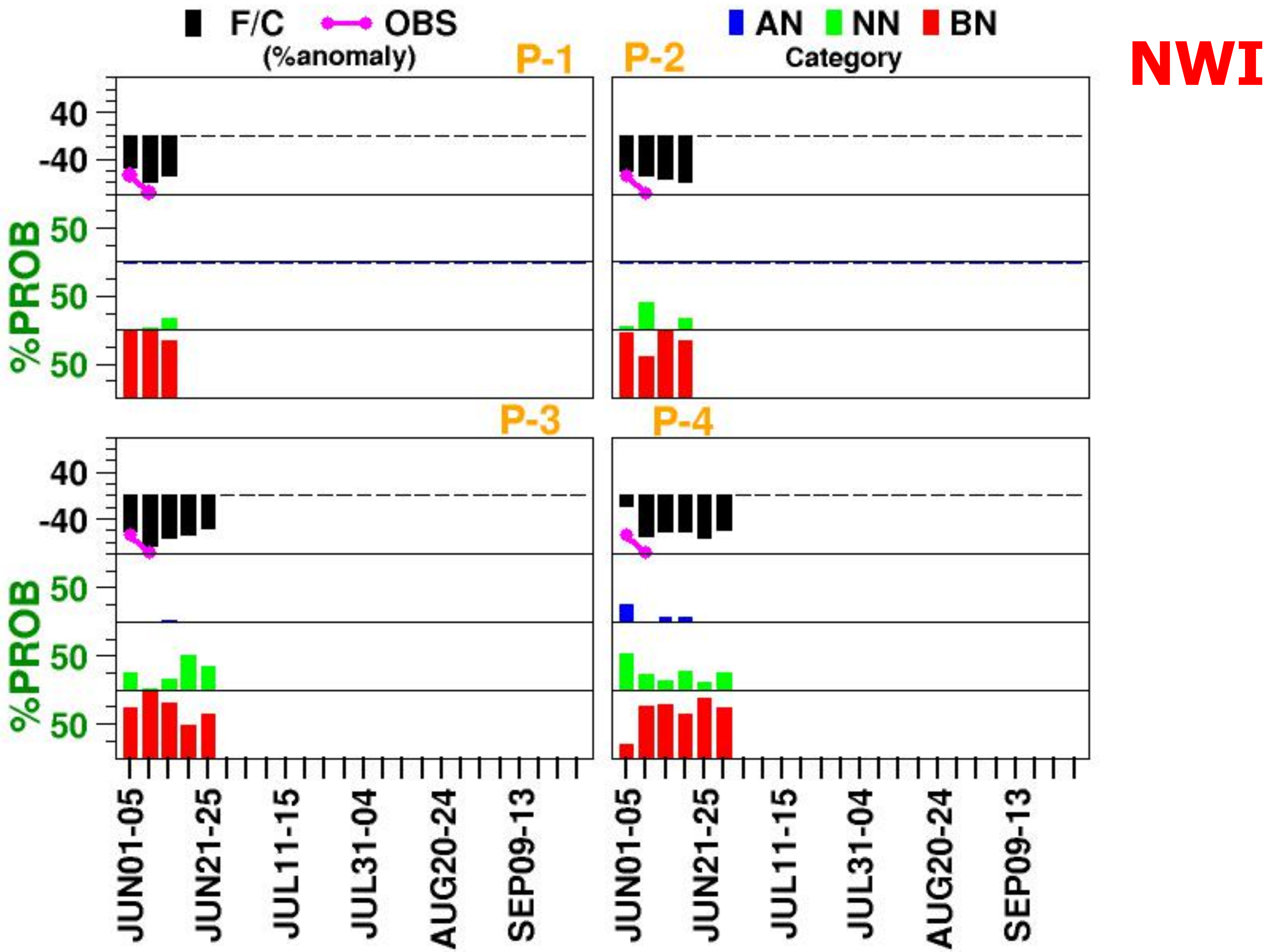

Verification of area averaged rainfall over homogeneous regions predicted by MME

SPI

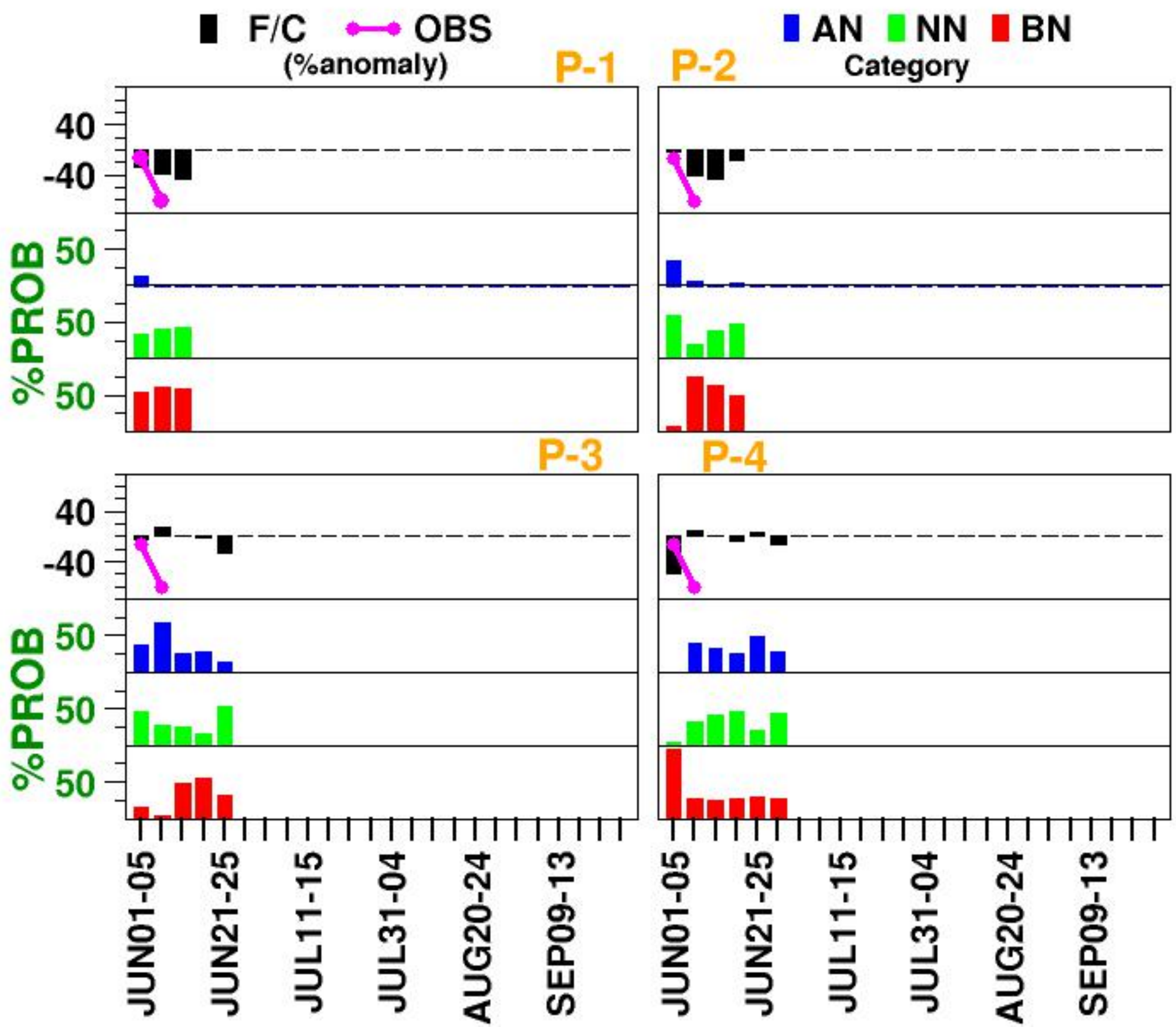

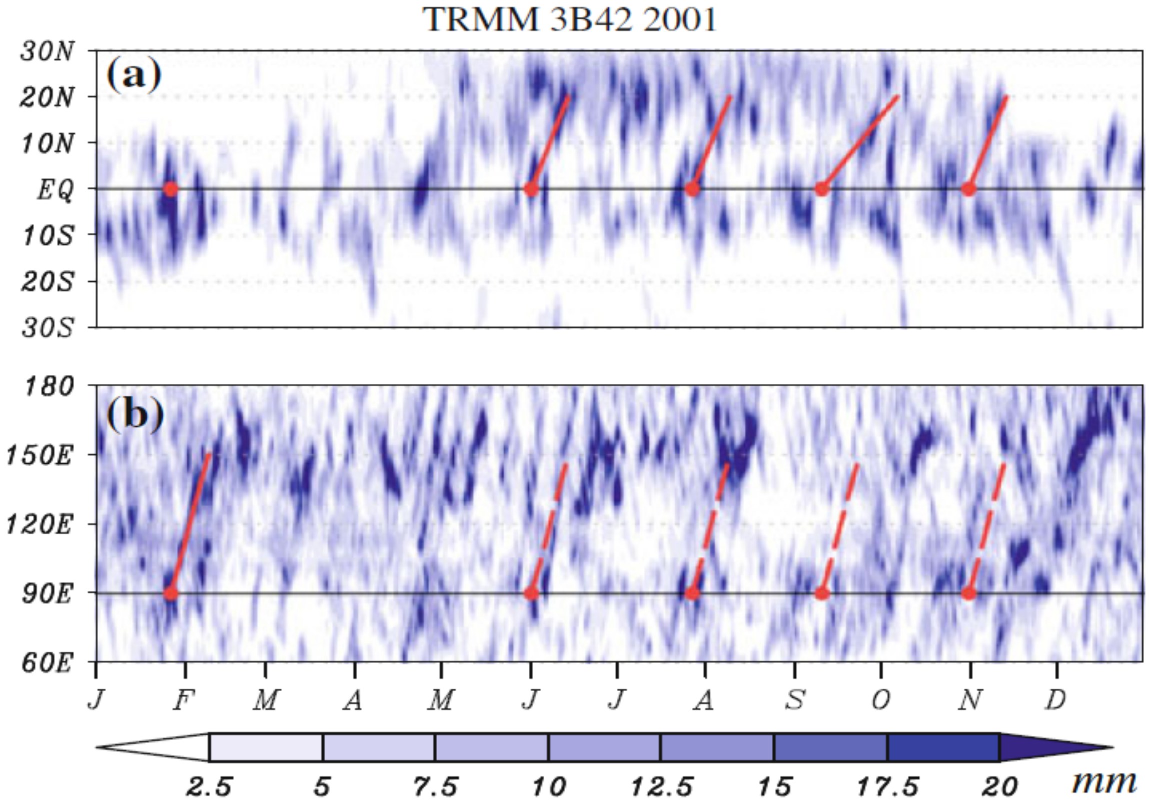

Fig. 1 Daily precipitation (tropical rainfall measuring mission product 3B42) associated with the ISO for the year 2001. **a** Latitude-time plot over the eastern Indian Ocean averaged between 80 and 100°E and (**b**) longitude-time plot along the equator between 7.5°S and 7.5°N. Each *red closed circles* indicates major convection associated with significant ISO events, determined by our analysis to be introduced in Sect. 4 (see also Fig. 4), sitting around the central Indian Ocean (90°E, 0°). *Solid* and *dashed lines* show reference phase speed corresponding to (**a**) northward propagation at approximately 1–2 ms^{-1} and (**b**) eastward propagation at approximately 6 ms^{-1}. The *solid lines* are intended to represent rather apparent convection exists

Northward propagation and Eastward propagation

Kikuchi and Wang, 2012

- While Kikuchi et al. 2012 demonstrate that MJO and BISO are distinct, their method of separation is not useful for Real Time monitoring and forecast verification as they use time filtering.

Clim Dyn (2013) 40:493–509
DOI 10.1007/s00382-012-1544-4

Real-time multivariate indices for the boreal summer intraseasonal oscillation over the Asian summer monsoon region

June-Yi Lee · Bin Wang · Matthew C. Wheeler ·
Xiouhua Fu · Duane E. Waliser · In-Sik Kang

Their Method

- MV-EOF analysis of daily mean OLR and 850 hPa zonal winds (U850)
- 1^{st} May to 31^{st} October, over the ASM region (10S-40N,40-160E)
- Anomalies obtained by removing the slow annual cycle (mean and first three harmonics) as well as effect of interannual variability by subtracting the mean of last 120 days.

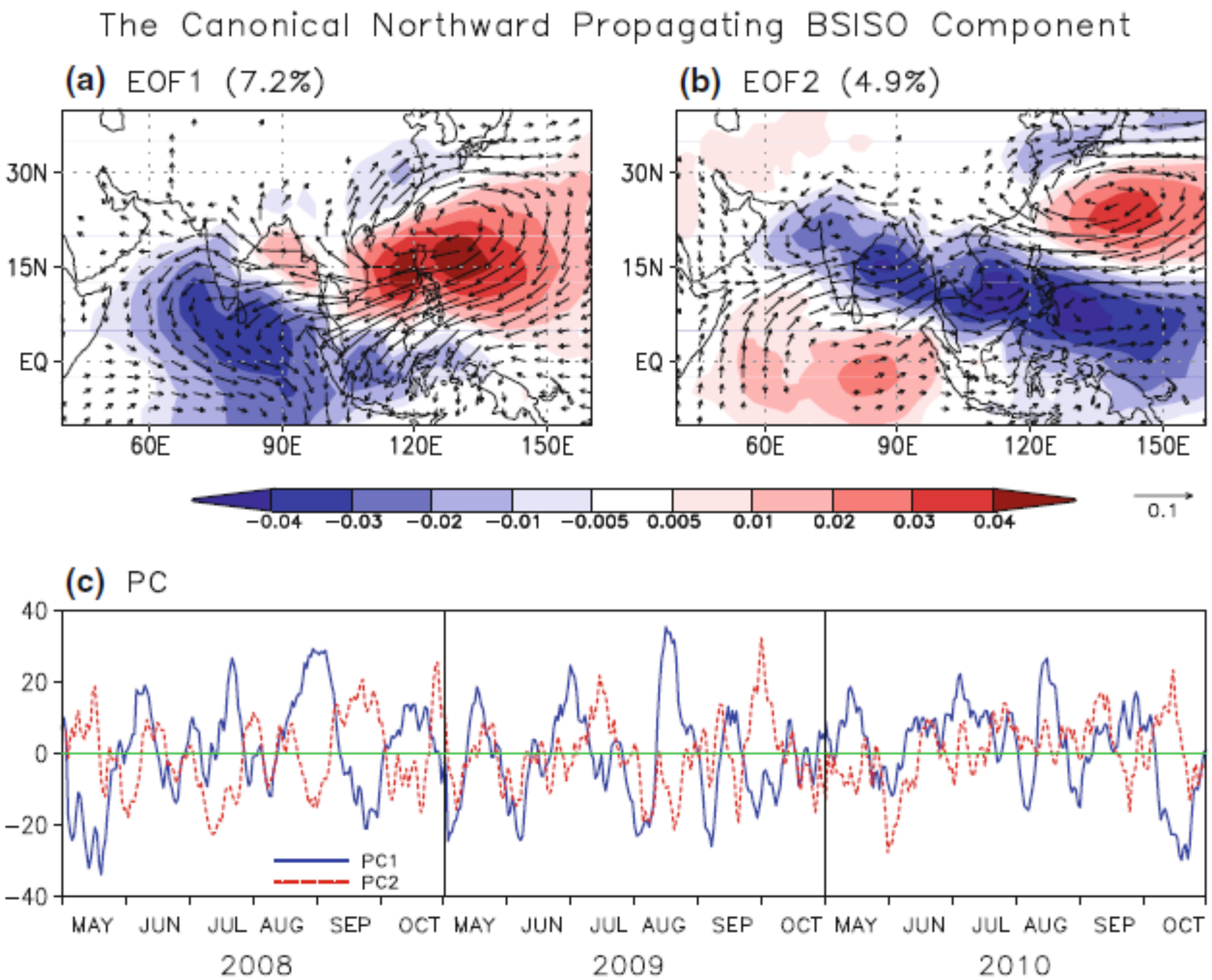

Fig. 2 Spatial structure (**a**, **b**) and PC time series (**c**) of the first two leading MV-EOF modes of daily OLR (*shading*) and zonal wind at 850 hPa (U850) anomalies normalized by their area averaged temporal standard deviation over the ASM region (33.04 W m^{-2} for OLR and 4.01 m s^{-1} for U850). To display the full horizontal wind vector, the associated meridional wind at 850 hPa (V850) was obtained by regressing V850 anomaly, normalize by its area averaged standard deviation (3.14 m s^{-1}), against each PC. The MV-EOF modes were obtained during MJJASO for the 30 years of 1981–2010

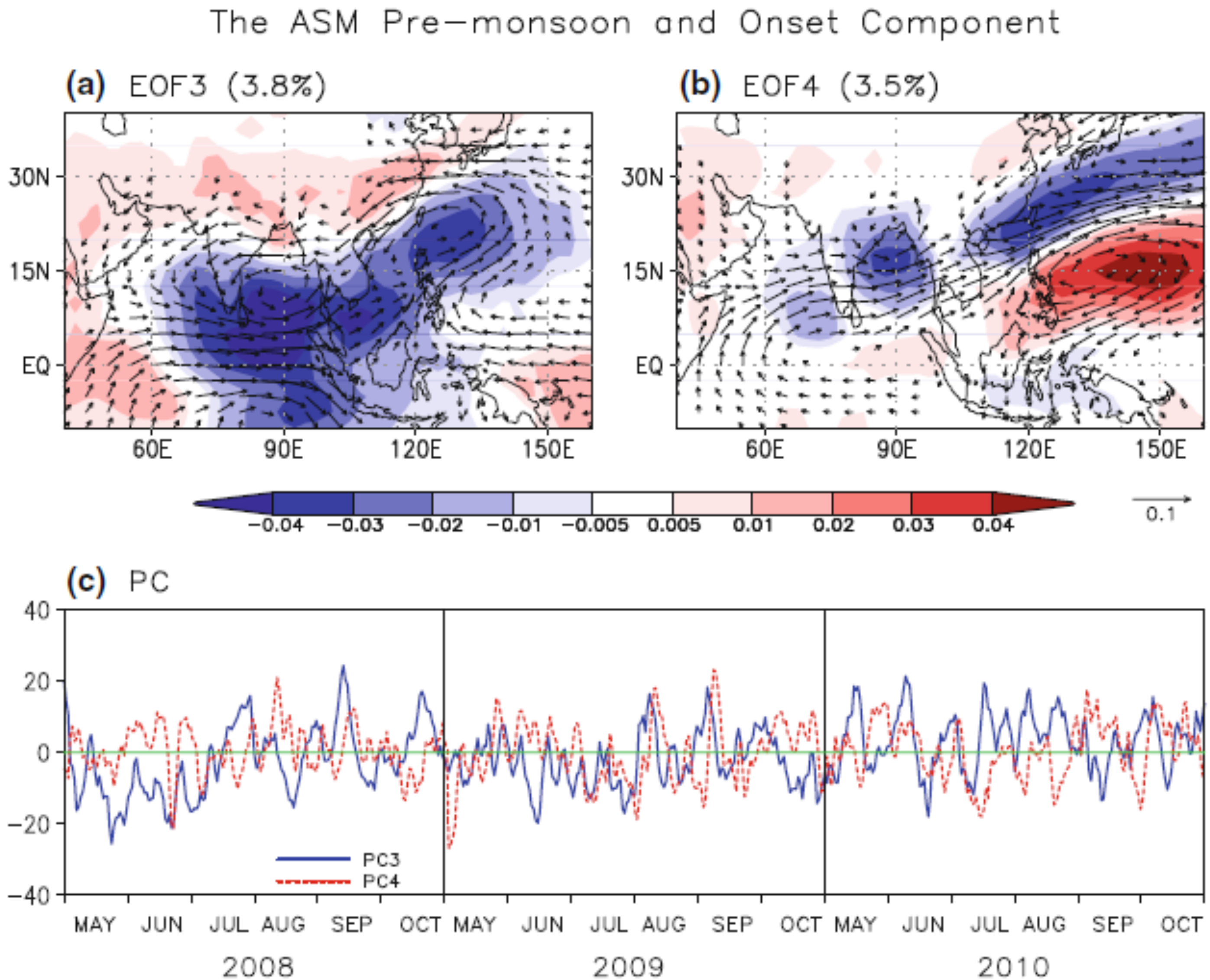

Fig. 3 Same as Fig. 2 except for the 3rd and 4th modes

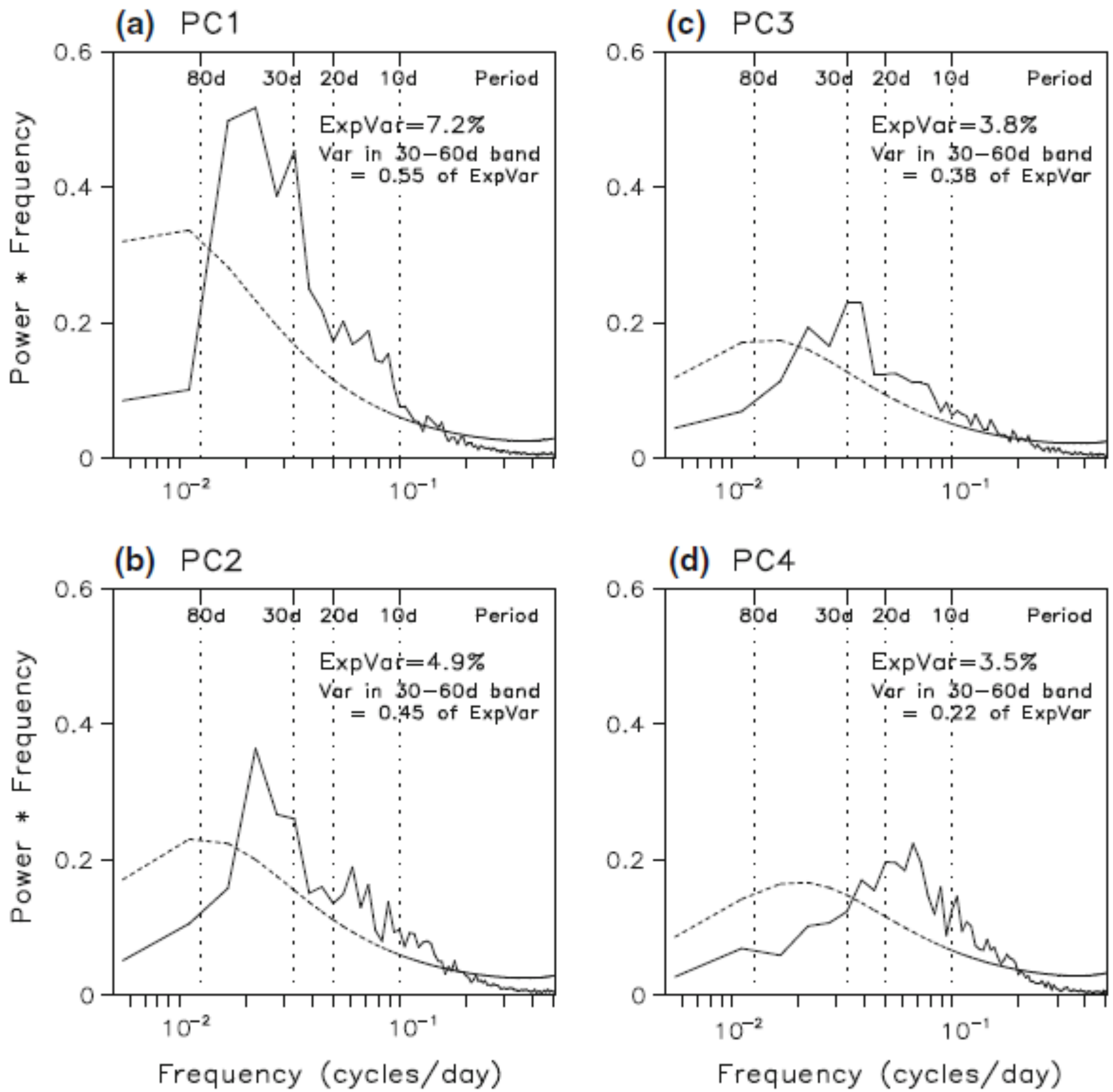

Fig. 5 Power spectra of each PC of the first four MV-EOFs. It was separately calculated each year with 184 sample size during MJJASO and then averaged over the 30-years. The plotting format forces the area under the power curve in any frequency band to be equal to variance. The total area under *each curve* is scaled to equal the explained variance (Exp Var) by that EOF. The fraction of ExpVar in the 30- to 60-day band for each PC is given. The *dashed curve* is the red-noise spectrum computed from the lag 1 autocorrelation

The problem!

PC3 and PC4 captures little of 30-60 day variance, an important component of MISO!!

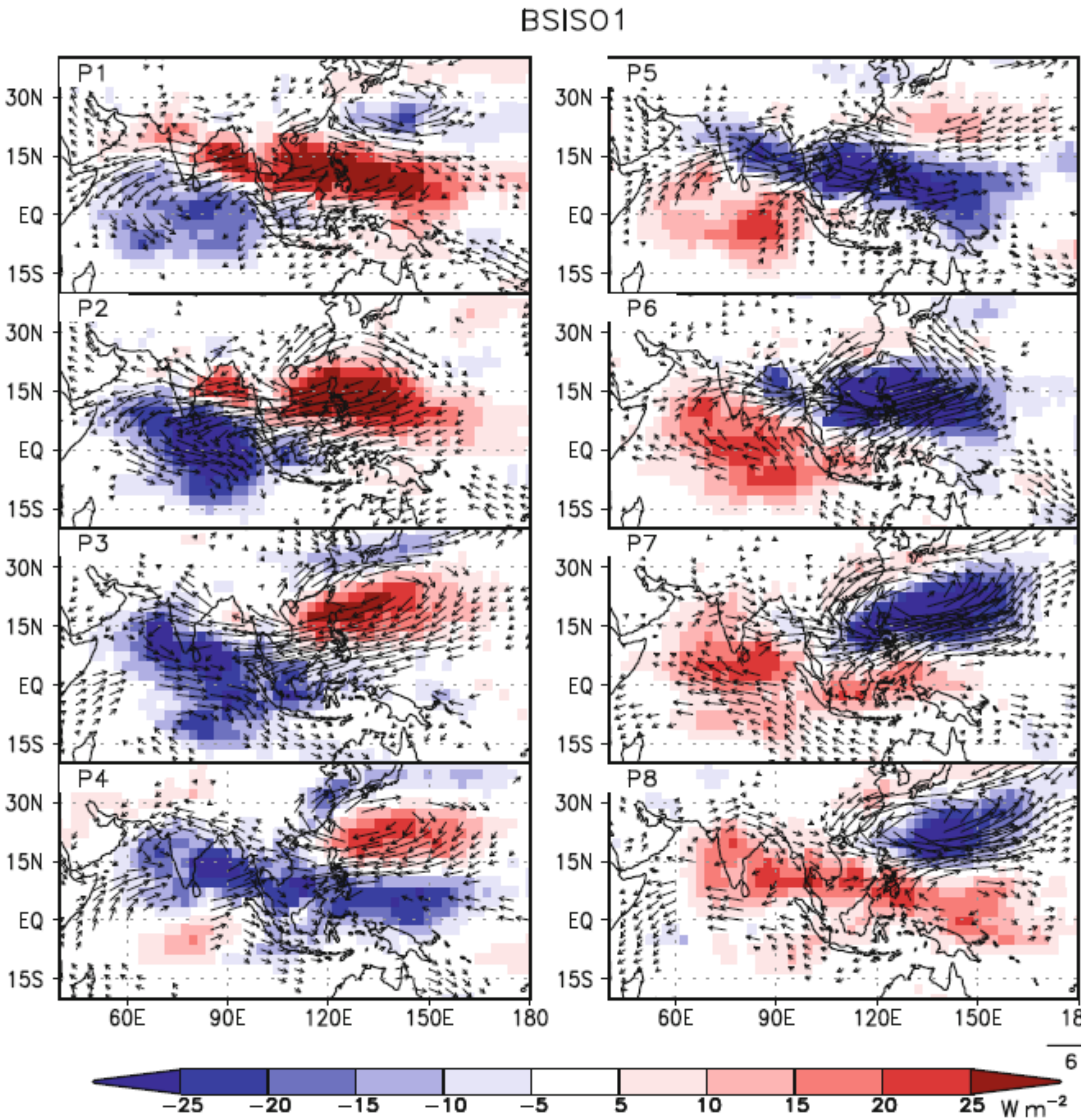

Fig. 9 The life cycle composite of OLR (*shading*) and 850-hPa wind (*vector*) anomaly reconstructed based on PC1 and PC2 of BSISO1 in 8 phases. Composite maps shown are masked to exhibit only anomalies that exceed a two-tailed Normal-z test at the 95 % confidence level

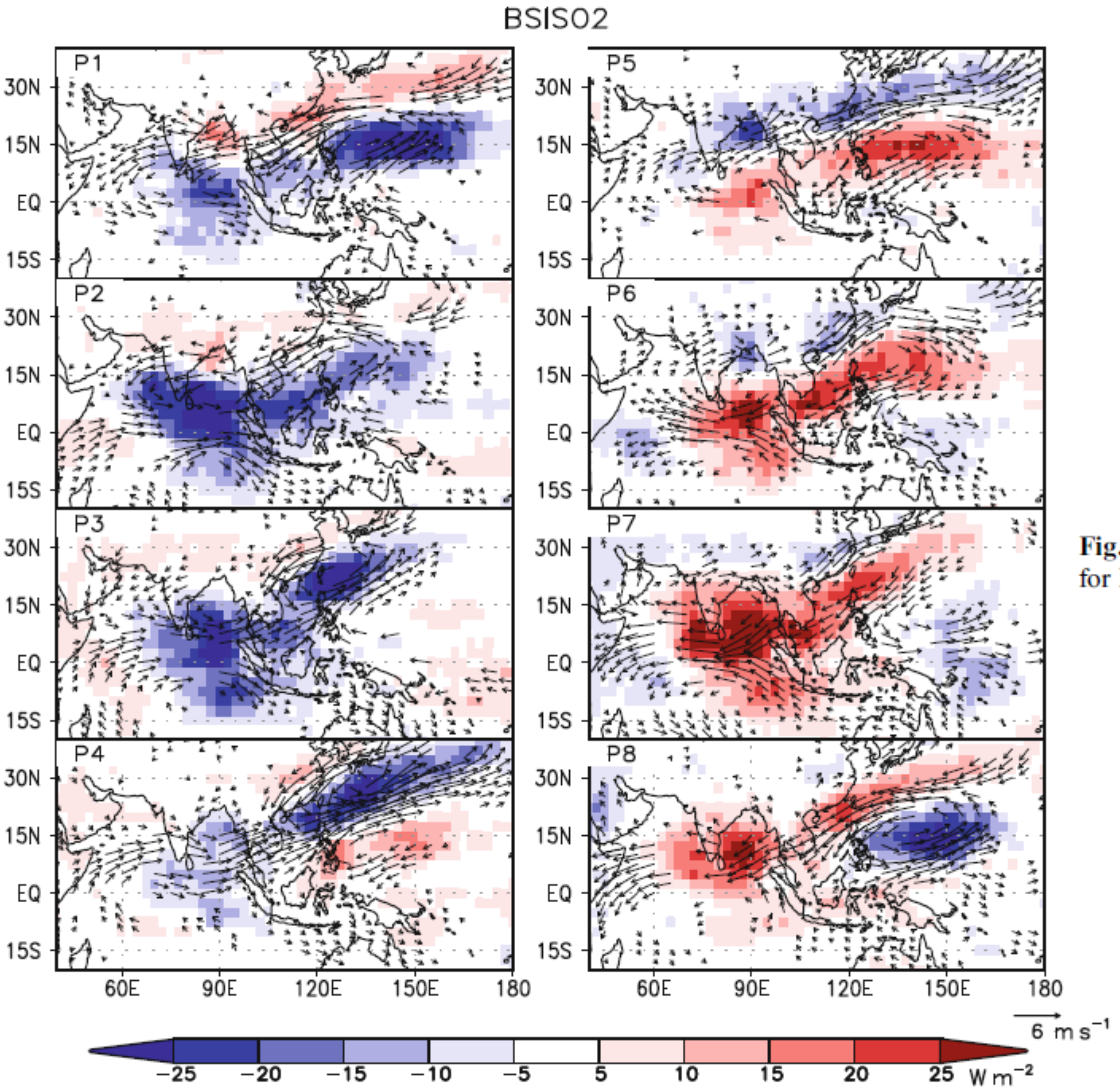

Fig. 10 Same as Fig. 9 except for PC3 and PC4 of BSISO2

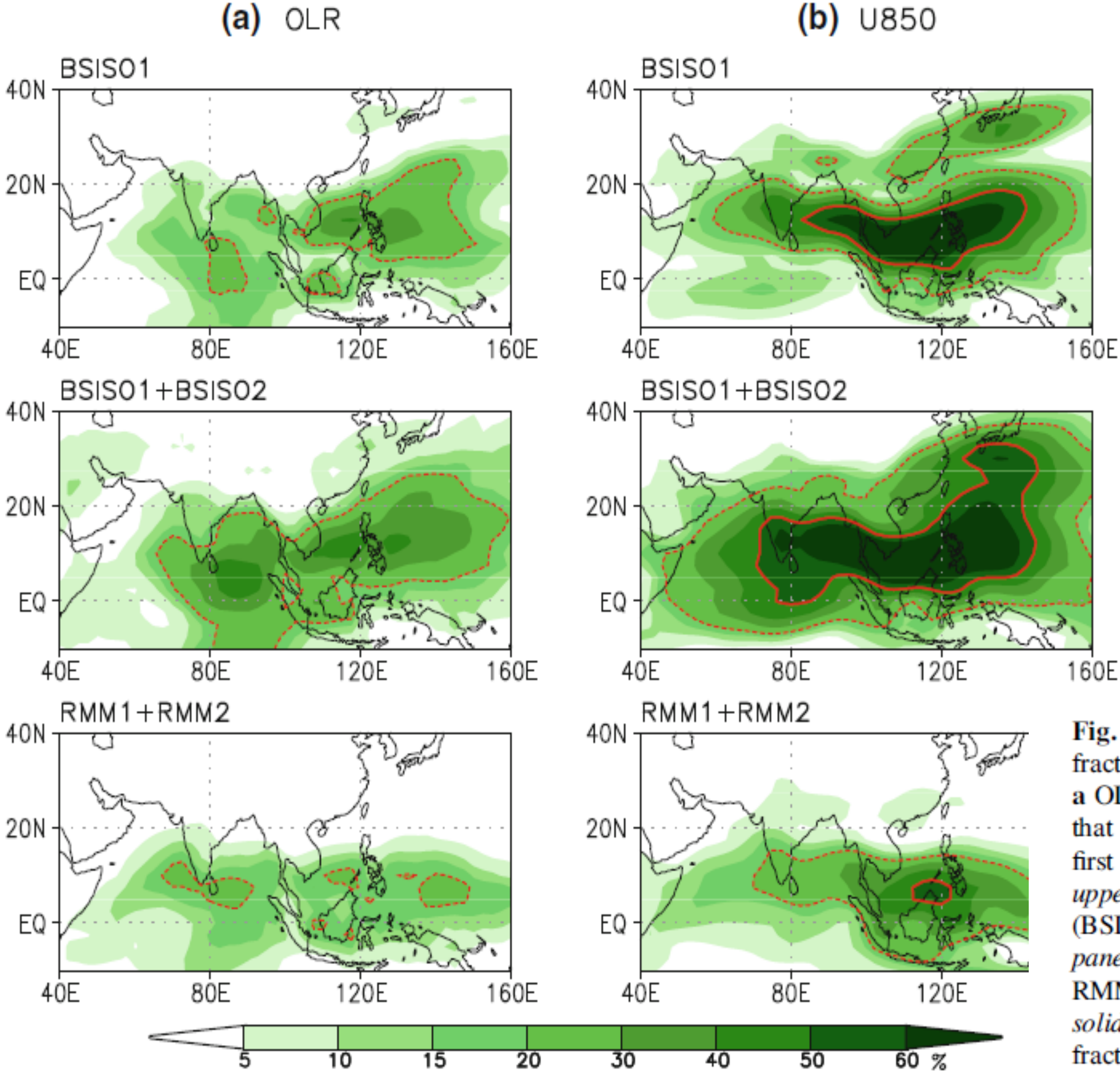

Fig. 12 Spatial distribution of fractional variance of pentad **a** OLR and **b** U850 anomaly that are accounted for by the first two PCs (BSISO1 only in *upper panels*), the first four PCs (BSISO1 and BSISO2 in *middle panels*) and the two-component RMM index (*lower panels*). *Red solid* (*dashed*) *line* indicates fractional variance at 50 % (20 %)

Madden-Julian Oscillation

(a.k.a. Intraseasonal, 40-50, 30-60 Day Oscillation)

- Intraseasonal Time Scale: ~40-60 days
- Planetary-Scale: Zonal Wavenumbers 1-3

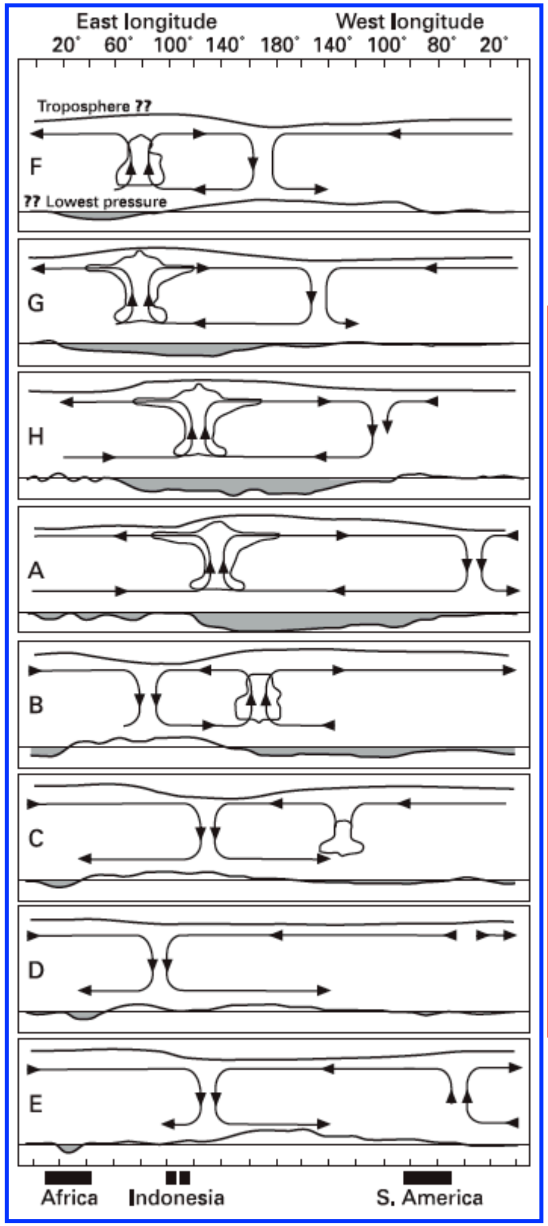

Madden & Julian, 1972

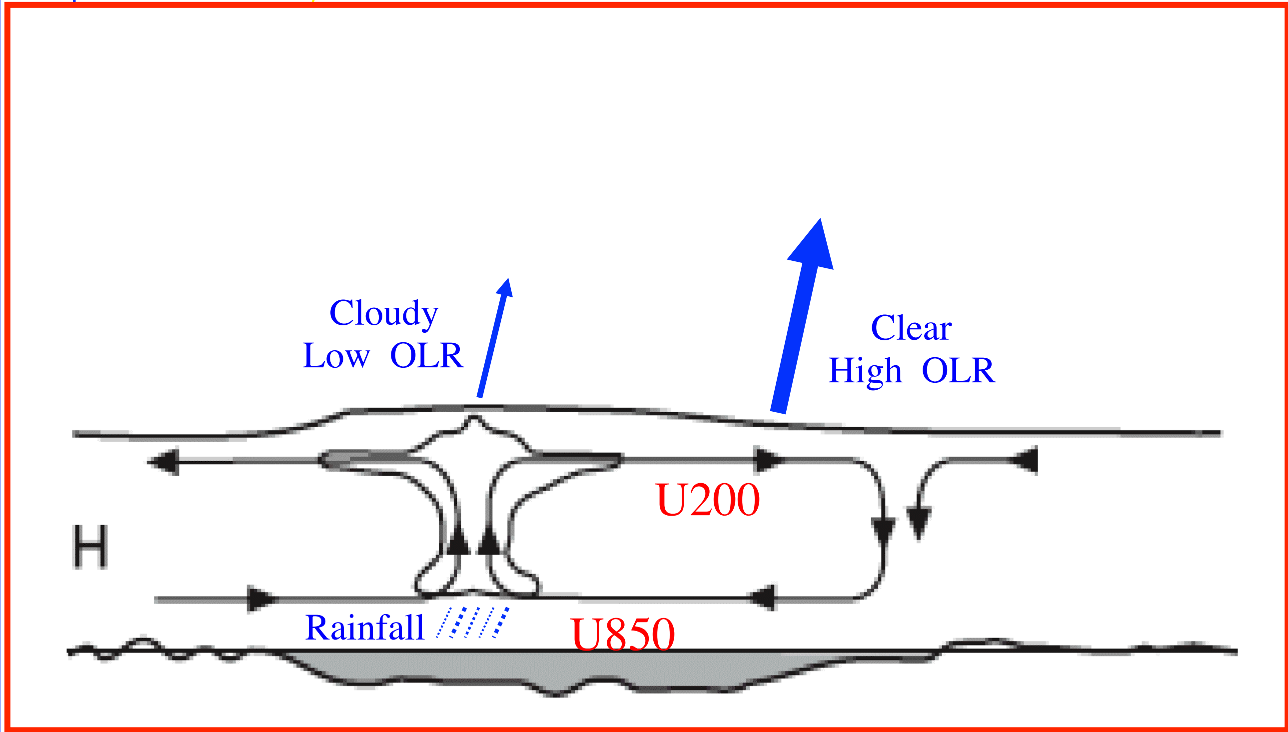

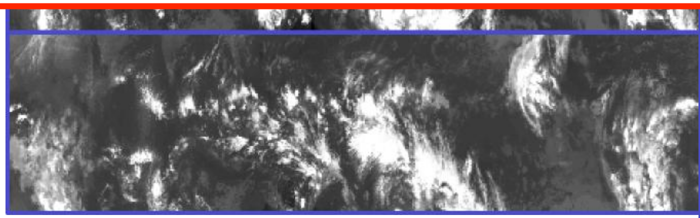

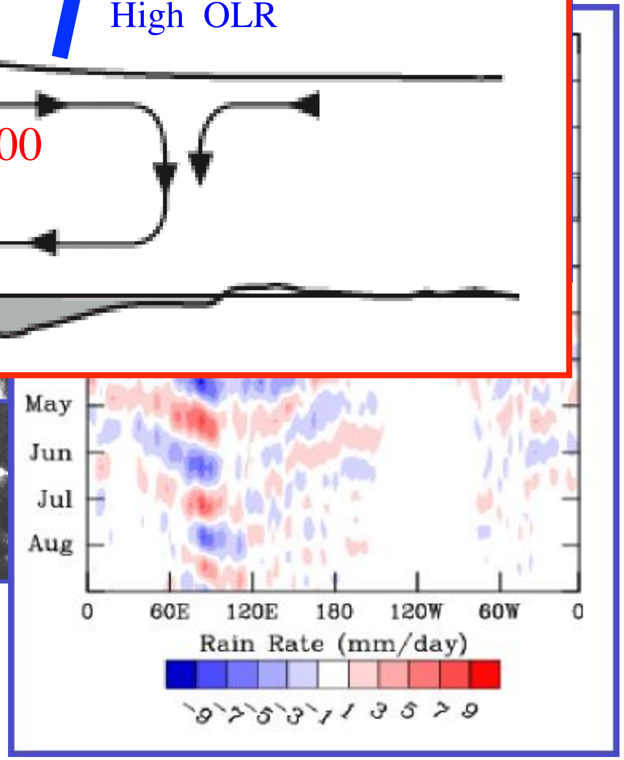

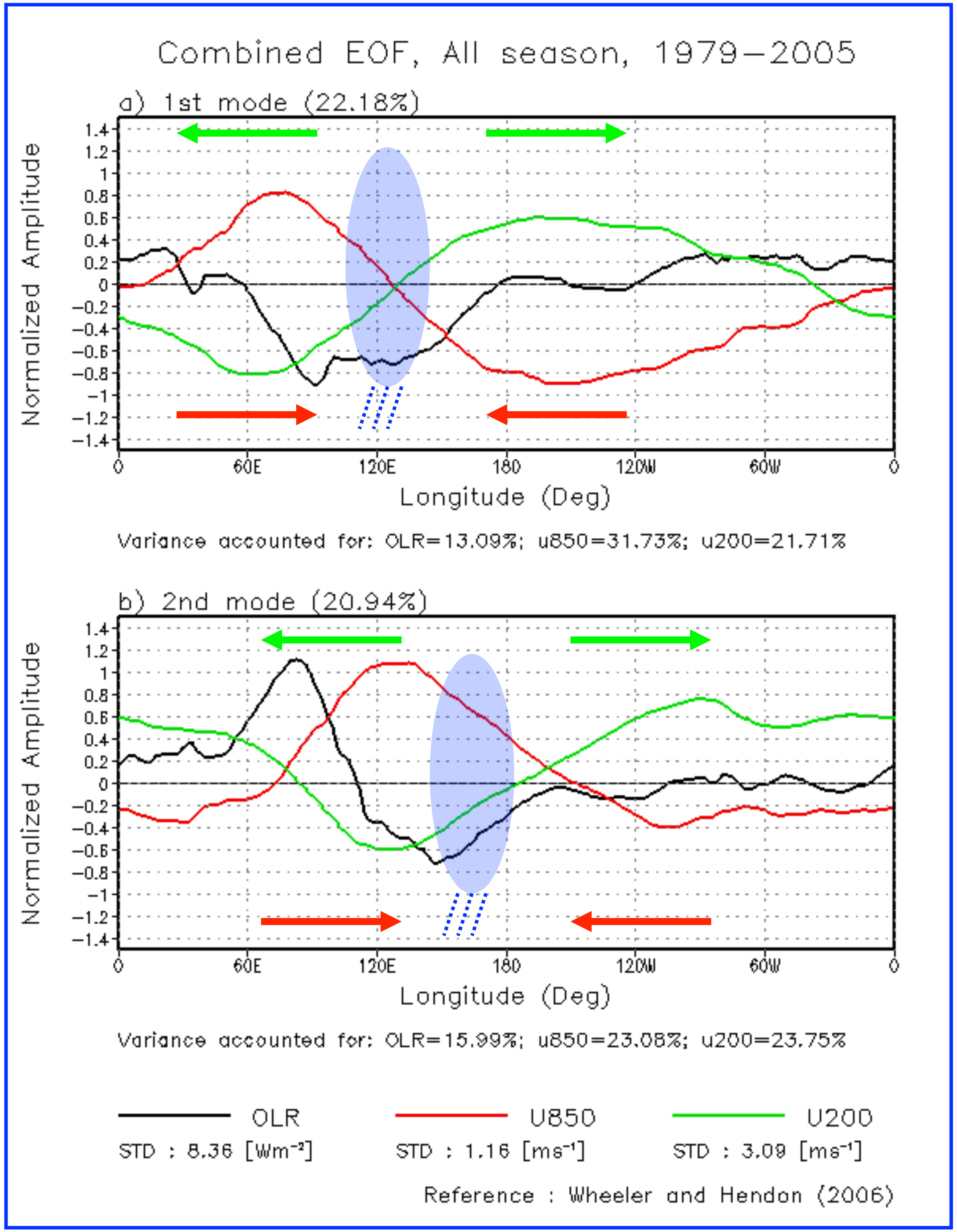

Basic Dynamical Structure

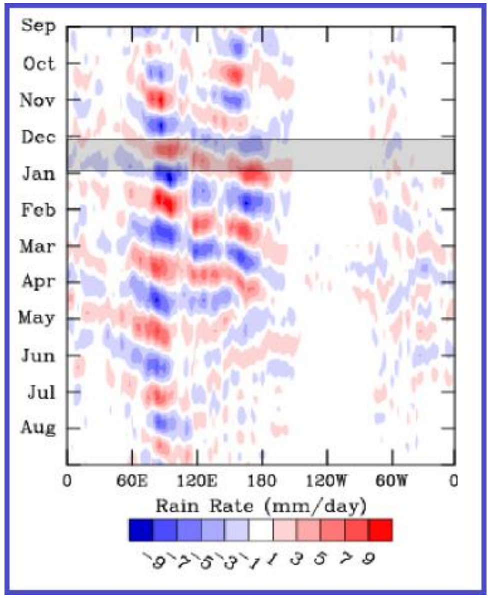

The 1st and 2nd Combined EOF's Capture the Equatorial Convective and Baroclinic Structure of the MJO

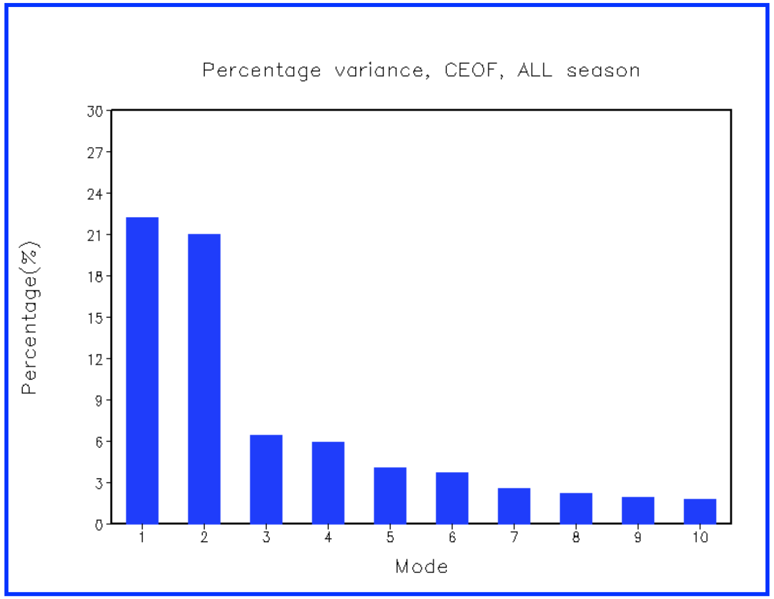

PC's of 1st and 2nd Combined EOF's

Significant Power at 50 days
90-deg out of phase and Coherent (0.77)

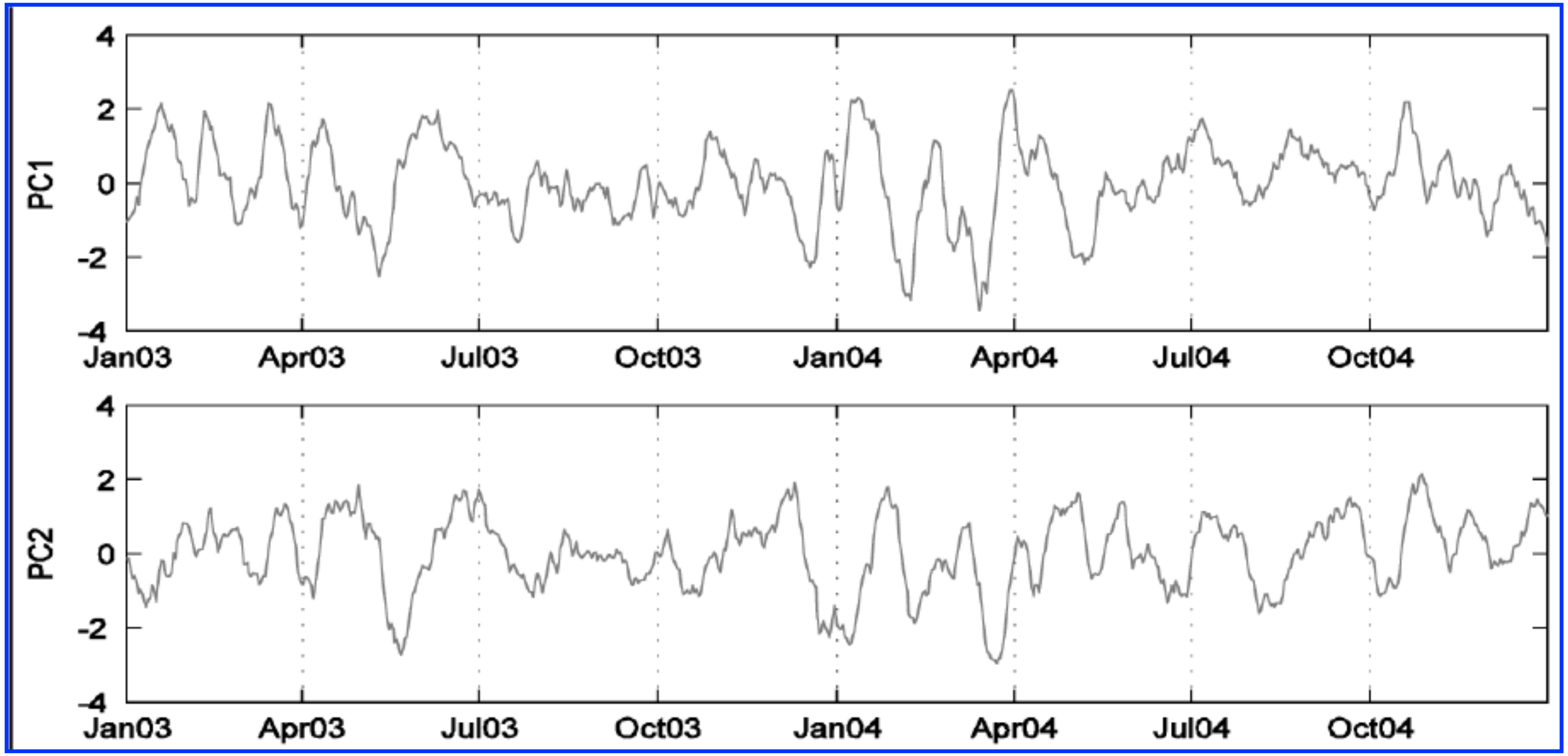

PC's of 1st and 2nd Combined EOF's

Significant Power at 50 days
90-deg out of phase and Coherent (0.77)

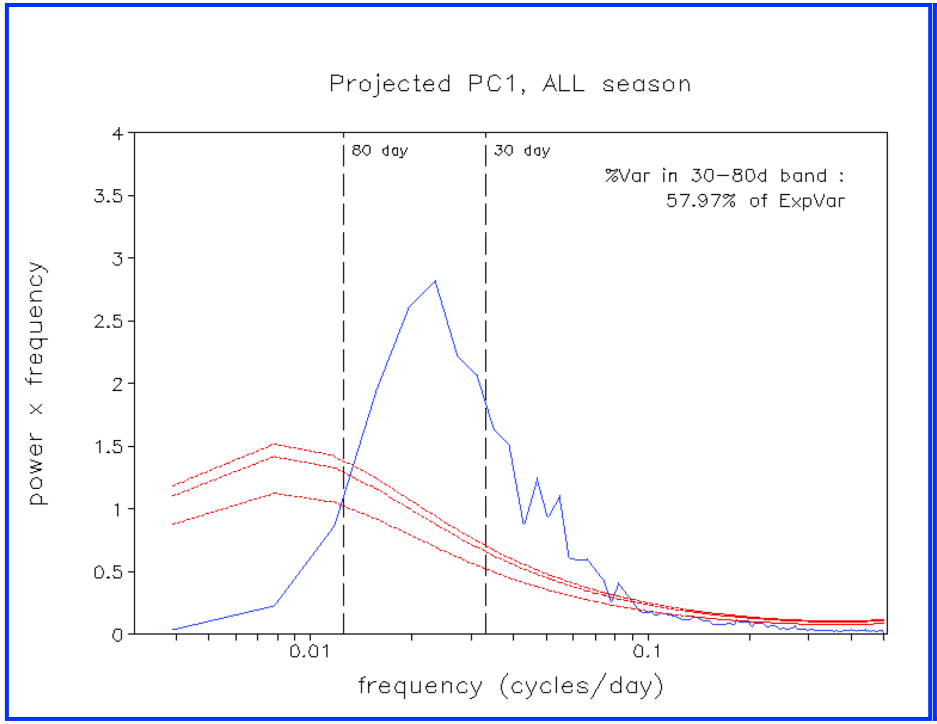

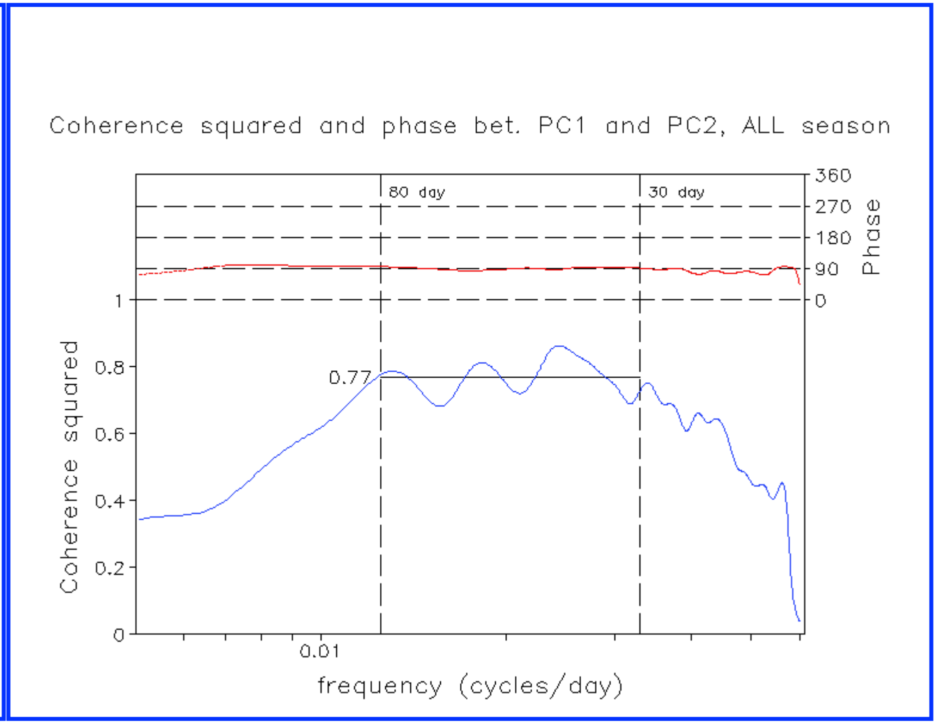

MJO Life-Cycle Composites

Rainfall (x,y)

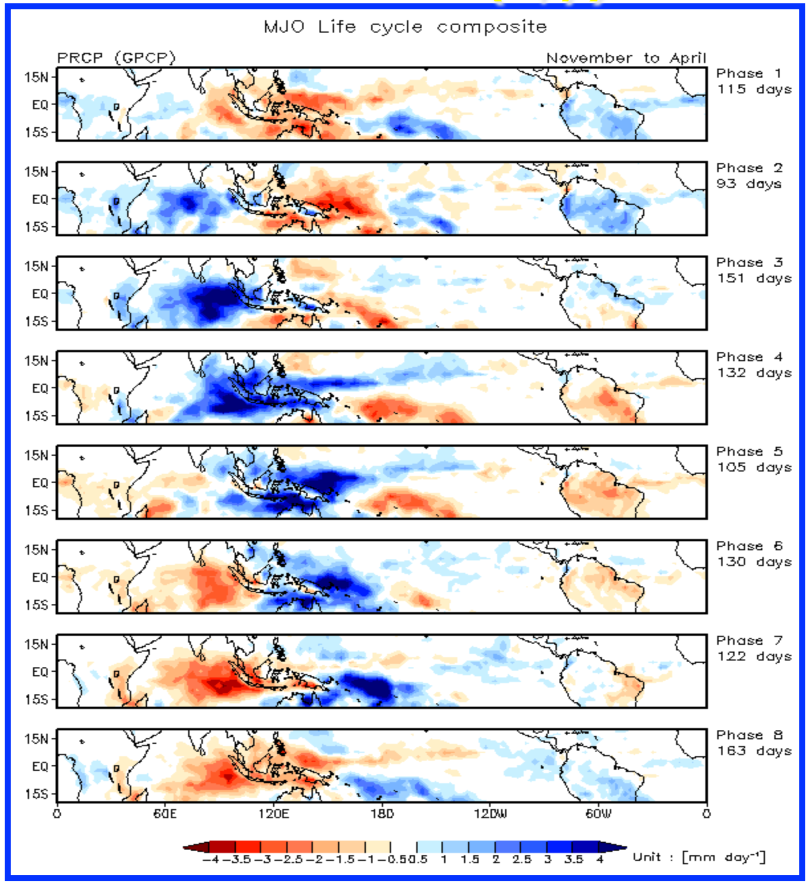

Zonal Wind (x,p)

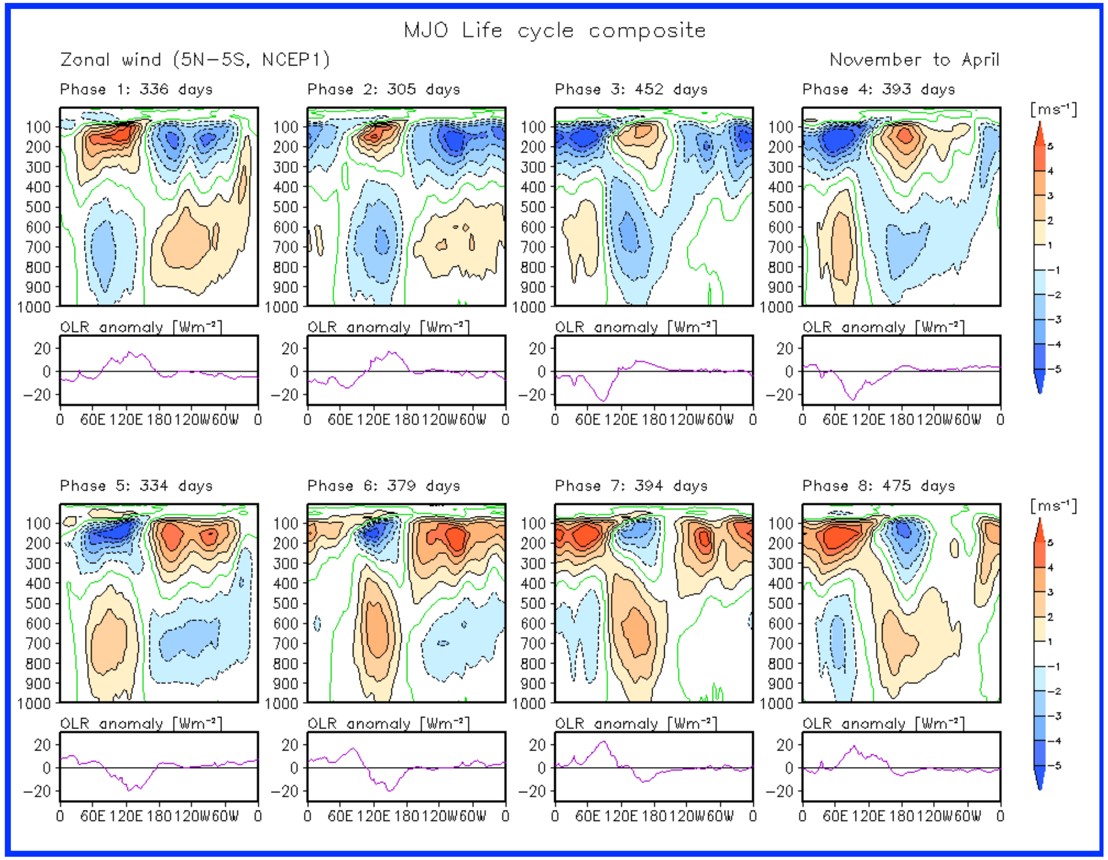

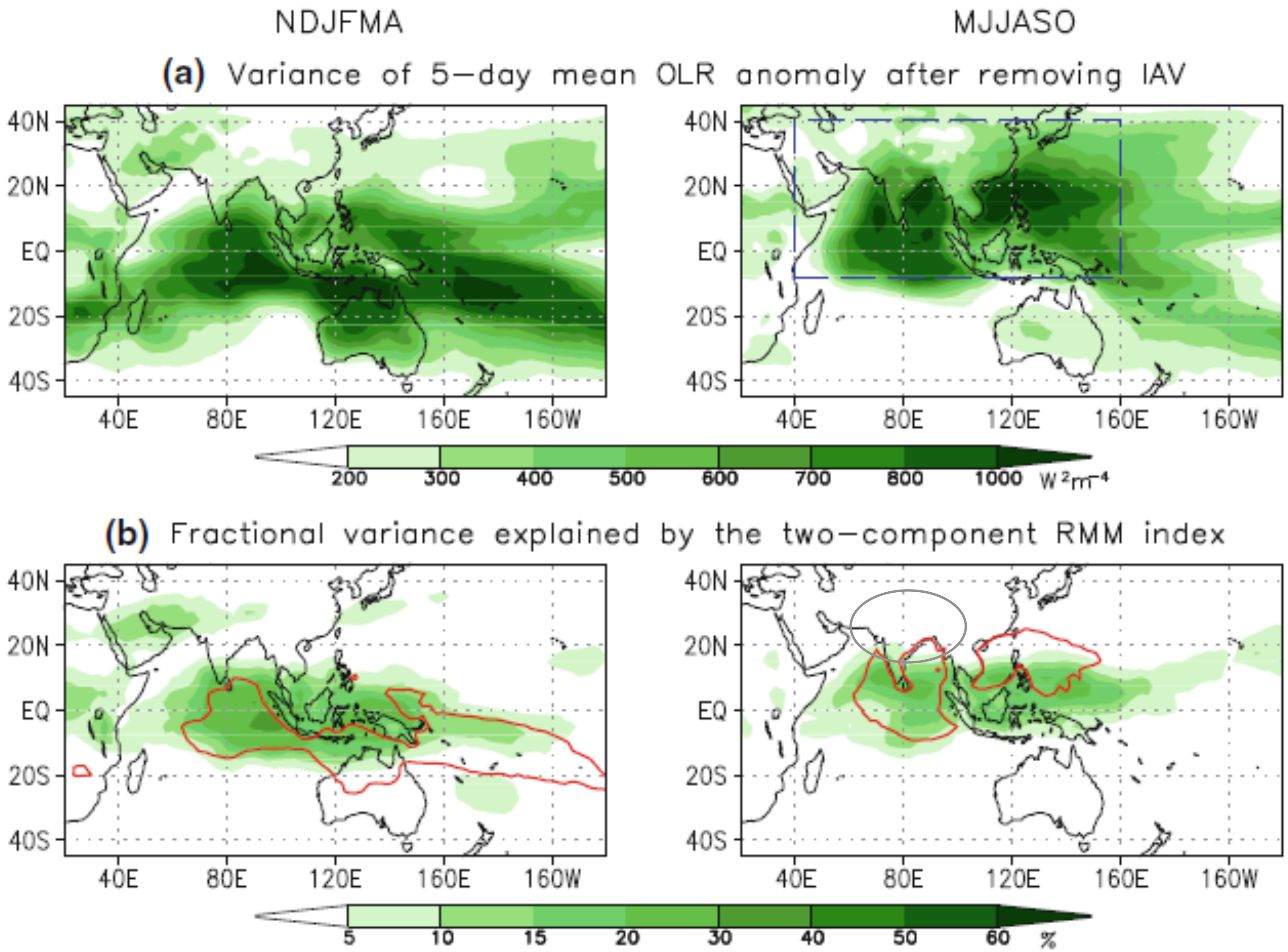

ig. 1 **a** Variance of pentad mean OLR anomaly ($W^2\ m^{-4}$) after emoving climatological annual cycle and interannual variability uring November to April (NDJFMA) and May to October MJJASO), respectively. **b** Fractional variance (%) of 5-day mean OLR anomaly accounted by the two-component RMM index. *Blue dashed line* in right-hand side of **a** indicates the Asian summer monsoon (ASM) domain. *Red contour* in **b** represents OLR variability center with variance larger than 800 $W^2\ m^{-4}$ shown in **a**

The RMM1 and RMM2 indices Do Not capture any variance over the Indian continent!

Ongoing and Future works:

Preliminary results:

ROC & AUC

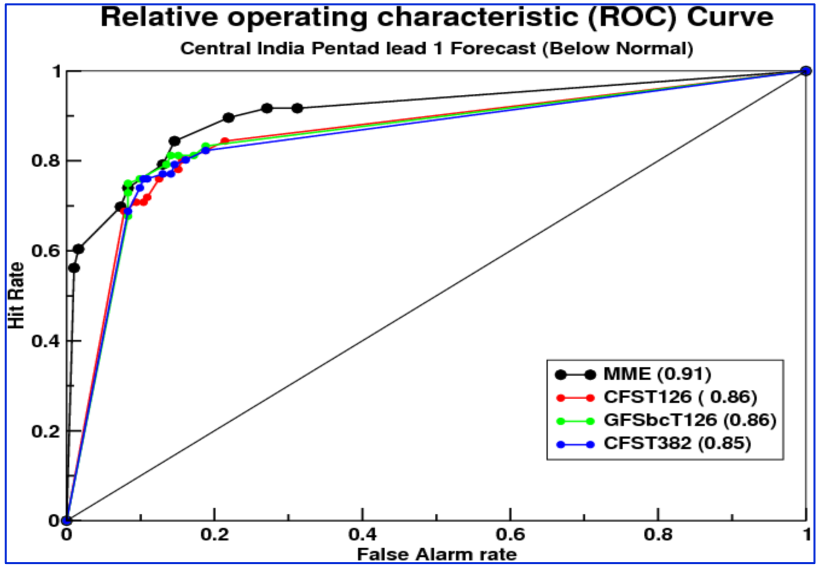

GFSbc
MME

CFST126
CFST382

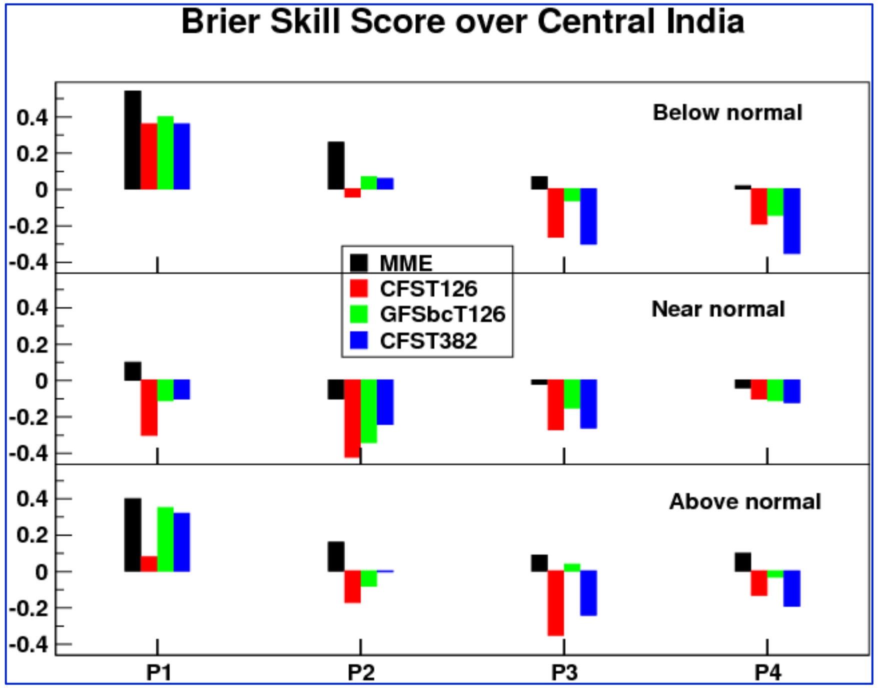

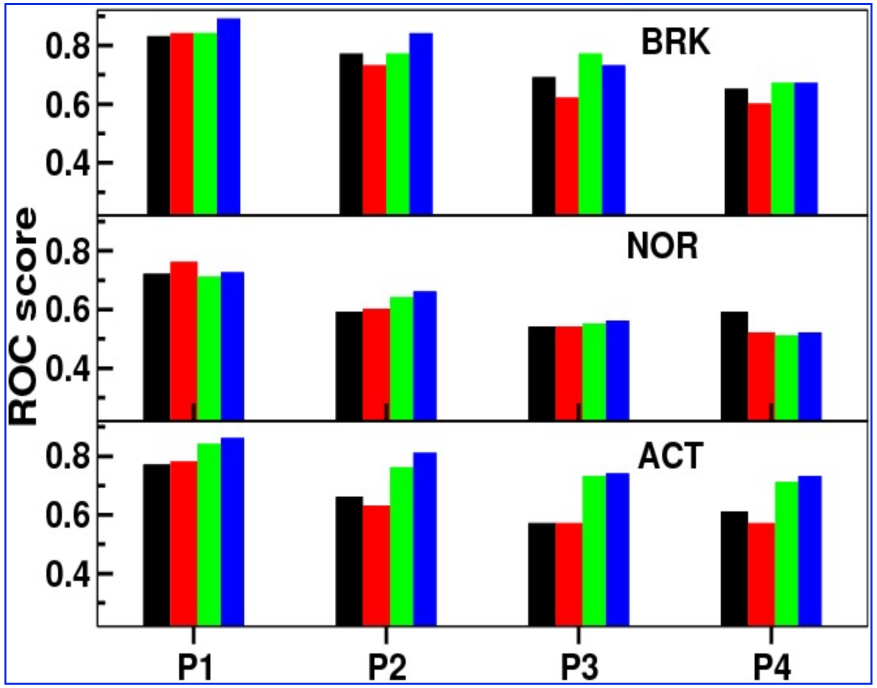

Standard Forecast Verification: Bivariate correlation and RMSE

$$cor(\tau) = \frac{\sum_{t=1}^{N}\left(a_1(t)b_1(t,\tau)+a_2(t)b_2(t,\tau)\right)}{\sqrt{\sum_{t=1}^{N}\left[a_1^2(t)+a_2^2(t)\right]}\sqrt{\sum_{t=1}^{N}\left[b_1^2(t,\tau)+b_2^2(t,\tau)\right]}}$$

$$RMSE(\tau) = \sqrt{\frac{1}{N}\sum_{t=1}^{N}\left\{\left[a_1(t)-b_1(t,\tau)\right]^2+\left[a_2(t)-b_2(t,\tau)\right]^2\right\}}$$

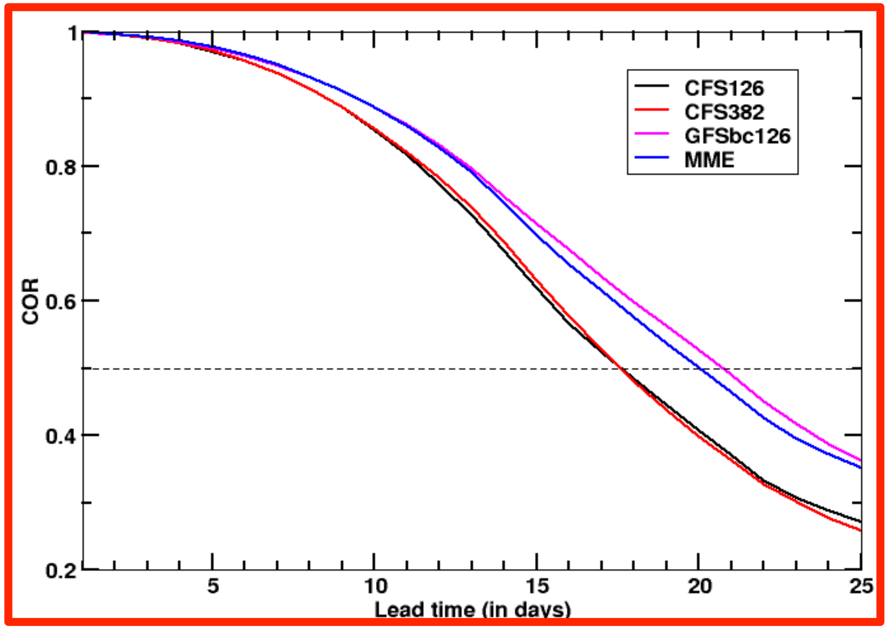

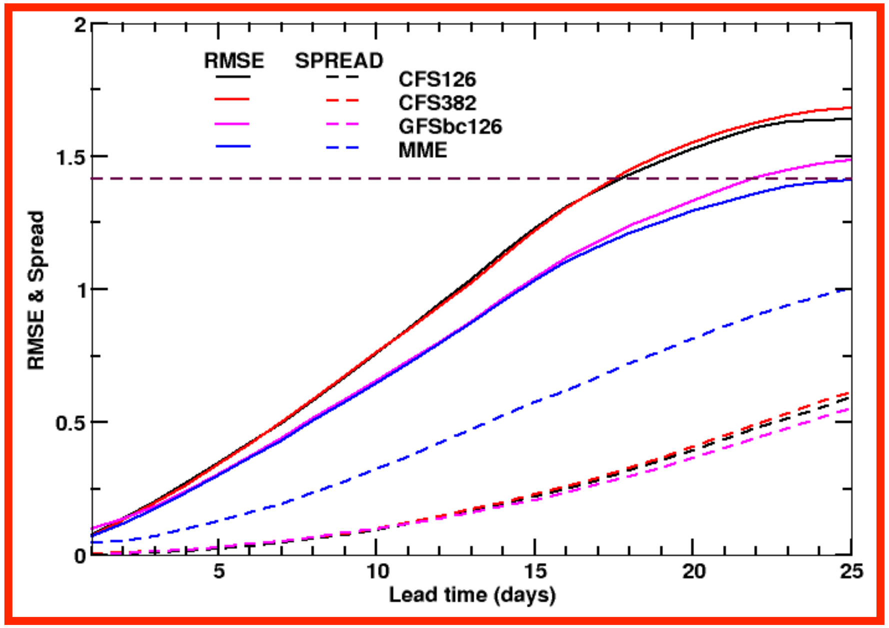

Summary & Conclusion

- The improvement in northward propagation in CFSv2 is not only due to improvement in physics in the atmospheric component. Air-sea interaction contributes significantly to northward propagation.
- Even with the presence of conducive vertical wind shear, the absence of humidity gradient and moistening of the atmosphere column north of convection hinders northward movement of convection in GFS.
- This moistening mechanism works only in the presence of an active ocean.
- In CFSv2, the lead-lag relationship between the atmospheric fluxes, SST and convection are maintained, while such lead-lag is unrealistic in the uncoupled simulations.
- This leads to the conclusion that high frequent and interactive ocean-atmosphere coupling is a necessary and crucial condition for the reproducing realistic northward propagation of MISO in this particular model.